An Abstract Of The Thesis Of

Philip L. Verplanck for degree of Master of Science in Geology presented on November 17, 1986 . Title: A Field and Geochemical Study of the Boundary Between the Nanga Parbat-Haramosh Massif and the Ladakh Arc Terrane, Northern Pakistan.

Redacted for Privacy

Abstract approved _____
Lawrence Snee

The Nanga Parbat-Haramosh massif (NPHM) is a north-south trending structural and topographic high, which interrupts the east-west trend of the Himalaya in northern Pakistan. Previously, the massif was thought to be bounded by the Main Mantle thrust (MMT), a north-dipping thrust along which the Kohistan-Ladakh arc was thrust south over the northern margin of the Indian continent. This study presents field and geochemical data suggesting that the eastern boundary of the massif, the Stak fault zone, is a young feature that displaces the suture zone.

The Stak fault zone marks the boundary between Precambrian kyanite-sillimanite bearing biotite gneiss of continental affinity and Cretaceous (?) arc lithologies of the western Ladakh terrane. The arc complex consists of amphibolitic country rock that has been intruded by gabbroic to tonalitic plutons. The protolith of the amphibolite is immature oceanic island arc tholeiitic basalt. The mafic to intermediate plutons are dominantly calc-alkaline and could have formed in

either a mature island arc setting or a continental margin setting. The Ladakh arc terrane exposes the upper section of an arc, below the sedimentary and volcanic cover.

The Stak fault zone is a 3-5 km wide zone containing at least four major high angle faults that separate blocks of various lithologies. The only true mylonite zone occurs along the westernmost fault. A faulted late stage dike is evidence for recent activity along the easternmost fault. The units along the western side of the fault zone are analogous to deep oceanic arc lithologies; tholeiitic amphibolite, banded gneiss, and a section of a layered mafic complex. The units along the eastern side of the fault zone are mineralogically and chemically correlative to the mafic plutons exposed in the western Ladakh terrane.

The geometry of the fault zone, the lack of suture zone lithologies, and the evidence for recent activity suggest that the Stak fault zone does not represent the suturing event, when the Kohistan-Ladakh arc was obducted onto the northern margin of India. Instead, the fault zone is likely formed in response to the recent uplift of the NPHM.

A Field and Geochemical Study of the Boundary Between the Nanga Parbat-Haramosh Massif and the Ladakh Arc Terrane, Northern Pakistan.

by
Philip L. Verplanck

A Thesis
submitted to
Oregon State University

in partial fulfillment of
the requirements for the
degree of

Master of Sceince

Completed November 17, 1986

Commencement June 1987

APPROVED:

Redacted for Privacy

Dr. Lawrence W. Snee, Assistant Professor of Geology in charge of major

Redacted for Privacy

Dr. J. G. Johnson, Chairman of the Department of Geology

Redacted for Privacy

Dean of Graduate School

Date thesis is presented November 17, 1986

Thesis presented by Philip L. Verplanck

ACKNOWLEDGEMENTS

I am indebted to an assortment of people who have made the completion of this thesis possible and enjoyable. The list is headed by Dr. Larry Snee who provided endless guidance, support, patience, and humor. I appreciate and admire his efforts. Numerous discussions with Drs. Roman Schmitt and Scott Hughes not only strengthened the thesis but also showed me what it takes to be a researcher.

Drs. Ali Humzi Kazmi and Robert Lawrence, and Ian Madin introduced me to the area and provided logistical, intellectual, and moral support. Funding for the field work was provided by NFS grant # INT 81-18403. The field work could not have been completed without the aid of personnel from Gemstone Corporation of Pakistan and Peshawar University. Special thanks go to Ian, Riaz, Shafique, Shokot, Quadam, Javed, Ajad, Karen, Larry, and Emily who shared in the joys as well as the gourmet meals.

Reactor facilities and counting equipment was provided by an unsponsored research grant from the O.S.U. Radiation Center. Technical assistance was provided by M.R. Conrady, T.V. Anderson, W.T. Carpenter, and A.G. Johnson.

The assortment of personalities in the geology and marine geology departments provided many special moments. The years spent with these folks were full of fun and humor.

Most of all I what to thank my wife, Emily, and family for their undaunting support. I admire the strength they showed in the past year and a half.

Table of Contents

List of Figures

List of Tables

A Field and Geochemical Study of the Boundary Between the Nanga Parbat-Haramosh Massif and the Ladakh Arc Terrane, Northern Pakistan.

INTRODUCTION

Background

The Nanga Parbat-Haramosh massif (NPHM) of northern Pakistan is an unusual geologic feature. The massif is a 20-40 km wide, north-trending belt of rocks of probable Indian subcontinental origin protruding northward into rocks of island arc affinities (Fig. 1.1). The massif cuts the regional east-west structural grain of the high Himalaya and separates two similar island arc terranes, Ladakh to the east and Kohistan to the west. The nature and origin of this unusual geologic relationship is not clearly understood. Although the east and west boundaries of the massif were approximately located by Wadia (1933,1937), the nature of the eastern boundary was obscure. The purpose of this study is to define the location and character of the eastern boundary of the Nanga Parbat massif.

The eastern margin of the NPHM is in northern Pakistan in the region referred to as the Deosai Plateau (Fig. 1.2). The western border of the study area is at the town of Shengus, 45 km east of Gilgit, and the eastern border is at the village of Dasu, 45 km west of Skardu. The Indus River cuts through the study area at an elevation between 2000 and 2500 m above sea level. The ridges range from 5000 to 6000 m, and

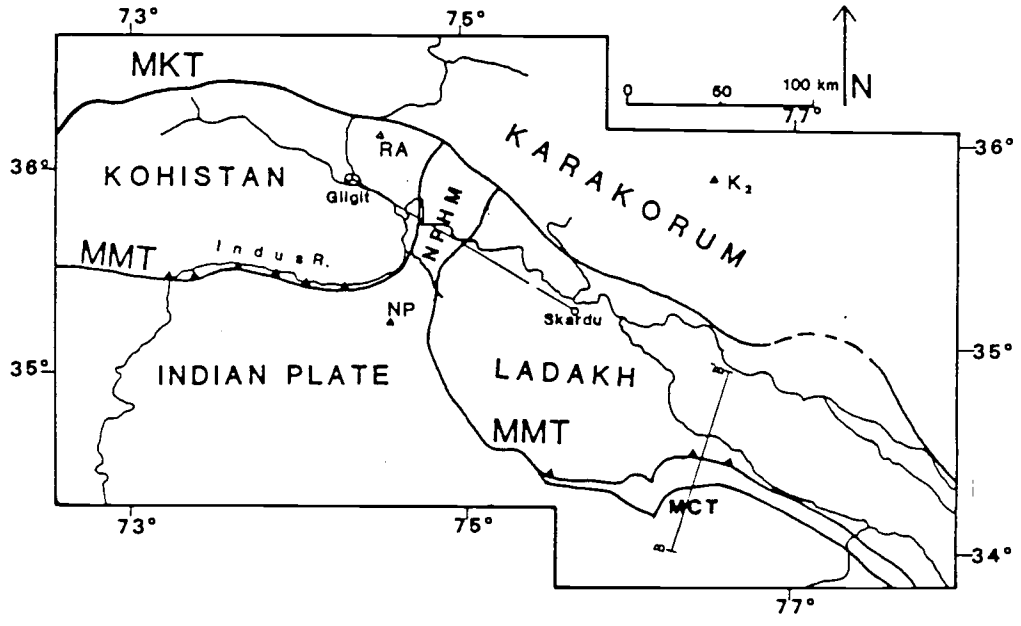

Figure 1.1. Location of Massif. Major structural boundaries in northern Pakistan are delineated.

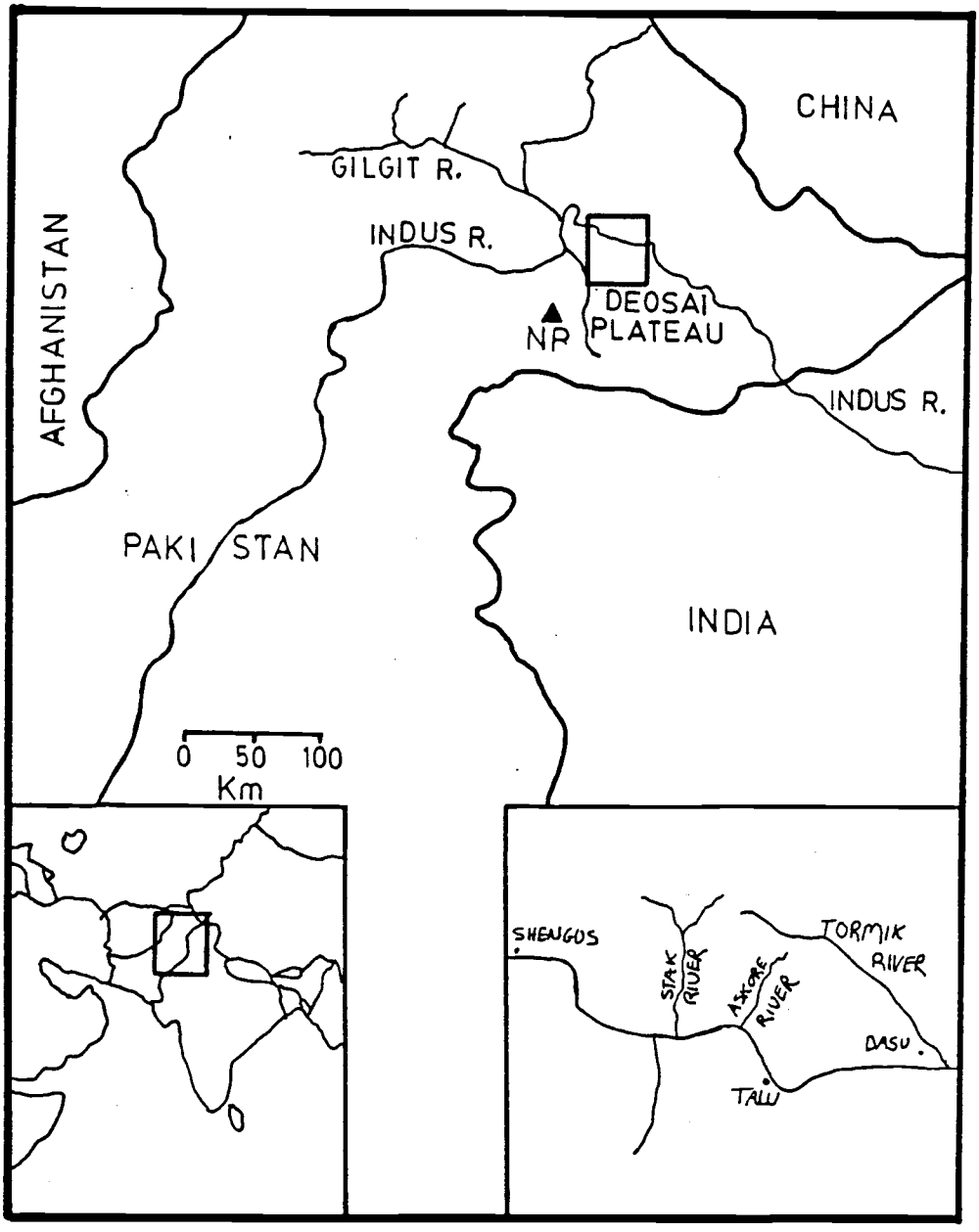

Figure 1.2. Location of Study Area.

an assortment of peaks rise to 7500 m. Nanga Parbat (8125m) lies 40 km to the south. The geology is extremely well exposed, because the climate is arid; approximately 5 cm of annual rainfall are recorded along the Indus gorge (Kureshy and Elahi, 1975). Bedrock is locally covered by landslide deposits, glacial debris, and glaciers.

Regional Setting

The NPHM interrupts the east-west structural grain of the Ladakh Range to the east and the Kohistan Range to the west. The massif is believed to be Indian continental rocks composed predominantly of biotite gneiss with subordinant amphibolites and migmatites (Madin, 1986). The gneiss varies from fine-grained, finely laminated, augen-rich to coarse-grained and coarsely foliated. The rocks in the Ladakh and Kohistan Ranges near the massif comprise gabbro, diorite, and amphibolite.

The massif is bounded by three contrasting terranes. To the north lies the Karakorum axial batholith of Asian (?) continental affinities, to the east and west lie the late Cretaceous Ladakh and Kohistan island arc terranes, and to the south lie Tethyan and cratonic sediments and associated plutons of Indian continental affinities.

The boundaries between these terranes and the massif are poorly delineated, for both political and logistical reasons. Tahirkheli (1979) used the limited available data to located approximately the unmapped boundaries around the massif. Tahirkheli proposed ,and it is now generally accepted, that the Kohistan and Ladakh arcs are sutured

to the Karakorum axial batholith by a vertical to north dipping thrust fault, named the Northern Suture Zone or the Main Karakorum thrust (MKT). Most regional geologic maps (Kazmi and Rana, 1982 and Desio, 1964) show the MKT as the northern boundary of the massif. Another north-dipping thrust fault, the Indus Tsangpo suture (in India) or the Main Mantle thrust (MMT; in Pakistan), sutures the Ladakh and Kohistan arcs to the Indian continental mass. This east-west trending structure contains typical suture zone material which includes large ultramafic bodies, dismembered ophiolites, blueschists, and greenstone assemblages. The eastern and western boundaries of the massif trend north/south and have been drawn as extensions of the Indus Tsangpo suture and MMT. The southern part of the massif is generally shown as a continuation of the Indian continental terrane.

The relative timing of the initiation of suturing along the MMT and MKT is debated because limited field data are available to constrain the geochronology. Reynolds et al. (1983) envisage that the sequence was first the collision of the Indian plate with the Ladakh-Kohistan arc during the late Cretaceous causing thrusting along the MMT and then subsequent collision of the Indian plate along with the arcs with the Asian continent along the MKT. Conversely, Coward et al. (1982), Peterson and Windley, 1985, and Debon et al.(1986) believe that the Ladakh/Kohistan arc was sutured to the Asian mass during the early Cretaceous and then the Indian plate collided with the arc and Asian plate. Klootwijk et al. (1985) use paleomagnetic evidence to show that since 50 My the Indian plate and the Ladakh arc had the same magnetic polar wander paths; thus, suturing of India and Ladakh along the Indus Tsangpo Suture Zone took place in the early Eocene.

Previous Work

Because of poor access and rugged terrain, little geologic work has been attempted in the study area, although some work has been done in adjacent areas. For the past 50 years, the Indian Geological Survey has been mapping the region to the south. Wadia (1933, 1937) mapped much of northern Kashmir (Fig. 1.3), including the Astor River valley northward to the intersection with the Indus River. He believed that the Nanga Parbat massif was the core of a large antiform, and he mentioned that the lithologies on the eastern boundary of the massif are similar to the ones on the western boundary. The northern limit of the work is the northwest-trending divide between the Astor River valley and the Indus gorge to the north.

Misch (1935,1949) studied the Nanga Parbat region (Fig. 1.3) as part of the 1933 German climbing expedition. He entered the region from the south and observed an increase in metamorphic grade of the Salkala sediments of the Indian continent. He interpreted the gneisses of the NPHM as granitized metasediments, calling upon potassium metasomatism.

Desio and Zanettin (1964) mapped the region east of the study area as part of the 1954 Italian Karakorum Expedition; the resultant map overlaps the eastern edge of this study area. Primarily, they concentrated on the petrology of the major units, and made only a few observations on the contact relationships. Their mapping of the western Ladakh terrane was used as a base for this study.

With the advent of plate tectonics, Tahirkheli (1979) reevaluated the previous work and performed limited reconnaissance work, but he was

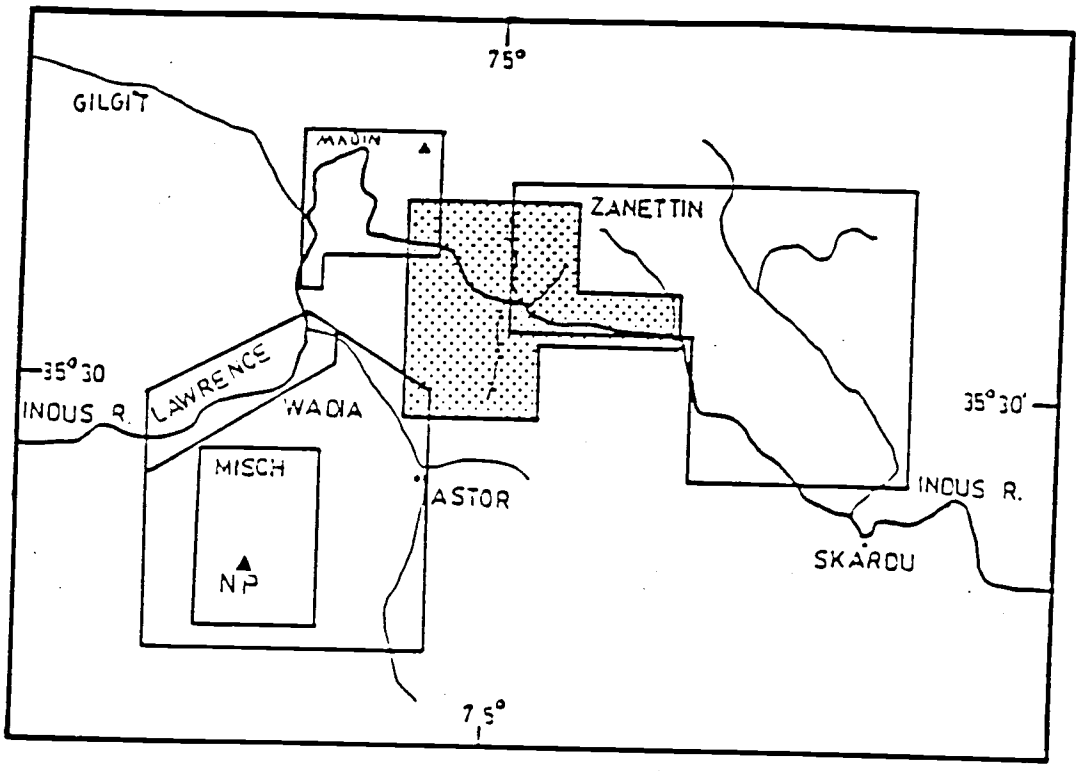

Figure 1.3. Location of Other Studies.

still hindered by poor access. The survey route for the Gilgit to Skardu road along the Indus gorge provided him access to the eastern boundary of the massif, which he took to be the Main Mantle thrust.

Zeitler (1985) collected samples from the massif and adjoining terranes to evaluate and quantify the uplift rates of various tectonic blocks in northern Pakistan. He concluded that the NPHM was rising at a rate of 4.5+-0.7 mm/yr from 0.7 my to the present and at a rate of 1.6+-0.16 mm/yr from 2.0 to 0.7 my These rates were based on the conclusions of his fission track cooling study. Overall, the NPHM has risen 5.2+-0.7 km during the past 2 million years.

The most recent study of the massif was completed by Madin (1986). He mapped the western boundary of the massif from Khaltaro to Bunji along the Indus River (Fig. 1.3). Our work overlaps at Shengus. He presents evidence showing that the western boundary is an active fault, which was first recognized by Lawrence and Ghauri (1983). The fault has both horizontal and vertical motion, specifically right lateral and east side up. It is hypothesized that the young fault displaces the MMT and is the western termination of the Main Central thrust (MCT).

Purpose and Procedure

The purpose of this study is to attempt to unravel the geologic history of the eastern side of the NPHM. Delineating and interpreting the structure that marks the eastern boundary is essential for understanding the origin of the massif and its apparently anomalous geologic character. To accomplish this purpose, two field seasons of detailed

geological mapping and sample collecting along the Indus gorge and its major tributaries from Shengus to Dasu were completed during the falls of 1984 and 1985. Reconnaissance work to the east, west, and south was performed to aid in the interpretation. Major and trace element geochemistry is used to define the nature of sources of the various lithologies within the massif, arc and fault zone. Finally, the results of the study are put into a regional geologic framework.

In the organization of this paper the lithology, structure, and geochemistry of the northeast section of the massif are first described: next, the same is done for the adjoining Ladakh terrane. A detailed knowledge of the adjoining terranes is necessary to interpret the boundary between them. Using this framework, the lithologic and chemical character of the rocks within the boundary zone are described and the geometry discussed. Finally, a model for the origin of the boundary is derived within the framework of the regional geology.

Analytical Methods

Samples were collected from the massif, arc, and fault zone betweeen them. The sample size was restricted to less than 10 kg due to the remoteness of the area. Sample preparation was performed in a clean environment. Weathered material was trimmed and the fresh portions were crushed in a Lamaire jaw crusher and rotary mill; both machines are equiped with 99.5% pure alumina plates. Representative aliquants of the sample were pulverized to less than 200 mesh in an alumina shatter box.

Aliquants were taken for major and trace element analyses. Major element analysis was done by X-ray fluorescence techniques at the

U.S. Geological Survey in Denver. Trace element abundances were acquired by sequential instrumental neutron activation analysis (INAA), following the procedure outlined by Laul (1979). At the OSU TRIGA reactor facility samples weighing 0.5-1.0 g, were irradiated with equivalent volumes of the U.S.G.S. standards AGV-1, BCR-1, BHVO-1, G-2, and SRM-1633, as well as OSU Radiation Center in-house standards. Gamma ray spectra were collected on ND600 and ND2200 multichannel analysers coupled with Ge(Li) crystal gamma ray detectors. Two counts, one week after irradiation and one month after irradiation, were performed to acquire data on the various isotopes. The raw data were reduced on the OSU Cyber computer system. All recognized interferences were corrected.

NANGA PARBAT-HARAMOSH MASSIF

An east-west cross section of the northern section of the NPHM is well exposed along the Indus Gorge. The section is dominated by two large north/northeast-trending antiforms, the Bulache antiform to the east and the Iskere antiform to the west (Fig. 2.1). The antiforms are separated by a fault, the Baraluma fault, as well as bounded by faults, the Stak fault zone on the east side of the massif and the Raikot fault on the west.

The Bulache antiform is composed of the Shengus gneiss, a multilithologic amphibolite facies gneiss. The dominant lithology, approximately 90%, is fine-grained, finely laminated, biotite-garnet gneiss. The laterally continuous layers make the unit distinctive. Subordinant lithologies are pods and layers of medium- to coarse-grained equigranular gneiss, augen gneiss, and calc-silicate gneiss; schistose interbeds; and amphibolite layers. The mineralogy is tabulated in Table 2.1.

Adjacent to the Baraluma fault, a relatively thick layer of amphibolite, the Baraluma amphibolite, crops out. It is composed of subequal amounts of hornblende and plagioclase, with subordinant amounts of quartz, garnet, and biotite.

Pegmatitic amd basaltic dikes intrude the gneisses. Although the pegmatites occur throughout the study area, dike swarms are centered near Shengus and Toghla. The basaltic dikes are less abundant and have only been observed in the eastern limb of the Bulache antiform.

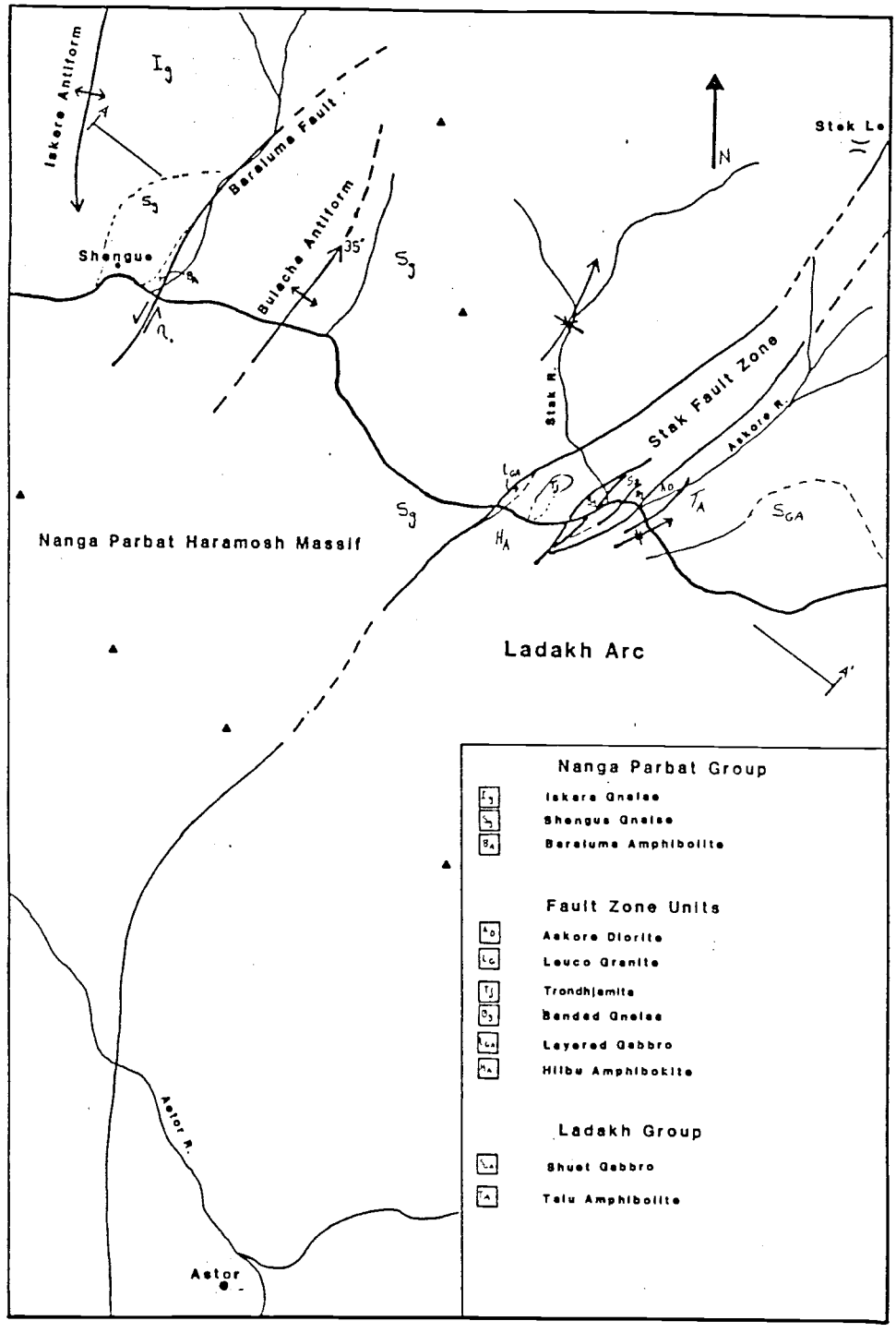

Figure 2.1. Generalized Geologic Map.

Table 2.1

Characteristic Mineralogy of Nanga Parbat-Haramosh Massif Units

P = Psammitic, Pe = Pelitic, C = Calcic, M = Mafic. X = major component, x = minor component, t = trace component.

Mineral	Shengus Gneiss			Equigranular Gneiss	Iskere Gneiss*			Baraluma Amphibolite	Mafic Dikes
	Pe	C	M	P	P	C	M	M	M
Plagioclase	X	x	X	X	X		X	X	x
K Feldspar	X			X	X		t		
Microcline		x				x			
Quartz	X	x	x	X	X	X	x	x	t
Biotite	x	x	x	x	x		x		x
Muscovite	x			x	x	x	t		
Almandine	x		x	t	x		x	x	
Sillimanite	x								
Kyanite	x								
Tourmaline	t				t				
Hornblende		x	X				X	X	X
Epidote	t	t	x			t		x	
Calcite		X				t	x		t
Grossularite		X				X			
Diopside		X				X			
Zoisite	t				t	t	x		
Sphene	t	t	t		t	t		t	
Zircon	t	t	t	t	t	t	t		
Apatite	t	t		t	t	t	t		
Opaques	t		t	t	t	t	t	t	t
Graphite	t								

* from Madin, 1986

Lithology Section

Shengus Gneiss

The Shengus gneiss occurs in a northeast-trending, north-plunging antiform (the Bulache antiform), which is the dominant feature of this part of the massif (Plate A2). The exposed thickness of the gneiss is approximately 12 km from the core of the antiform along the Indus river, to the upper part of the section in the upper Stak valley. Extensive thickening by isoclinal folding is likely. The unit is dominated by biotite gneiss, but interbeds of medium- to coarse-grained equigranular gneiss, calc-silicate gneiss, mica schist, and amphibolite are present. Fine-scale, laterally continuous layering makes the unit easily recognized. The layering consists of bands of alternating plagioclase, potassium feldspar, and quartz with biotite and muscovite. Lithologic layers are generally 1-25 cm thick and are laterally continuous with numerous garnet porphyroblasts up to 20 cm in diameter. Locally augen gneiss lenses contain porphyroblasts of potassium feldspar up to 15 cm long.

Along the Indus near the core of the antiform, the typical minerals at the base of the Shengus gneiss are quartz, plagioclase, potassium feldspar, sillimanite, biotite, and garnet with or without muscovite, sphene, hornblende, and zircon. The garnets contain inclusions of plagioclase, biotite, and muscovite, apparently indicating a prograde reaction. The mineral assemblage in this portion of the Shengus gneiss is representative of amphibolite facies metamorphism. The pressure and temperature conditions are displayed in Fig. 2.2.

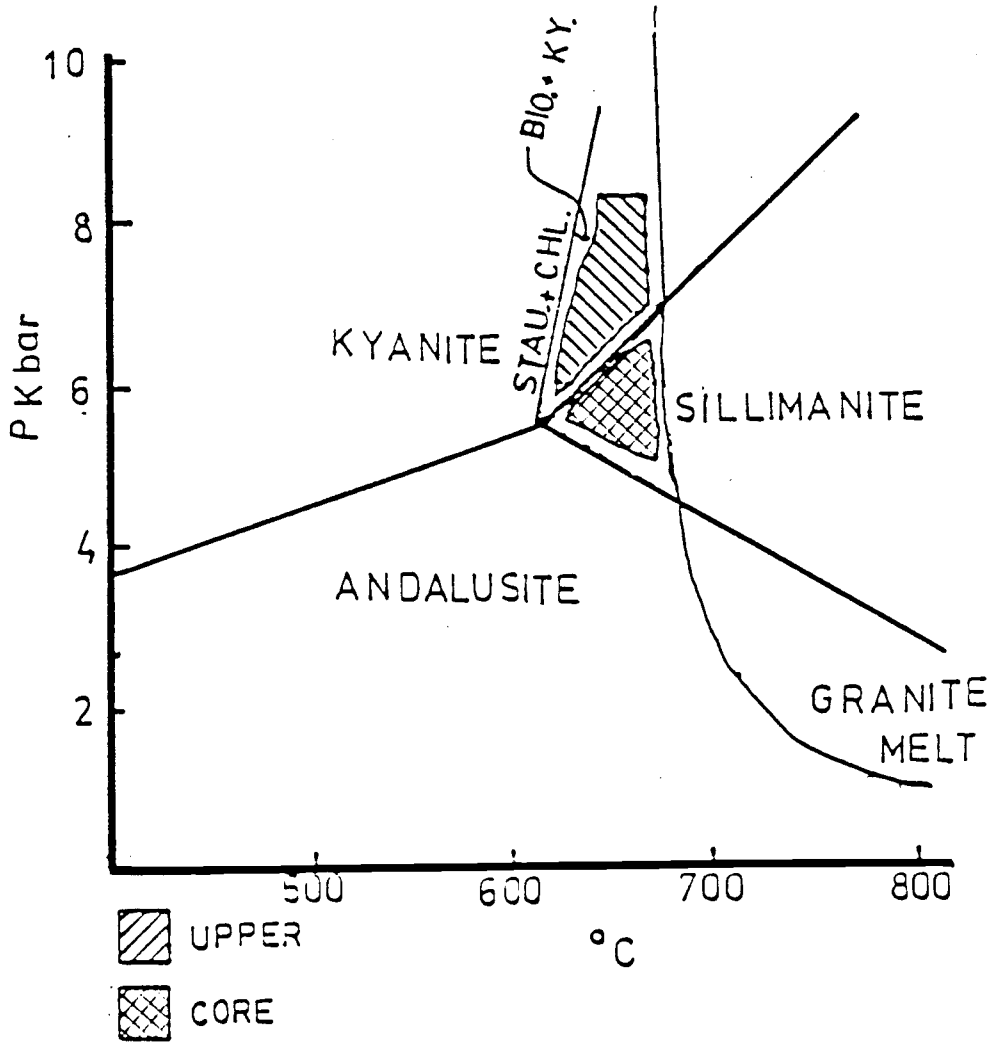

Figure 2.2. Pressure and Temperature Conditions (from Miyashiro, 1973).

Petrographically, samples from the core of the antiform exhibit a polygonal equigranular texture, which may have formed during static recrystallization at some time after regional metamorphism. Some of the plagioclase crystals exhibit a curious exsolution texture (Fig. 2.3) that most likely formed during slow cooling of the unit (J.Rice, personal comm.,1986).

A typical mineral assemblage from the gneisses of the upper Stak valley, at the highest sampled exposure in the section, consists of quartz, oligoclase, potassium feldspar, biotite, muscovite, garnet, and kyanite with or wthout graphite, sphene, and zircon. This mineral assemblage is representetive of amphibolite facies metamorphism, and the pressure and temperature conditions are displayed on Fig. 2.2. These samples exhibit a fabric that formed under more dynamic conditions than the samples from the bottom of the section. Grain-size reduction is exhibited by a mortar texture.

The mineralogy and lithologic variations point to sedimentary protolith for much of the Shengus gneiss. The presence of sillimanite, kyanite, muscovite, and graphite in relatively high abundances are evidence for the high aluminum and carbon content of the protolith and are indicative of a sedimentary origin. Calc-silicate and schistose interbeds are consistent with a sedimentary protolith. Thick, augen-bearing, gneissic layers of coarse-grained quartz, oligoclase, potassium feldspar, and biotite do occur within the unit and were probably derived from plutons that intruded the sedimentary or metasedimentary rocks. Subsequently, the entire sequence was metamorphosed and deformed.

Figure 2.3. Exsolution Texture in Shengus Gneiss.
Photomicrograph of a plagioclase grain. 1.31 mm across.

Baraluma Amphibolite

The Baraluma amphibolite occurs as layers within the Shengus gneiss near the town of Shengus (Plate A2). The unit crops out along the Skardu road on the west side of town by the checkpoint and on the east side of town along Baraluma Gah. The thickness of the unit is difficult to estimate, for it is highly contorted. The thickest section is along the west side of the Baraluma fault and is approximately 400 m thick.

The mineralogy consists of subequal amounts of hornblende and plagioclase along with minor amounts of biotite, quartz, and garnet. Plagioclase from the amphibolite on west side of Shengus has a distinctive exsolution texture (Fig. 2.4). The coarse-grained labradorite (An 55) has exsolved plagioclase of a different An content. At the molecular scale, this has been described by Champnes and Lorimer (1976), but this texture has never been reported at the microscopic scale. This texture is less well developed in some of the sections of Shengus gniess near the core of the antiform. If this texture formed by exsolution, it indicates a period of static,slow cooling of this part of the area, which is consistent with the texture in the nearby Shengus gneiss.

Pegmatites

Pegmatitic dikes occur throughout the massif; two areas, Shengus and the west side of the upper Stak valley (Plate A2), have high concentrations. The areas are 10 km apart and separated by two 6500

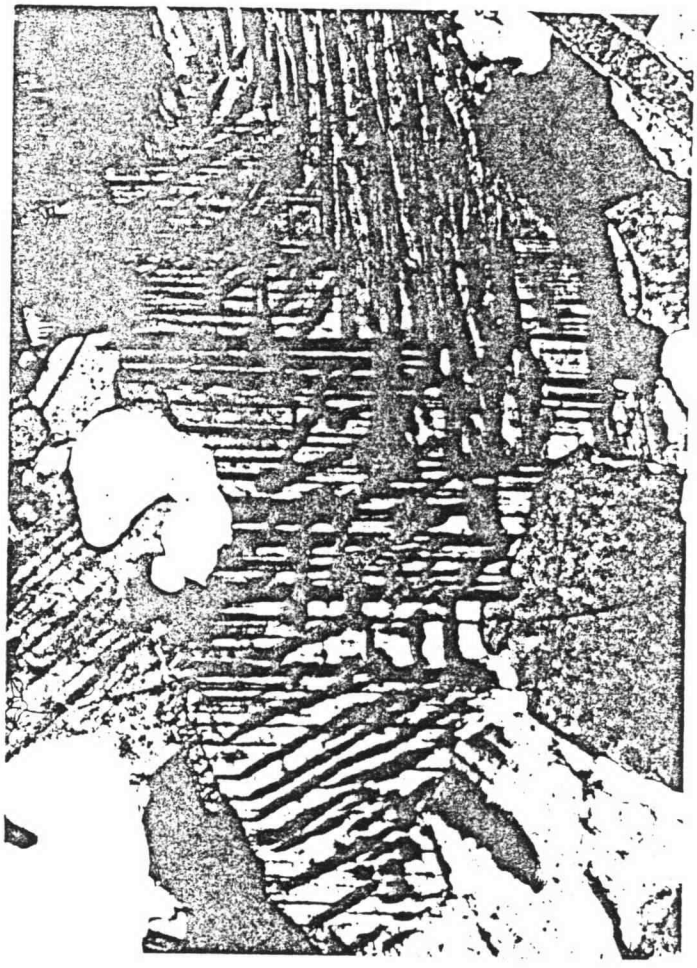

Figure 2.4. Exsolution Texture in Baraluma Amphibolite. Photomicrograph of a plagioclase grain. 1.31 mm across.

m high ridges. This makes it difficult to determine if the two swarms are part of the same group. The swarms occur at different elevations and have distinctive mineralogies.

The Shengus pegmatites are one to two meters wide and occur at an elevation of 2500 to 3000 m and are presently being mined for aquamarine by the Gemstone Corporation of Pakistan (GEMCP). The pegmatites intruded along joint sets with attitudes of N50E 42W and N10E 65W. The mineralogically most fertile pegmatites were emplaced adjacent to the Baraluma amphibolite and they are normally bounded on one side by the gneiss and on the other by the amphibolite. The minerals consist of massive quartz, plagioclase, potassium feldspar, with minor amounts of muscovite and beryl (aquamarine), and trace amounts of garnet and schorl. Lepidolite and spodumene are reportedly present (Ali, personnel comm., 1985). The aquamarine crystals occur in clay filled cavities along with crystalline quartz, orthoclase, cleavelandite, and muscovite.

Pegmatites along the west side of the upper Stak valley are also in the Shengus gneiss and are being mined by GEMCP for bicolored tourmaline crystals. The pegmatites are generally concordant to foliation and in some places are deformed by faulting and folding. Approximately 80% of the pegmatites studied were parallel to subparallel to foliation. The richest pegmatites occur between the elevation of 3500 and 4500 m. One to two meter thick pegmatites are crudely zoned with massive quartz near the middle. Massive potassium feldspar, quartz, and plagioclase are the dominant minerals with minor amounts of muscovite, biotite, and schorl, and trace amounts of epidote, fluorite, and opaque minerals. The upper 20 cm are rich in

schorl oriented perpendicular to the contact. The bicolored tourmaline crystals occur in clay filled fractures and cavities in association with orthoclase, quartz, cleavelandite, muscovite, clear topaz, and schorl (Fig. 2.5). Tourmaline usually grades from a dark green core to a pink or clear termination. In rare cases, the dark green core grades to a deep blue termination.

Mafic Dikes

Within the antiform, fine-grained mafic dikes up to a meter wide crosscut the foliation of the Shengus gneiss. The extent of diking cannot be estimated because the mafic dikes are not easily visible within the weathered gneiss. The dikes do stand out along the Skardu roadcut. Two sampled dikes, occurring 5 and 11 km west of the Stak fault zone, consist of hornblende, biotite, and plagioclase. The unoriented biotite appears to be secondary, grown at the expense of the amphibole. The dikes seem to have undergone a mild static metamorphic event, for they are not contorted.

Geochemistry and Its Implications

Whole rock geochemistry is a valuable technique to determine the nature of the protolith of metamorphic rocks such as the Shengus gneiss and Baraluma amphibolite as well as to define the nature of the igneous rocks such as the mafic dikes that intrude the massif. At the microscopic scale regional metamorphism causes a redistribution of the major elements, but at the megamacroscopic scale metamorphism is

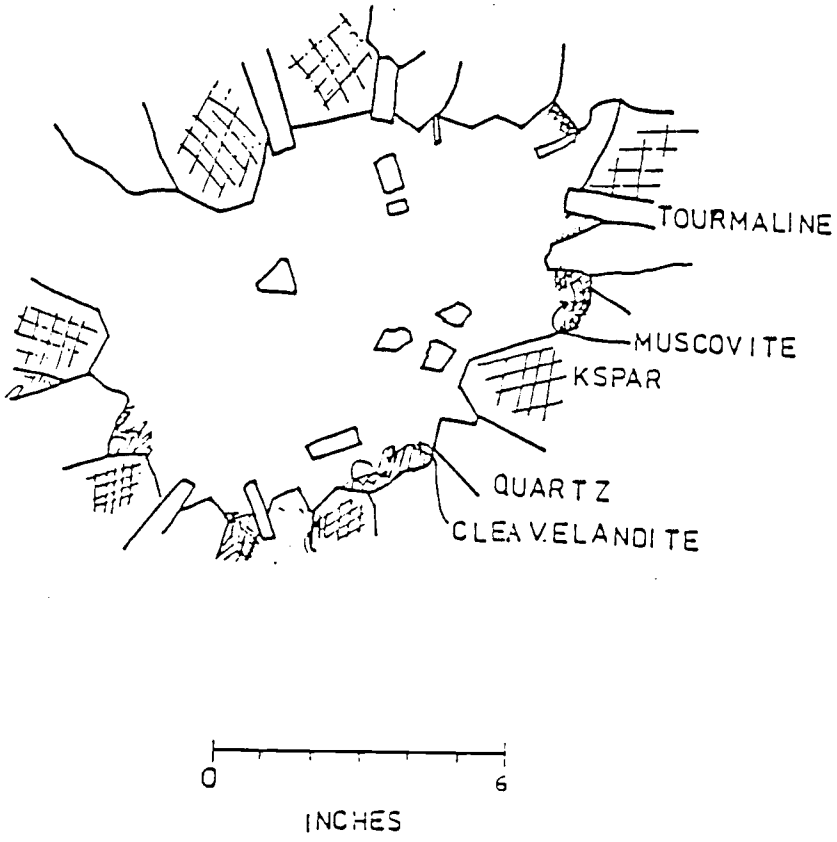

Figure 2.5. Pegmatite Cavity.

believed to be isochemical (Eskola, 1939). This is a valid assumption unless an aqueous phase is present. Certain trace elements, particularly the rare earth elements (REEs), are relatively immobile during upper amphibolite facies metamorphism (Frey et al, 1968, Meuke etal, 1977).

Major and trace element data of 12 samples of the Nanga Parbat terrane are presented in Table 2.2. Six to ten kg samples were used to ensure sample homogeneity because of the layered and porphyritic nature of the gneisses.

Major Element Geochemistry

To visualize better the data and gain insight into the nature of the protolith, major element concentrations are plotted on ACF diagrams ($A=Al_2O_3+Fe_2O_3-(Na_2O+K_2O)$, $C=CaO-3.3(P_2O_5)$, and $F=FeO+MgO+MnO$). Nockolds (1954) developed the ACF diagram to compare the chemical composition of metamorphic rocks with those of sedimentary and igneous rocks in an attempt to identify the protolith (Fig 2.6). Depending on the extent of weathering, sedimentary rocks tend to be enriched in Al_2O_3 and depleted in FeO, MgO, Na_2O, K_2O,and CaO.

Mafic units, such as amphibolites and mafic dikes of the NPHM, can be plotted on diagrams, such as AFM ($A=Na_2O+K_2O$, F=FeO*, and M=MgO), SiO_2 vs FeO*, and SiO_2 vs FeO*/MgO, to see if they are of tholeiitic or calc-alkaline series. The chemical variation resulting from crystal fractionation of a tholeiitic magma consists of iron enrichment (and magnesium depletion) followed by sodium and potassium enrichment (Fig. 2.7). The Skærgaard trend is a good example. The calc-alkaline trend consists of sodium and potassium enrichment without pronounced iron

	Finely Laminated Gneisses			Equigranular Gneisses			Iskere Gneiss	Amphibolites		Malic Dikes		Percent
Sample no.	4036	4047	4052	4030	4081	4131C	3173	3020C	4014	4130A	4131A	Uncertainity
SiO2	72.2	71.8	71.2	71.1	77.3	73.5	67.7	53.3	50.2	49.6	47.1	1-3
TiO2	0.39	0.38	0.83	0.42	0.18	0.27	1.14	1.78	1.94	1.79	1.55	1-3
Al2O3	14.5	15.1	15.9	15.0	11.8	14.7	14.3	15.4	15.0	13.9	16.3	1-3
Fe2O3	0.39	0.27	0.36	0.56	0.25	0.42	0.69	3.58	1.73	1.89	1.82	1-3
FeO	1.55	1.20	3.55	2.40	1.70	1.46	4.32	10.20	9.97	11.00	9.89	1-3
MnO	0.02	0.02	0.04	0.04	0.02	0.03	0.05	0.21	0.19	0.22	0.19	1-3
MgO	0.56	0.63	1.25	0.84	0.10	0.58	0.87	2.62	6.49	6.74	8.30	1-3
CaO	0.95	0.55	0.58	1.21	0.80	1.02	1.97	8.50	10.40	11.30	10.40	1-3
Na2O	2.46	2.72	1.25	2.69	3.15	2.51	2.56	2.78	2.50	1.44	2.34	1-3
K2O	6.10	6.62	4.02	4.41	3.91	4.18	5.20	0.41	0.67	0.83	0.99	1-3
P2O5	0.26	0.24	0.05	0.16	0.05	0.12	0.31	0.40	0.21	0.19	0.16	1-3
H2O-	0.03	0.03	0.04	0.07	0.02	0.05	0.01	0.05	0.01	0.14	0.04	1-3
H2O+	0.56	0.76	0.68	0.98	0.44	0.94	0.72	1.06	1.50	1.43	1.68	1-3
Sc PPM	3.5	2.0	5.8	6.0	0.9	4.0	8.0	31	33	45	37	1-2
Cr	5	3	40	20	2	10	10	40	-	150	145	2-4
Co	3.1	2	34.6	24.2	17.4	3	5.3	43	134	42.2	54	2-3
Ni	-	-	30	-	20	-	10	70	50	60	110	10-20
Rb	290	290	150	260	210	200	250	-	-	120	50	10-30
Sr	-	-	-	-	-	-	-	-	-	-	-	10-30
Cs	-	3.7	3.5	-	7.9	-	2.8	0.44	-	-	5.3	10-30
Ba	360	710	-	490	1010	610	720	90	-	-	70	5-10
La	135	69.3	103	42.9	103	29.0	137	29.4	22.9	10.7	7.89	1-3
Ce	-	-	-	-	194	60.5	267	41.7	56.3	27.9	21.5	5
Nd	54	71	56	40	94	32	78	-	24	-	-	10-30
Sm	26.60	20.10	21.70	7.66	18.91	6.56	23.30	11.50	6.72	4.80	3.64	1
Eu	1.42	0.66	1.94	0.87	2.56	0.82	0.96	3.47	1.77	1.47	1.17	1-3
Tb	1.6	0.88	1.6	0.81	3.4	0.65	2.2	1.8	0.42	0.85	0.73	5-10
Yb	-	-	-	-	9.6	-	6.6	6.9	2.4	0.5	2.4	5-10
Lu	0.33	0.21	0.26	0.25	1.3	0.25	0.81	0.98	0.30	0.51	0.43	5-10
Zr	350	250	350	120	400	130	700	350	100	-	-	30
Hf	6.8	5.4	9.0	5.0	13	3.1	20	7.8	4.0	3.3	2.6	5-10
Ta	0.65	0.75	3.2	2.7	4.1	1.2	2.0	1.5	1.5	0.64	0.44	5-15
Th	108	121	72	33	28	17	54	4.3	3.1	2.3	0.85	5-15

Table 2.2. Chemistry of Nanga Parbat Samples.
Note: Percent uncertainty derived from statistical error and reproducibility of data.

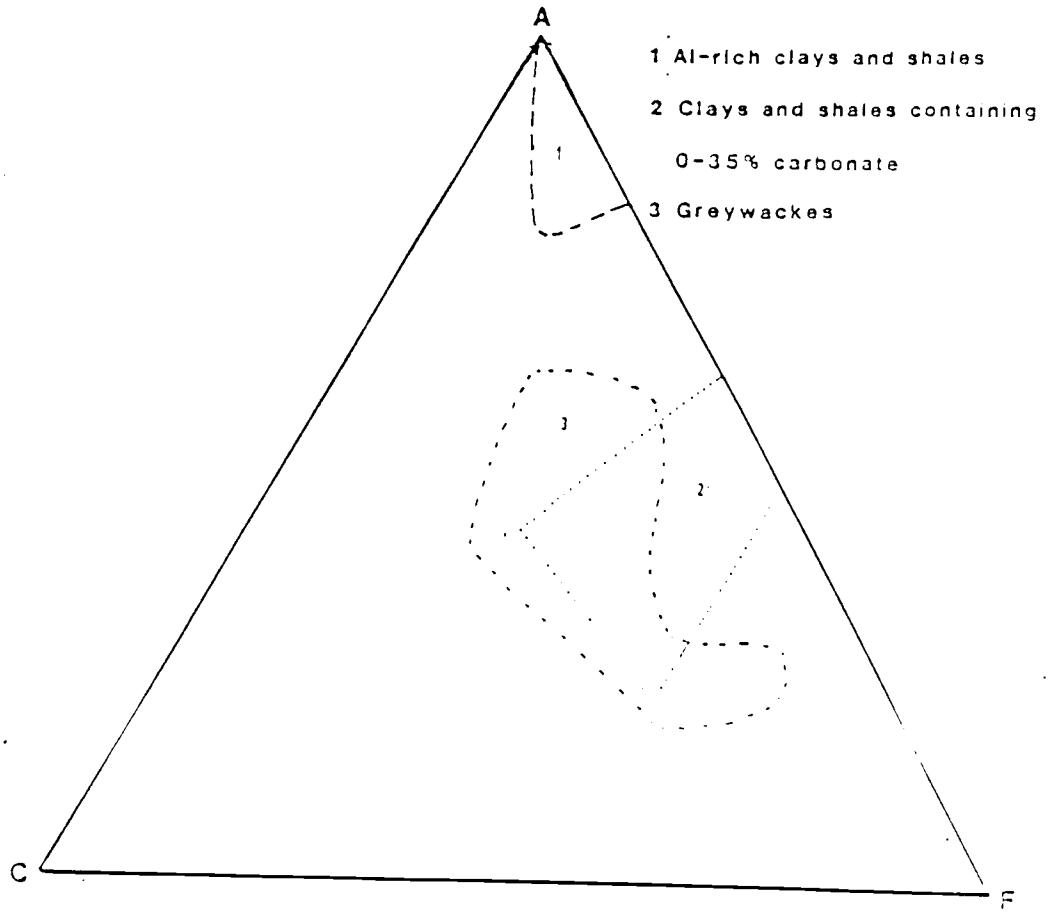

Figure 2.6. ACF Diagram. Delineating protolith fields.

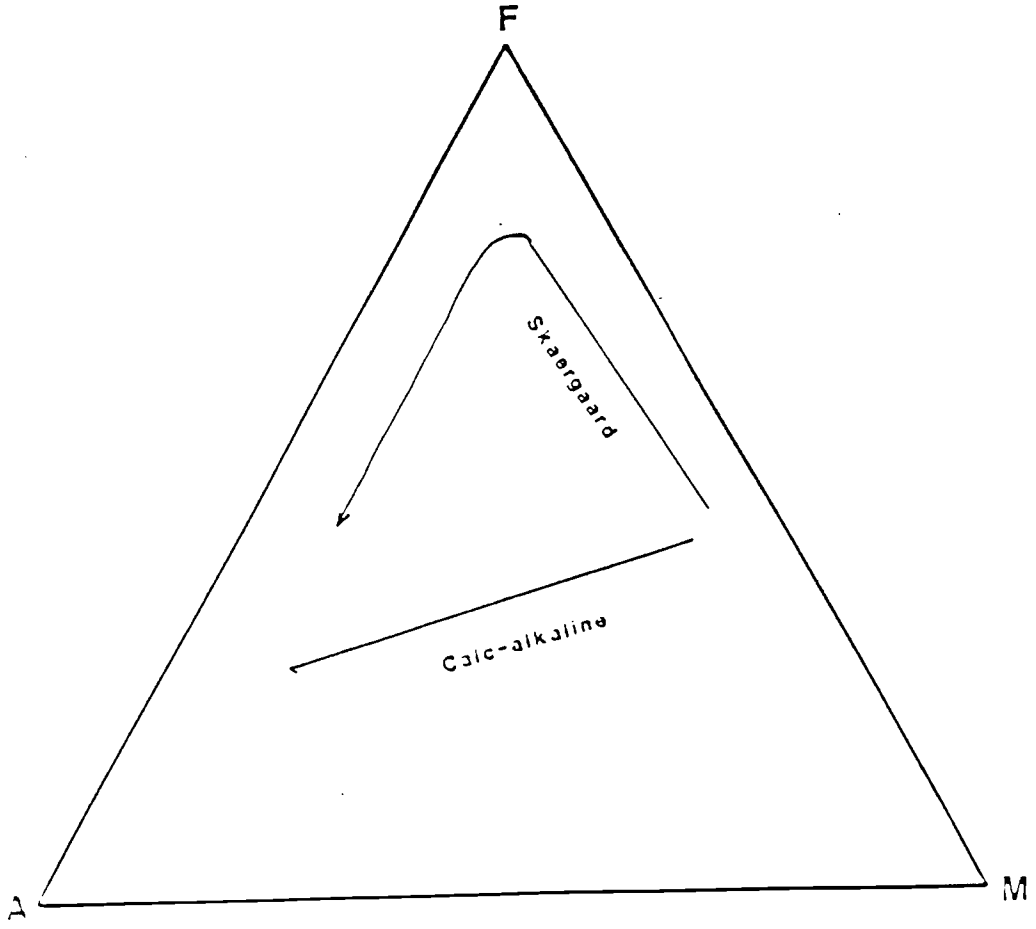

Figure 2.7. AFM Diagram. Delineating tholeiitic and calc-alkaline fractionation trends.

enrichment. Miyashiro (1974) used FeO*/MgO vs SiO_2 and FeO*/MgO vs FeO* diagrams to distinguish tholeiitic from calc-alkaline magmas.

Shengus Gneiss

In this discussion the Shengus gneiss is divided into two parts, finely laminated gneiss (representing 90-95 % of the overall unit) and equigranular gneiss (representing 5-10 % of the unit). Equigranular gneiss occurs as pods and lenses within the finely laminated gneiss. Three samples of each gneiss from various locations were analyzed. In addition one sample of the Iskere gneiss, a biotite-rich orthogneiss collected from western NPHM outside the study area, was analyzed.

The chemical data on the gneisses are variable, which is to be expected due to the variability in mineralogy and the large study area. Although a few samples can not adequately characterize this terrane, some general chemical trends are apparent.

Although the gneisses are lithologically different, the major element chemical data are not distinctive due to the large variation. The finely laminated gneisses have a restrictive range in SiO_2 (71.1%-72.2%) and Al_2O_3 (14.5%-15.9%) while the equigranular gneisses are quite variable, 71.1%-77.3% and 11.8%-15.0% respectively. The samples of the gneiss plotted on the ACF diagram (Fig. 2.8) show some scatter in the data due to the variety of lithologies sampled. The gneisses plot towards the A end of the plot as a group, and the two types of gneisses are indistinguishable. The group of samples plots within the field of clay defined by Nockolds (1954), but it overlaps the upper part of the graywacke field.

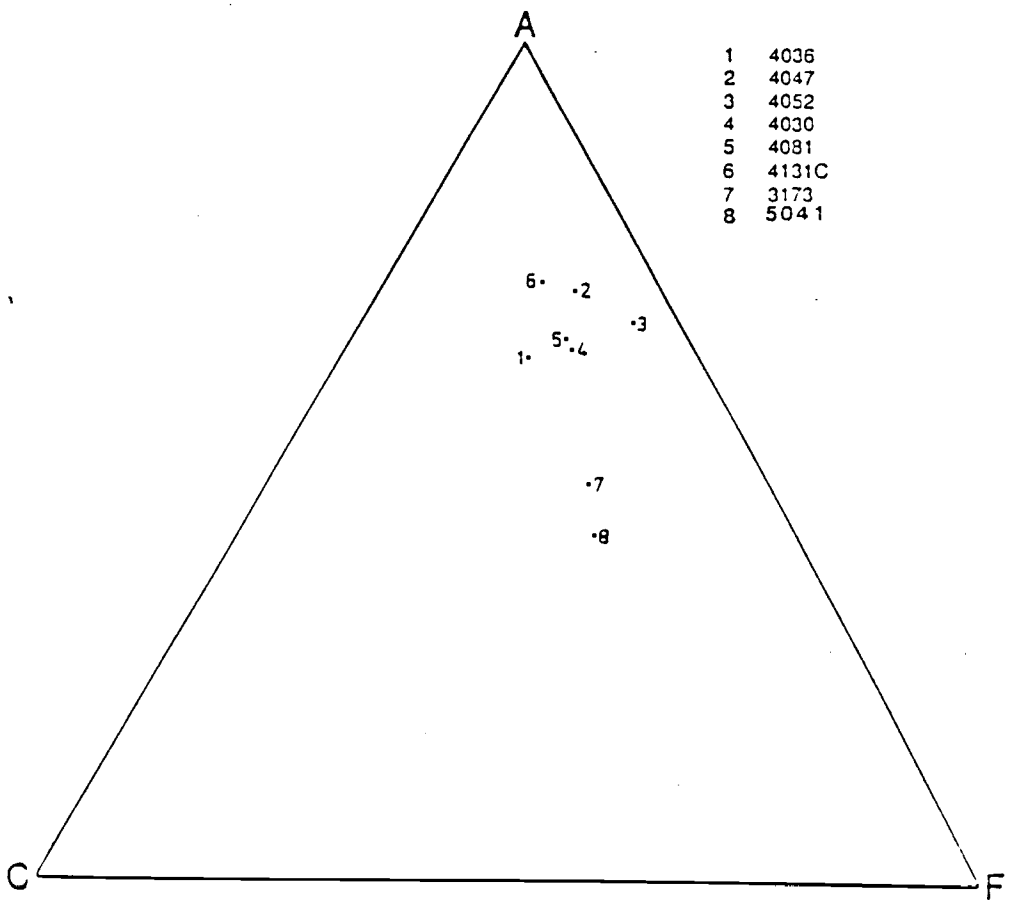

Figure 2.8. ACF Diagram of Gneisses. Samples from the massif.

The ratio of molecular percent of Al_2O_3/Na_2O+K_2O+CaO for all the gneisses is greater than 1.0. This range is that of peraluminous systems and exemplifies the enriched alumina content.

Two samples that do not plot within the group are 3173 and 5041. Sample 3173 is from the Iskere gneiss, a coarse-grained equigranular orthogneiss, cropping out to the west of the study area. The gneiss plots within the range of alkali granites, which is consistent with the orthogneiss classification. Sample 5041 is a biotite schist that has been hydrothermally altered. Coarse, hydrothermal calcite is visible in thin section. Secondary calcite will skew the plot to the C end of the diagram.

Baraluma Amphibolite

The Baraluma amphibolite (4014) consists of 50.20% SiO_2, 15.00% Al_2O_3, 12.80% Fe_2O_3*, and 10.40% CaO. The data plotted on the ACF (Fig. 2.9) diagram lie near the middle of the triangular diagram but slightly away from the C endmember. The major element data are consistent with derivation of the amphibolite from a protolith that was either igneous, basalt or gabbro, or sedimentary, clay-rich carbonate such as marl. Chemically, these lithologies can be identical.

Another amphibolite (3020C) from west of the thesis area was sampled. Field evidence suggests a sedimentary protolith. The amphibolite is interlayered with marble (Madin, 1986). This amphibolite has major element concentrations similar to the those of the Baraluma amphibolite, although it is slightly more enriched in Fe_2O_3* and depleted in MgO.

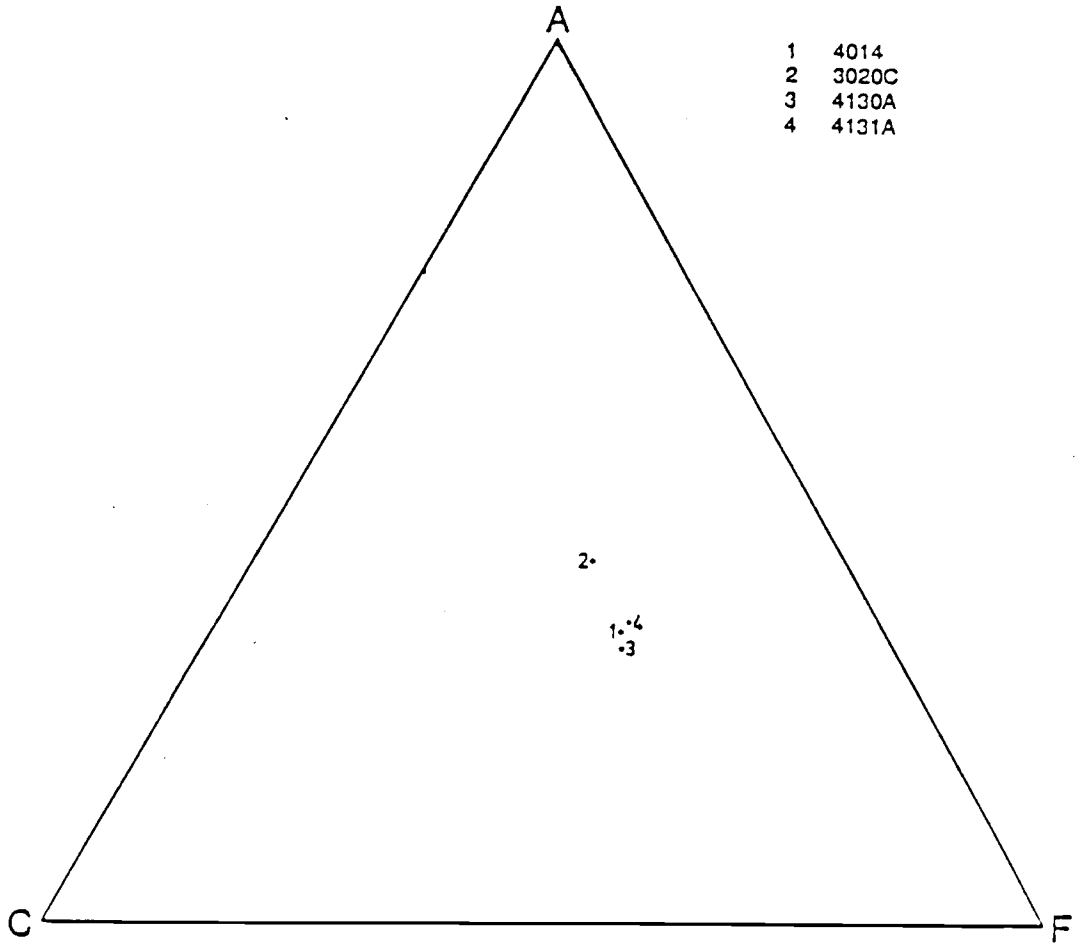

Figure 2.9. ACF Diagram of Mafic Units. Samples from the massif.

Mafic Dikes

The two mafic dikes (4130A and 4131A) that intrude the Shengus gneiss have similar, but not identical, major element concentrations. Sample 4130A is slightly more enriched in SiO_2, Fe_2O_3*, and CaO as well as being depleted in Al_2O_3, MgO, and Na_2O. Both lie within the tholeiitic basalt field on the FeO*/MgO vs. FeO* and FeO*/MgO vs. SiO_2 (Fig. 2.10).

Trace Element Geochemistry

Because the REEs are relatively immobile during amphibolite facies metamorphism, they can be used to identify the protolith. In plutonic systems the REEs tend to reflect the nature of the source region (Haskin, 1984). The REEs are generally plotted on a semilog scale with the elements plotted in decreasing ionic radii on the abscissa and the chondrite normalized concentrations on the ordinate. The concentrations are generally normalized to chondritic abundances to overcome the Oddo-Harkins effect, i.e. even atomic number elements have higher solar abundances than their neighboring odd atomic number elements because of their greater nuclear stability. The normalized concentrations used in this study are those of C1 chondritic abundances determined by Anders and Ebihara (1982).

Shengus gneiss

Chondrite-normalized REE plots of the finely laminated gneiss,

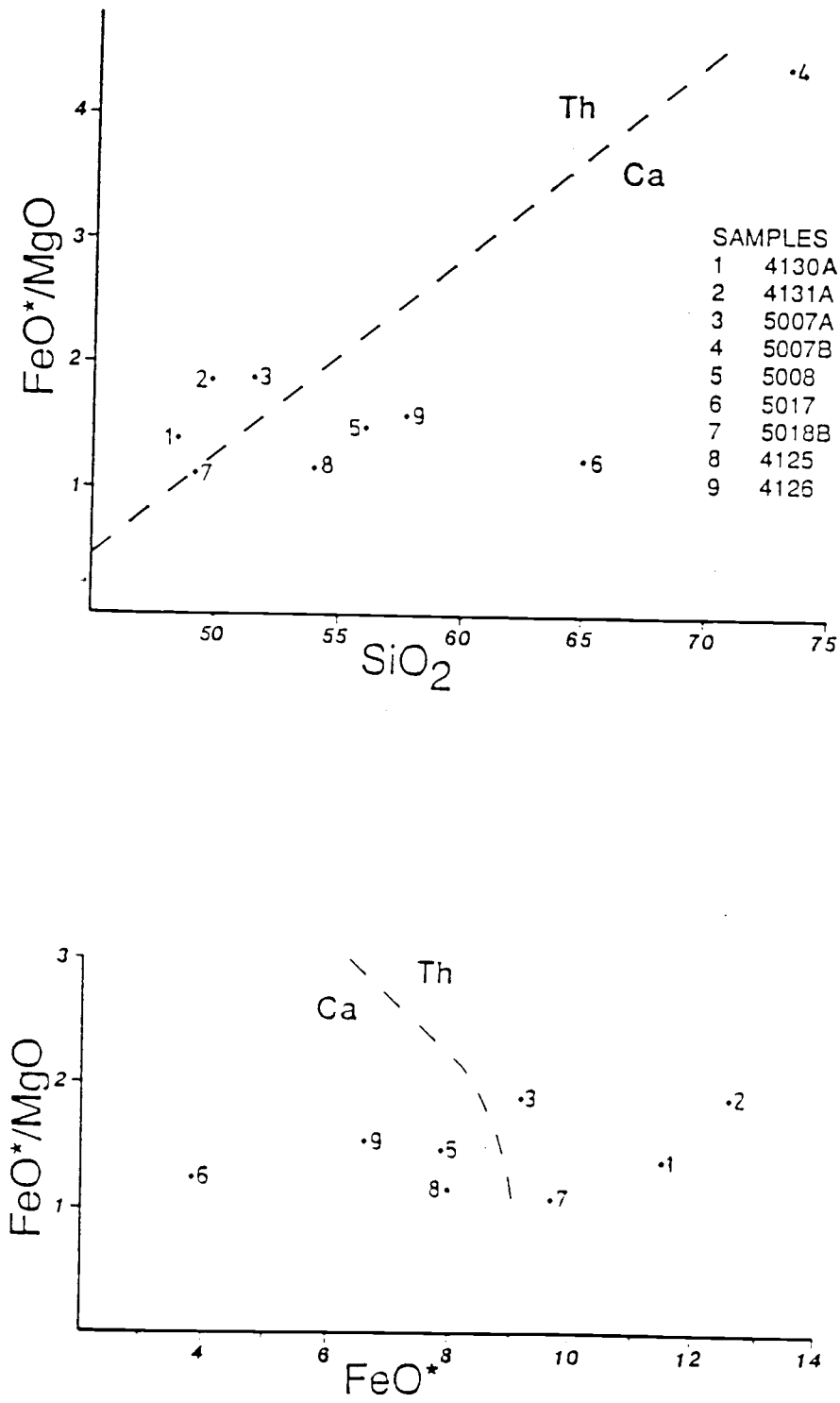

Figure 2.10. Feo* vs. SiO_2 and FeO*/MgO vs. FeO* for the Basaltic Dikes and Ladakh Lithologies. Tholeiitic and calc-alkaline discrimination line from Miyashiro (1974).

equigranular gneiss, and Iskere gneiss show fractionation of the light rare earth elements (LREE) and heavy rare earth elements (HREE) along with a negative europium anomaly (Fig. 2.11, 2.12, and 2.13). This pattern reflects a highly evolved source for the protolith. To generate these concentrations, evolved continental material is needed.

The finely laminated and equigranular gneisses have distinctive trace element concentrations. The finely laminated gneiss shows extreme fractionation, for the (La/Lu)cn is 40 (cn= chondrite normalized) and the negative europium anomaly is large. The equigranular gneiss tend to be less fractionated, (La/Lu)cn = 10, as well as having a smaller Eu anomaly. The slope of the HREE is greater for the finely laminated gneisses than for the equigranular gneisses.

The two types of gneisses are distinctive in other trace elements. In general the Zr/Hf is greater and the Rb/K_2O is smaller in the finely laminated gneiss. The Th values are greater, approximately four times greater, in the finely laminated set.

When compared to data of the North American shale composition (Haskin, 1968), the finely laminated gneisses exhibit extreme fractionation. The composition of the North American shale is believed to represent the composition of average continental crust. Both patterns show the LREE enrichment and Eu anomaly, but the patterns from the gneisses are much more pronounced.

Baraluma Amphibolite

The trace element data for the plagioclase rich Baraluma amphibolite shows LREE enrichment and slight HREE enrichment (Fig.

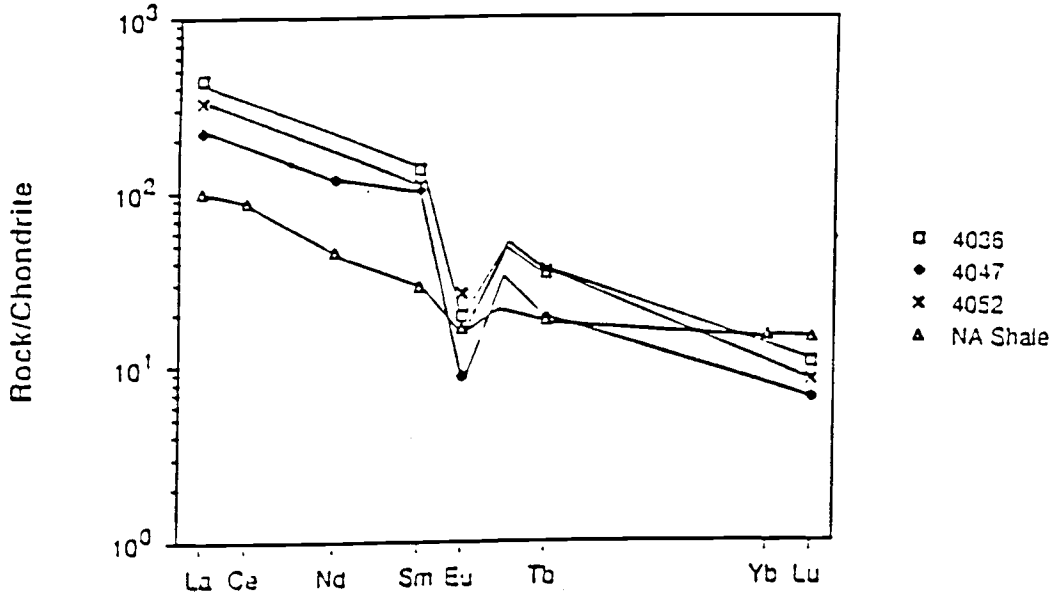

Figure 2.11. REE Diagram of Finely Laminated Shengus Gneiss. Samples normalized to C1 chondrites.

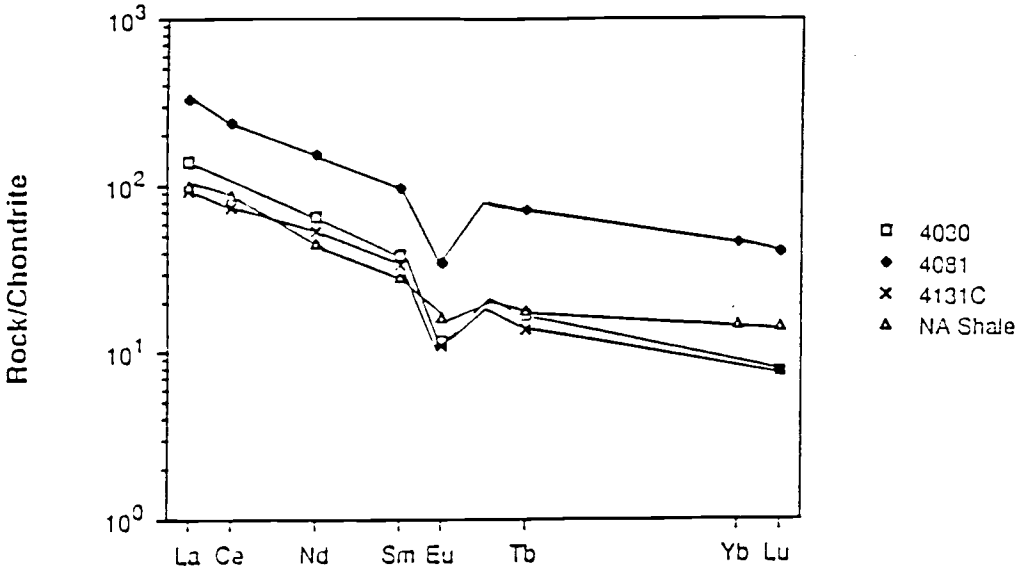

Figure 2.12. REE Diagram of Equigranular Gneisses.
Samples normalized to C1 chondrites.

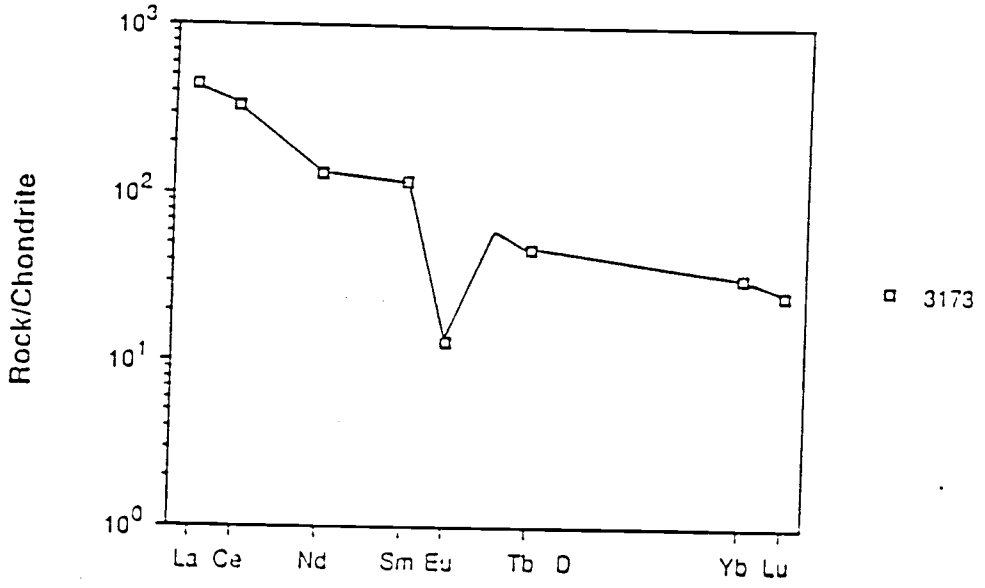

Figure 2.13. REE Diagram of Iskere Gneiss. Samples normalized to Cl chondrites.

2.14). Both patterns exhibit a fairly constant negative slope. Thorium is slightly enriched and the Sc is somewhat depleted. These data are not as conclusive as the data from the gneisses, but they suggest a continental affinity. The shape of the curve and total REE concentration is significantly different from those of island arc rocks of similar mineralogy. The field data are consistent with a continental source, for the amphibolite is within a package of continental material.

Mafic Dikes

Two late stage mafic dikes were analyzed to gain insight into the nature of their source (Fig. 2.15). The REE patterns show slight LREE enrichment with the (La/Lu)cn = 1.9 and 2.4. Both dikes have similar patterns, but the total REE concentration is slightly lower in the sample closest to the fault zone. These patterns are typical of rocks with island arc affinities.

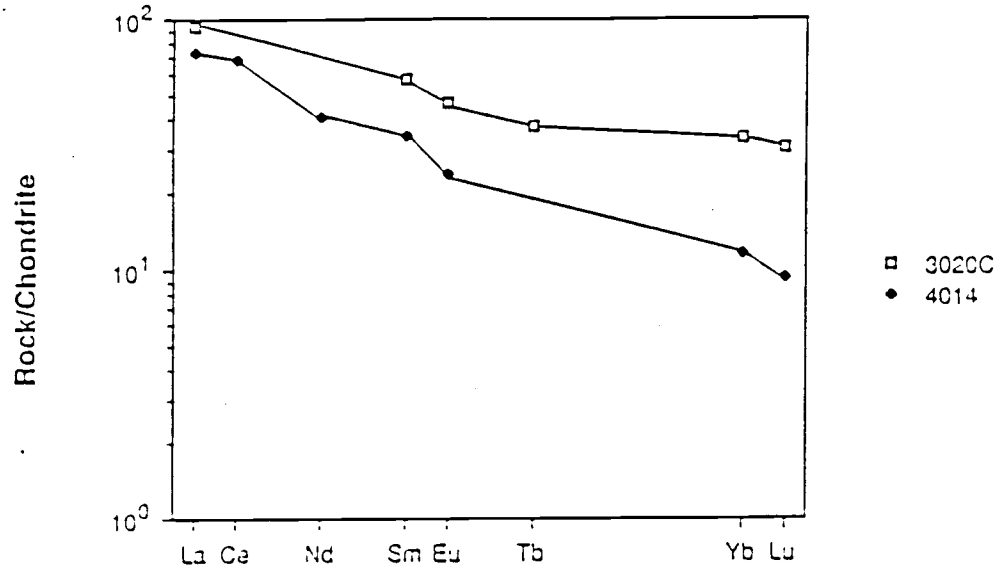

Figure 2.14. REE Diagram of Amphibolites. Samples normalized to Cl chondrites.

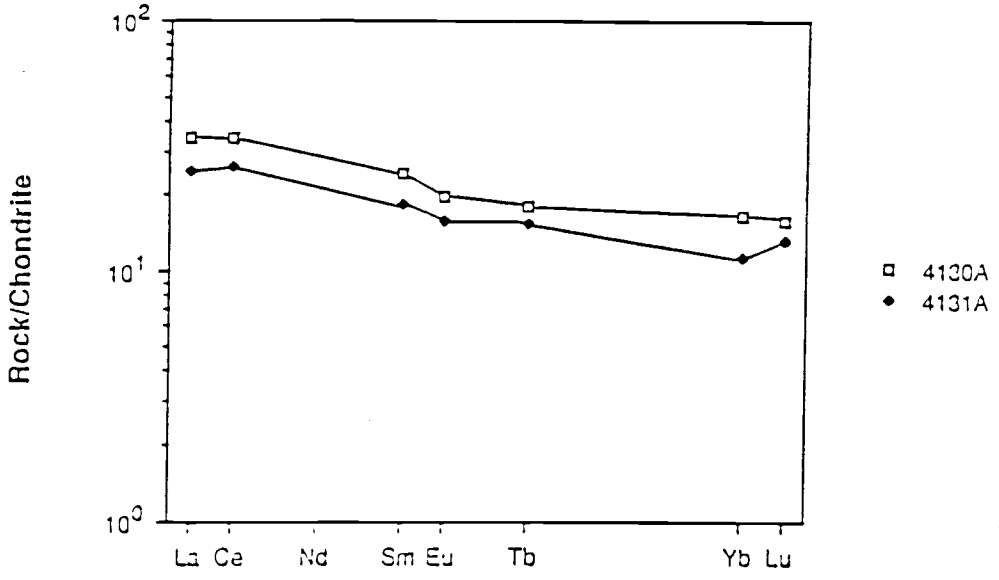

Figure 2.15. REE Diagram of Basaltic Dikes. Samples normalized to Cl chondrites.

Nanga Parbat Structure

As previuosly mentioned, the northeast-trending, north-plunging Bulache antiform dominates this part of the massif. This structure is asymmetric, with the western limb dipping 75-85°W and the eastern limb dipping 40-60°E. The antiform is a large structure with an exposed amplitude of 2 km. A detailed study of the foliation in the gneiss reveals an early deformational event exhibited by tight intrafolial folds. These folds are present at all scales, microscopic, mesoscopic, and even megascopic. In the adjacent study area, Madin (1986) documented a second deformational event, a north/south compressional event, that preceeded the east/west compressional event that formed the Bulache antiform. In this study area the second deformational event was recognized in the Shengus gneiss in Shengus and in the upper Stak Valley at the head of Toghla Canyon.

The Bulache antiform is bounded on the west side by the Baraluma fault (Fig. 2.16) and on the east side by the Stak fault zone (Fig. 2.17). The Baraluma fault is characterized by a gouge zone that is 50-70 m wide, hotspring activity, hydrothermal alteration, and a series of adjacent smaller faults. Due to the distinctive hydrothermal alteration, the fault can be traced in the field and on aerial photographs northeastward and south-westward.

To the west of the study area is a similar asymmetric antiform, the north-trending Iskere antiform. At Shengus the Baraluma fault separates the two. To the south along the Astor River the massif narrows and only one antiform is present (Wadia, 1933). It is conceivable that the Baraluma fault juxtaposed a part of the once

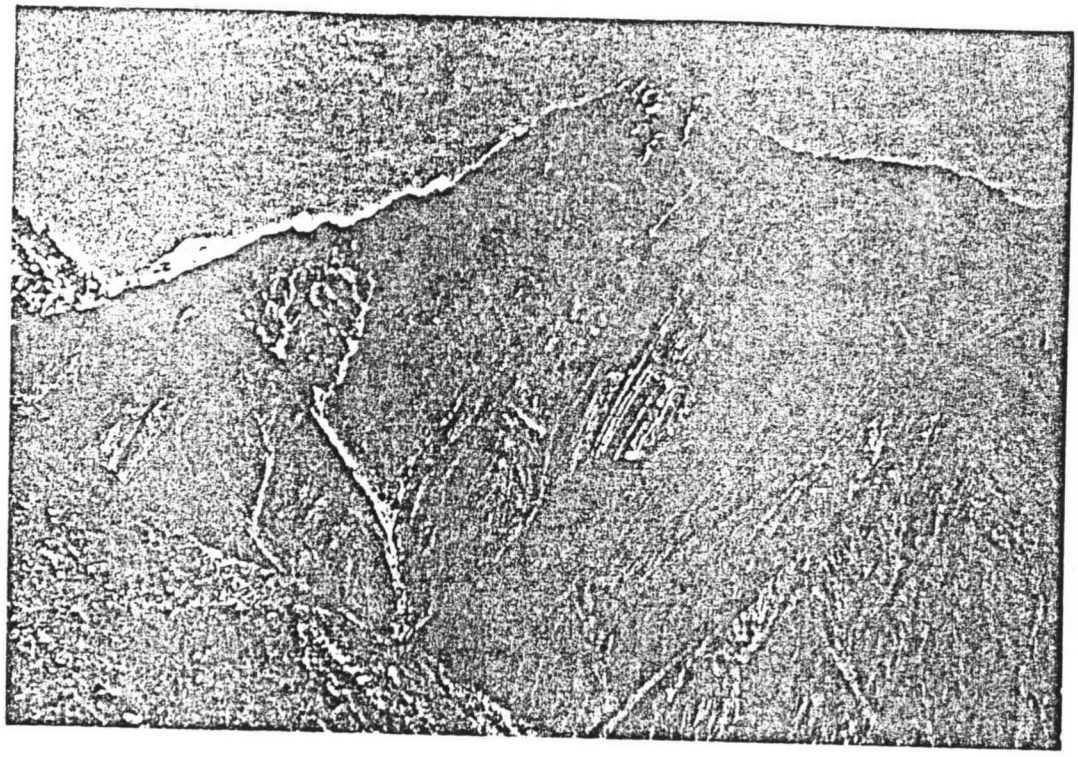

Figure 2.16. Photograph of West Limb of the Bulachi Antiform. View looking north from Shengus at the steep west limb of the Bulache antiform. Grey, hydrothermally altered, area on the left marks the trace of the Baraluma fault.

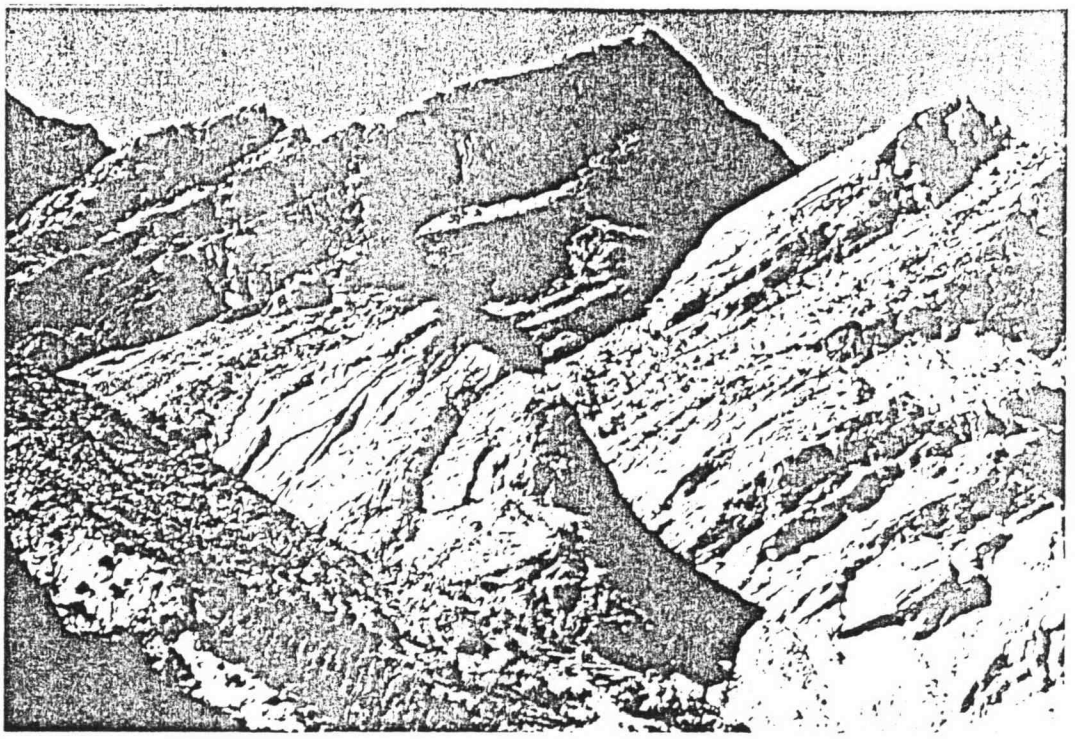

Figure 2.17. Photograph of the East Limb of the Bulache Antiform. View from Hilbu looking southwest at gentle east dipping limb of the Bulache antiform.

continuous antiform against another portion of the same antiform, creating two side-by-side structures in the northern part of the massif. The Bulache antiform has a northeast trend whereas the Iskere antiform trends north-south. This divergence in trends is apparently a result of approximately 30 degrees of rotation along the fault.

By using fission track data from apatites and zircons, Zeitler (1985) documents 5.2+-0.7 km of uplift within the past 2.0 My. The Baraluma fault and the Bulache antiform are the most recent structural features and may well have formed during the uplift.

The Shengus pegmatites appear to be late syn- to post-tectonic, for they are not cut by the major fault but are cut by some of the smaller ones. The pegmatites are displaced 10 to 20 m with the east side being upthrown.

Section Summary

Evidence from field, petrographic, and chemical data can be evaluated to draw some conclusions pertaining to the geologic history of the northeast section of the NPHM. Due to the complexity of the region, the evidence is not definitive but does shed light on the nature of the source rock and metamorphic and structural evolution of the massif.

The lithological, mineralogical, and chemical data of the fine-grained, finely laminated portion of the Shengus gneiss suggests a sedimentary protolith. The biotite-garnet gneiss is interlayered with calc-silicate gneisses, mica schists, and amphibolites. The abundance of aluminum rich minerals, kyanite, sillimanite, and muscovite, as well

as traces of graphite, are indicative of a sedimentary protolith. Chemically, the gneiss is rich in Al_2O_3 and depleted in CaO and Na_2O, suggesting weathering in the provenance of the gneiss.

The most likely candidate for the source of the Shengus gneiss is the high-grade metamorphic basement material of the Indian continental plate. Madin (1986) suggests that the gneiss represent Precambrian, possibly late Proterozoic basement material, not Tethyan or Indian cratonic sediments. This conclusion is based on the fact that the Shengus gneiss has experienced the same deformational history as the Iskere gneiss. A concordant U-Pb date of 1.8 +-0.2 Ga (R.Zartman, pers. comm., 1985) was obtained from zircon crystals in the Iskere gneiss.

The chemical data can be utilized to constrain the provenance of the protolith. The REE pattern for the Shengus gneiss is extremely LREE enriched and has a large negative Eu anomaly. This pattern is typical of continental granitic rocks that formed by fractional crystallization. The negative Eu anomaly is consistent with plagioclase fractionation. The similarity to continental granites suggests that the sediment was deposited near the plutonic source area.

Along with the finely laminated gneiss, the Shengus gneiss contains medium- to coarse-grained equigranular gneissic portions. Lithologic and mineralogic evidence suggests an igneous protolith, for the gneiss appears to intrude the sedimentary package. The chemical data is inconclusive, for the gneiss has a wide range in composition. On the ACF diagram the samples cluster with the finely laminated gneisses.

The metamorphic and deformational history of the gneiss is

extremely complex. The mineralogy may be derived wholly from the Himalayan orogenic event, or it may represent a partial overprinting on a previous event. The curious exsolution texture in the plagioclases suggests that the gneiss underwent a long period of slow cooling.

A change in metamorphic grade within the Shengus gneiss from the sillimanite to kyanite zone occurs within the Bulache antiform. Due to the nature of the terrain, the location and nature of the transition could not be defined. If the change in zone is sharp, it is probably the result of a major structure.

In the structural analysis of Madin (1986) on the northern section of the NPHM he describes the three deformational events and assigns tectonic events to each phase of deformation. The earliest and most fundamental structure is the folding of the original (?) layering creating tight, isoclinal, intrafolial folds in the gneiss. Madin relates this structure with a pre-Himalayan event, likely Proterozoic or early Paleozoic in age. The second deformational event is responsible for the set of folds with east/west oriented fold axis. This deformational event is likely related to the obduction of the Kohistan-Ladakh arc onto the northern margin of the Indian plate. The third and most recent event is the formation of the upright, asymmetric antiforms, the Bulache and Iskere antiforms. Late Cenozoic uplift is responsible for these structures (Madin, 1986).

By using fission track data from apatites and zircons, Zeitler (1985) documents 5.2+-0.7 km of uplift within the past 2.0 My. The Baraluma fault and the Bulache antiform are the most recent structural features and may well have formed in response to the uplift. The Baraluma fault strikes north/northeast from Shengus towards the upper

Stak Valley linking the syn- to post-tectonic pegmatite swarms. It may have provided a channel allowing the ascent of the magmatic fluids.

LADAKH TERRANE

To the east of the NPHM lies the Ladakh arc terrane, and it extends eastward through Ladakh into southern Tibet. The Ladakh terrane has been the subject of several comprehensive geologic studies (Honeggar et al, 1982 and Srimal, 1986) and a detailed evaluation of the western section of the Ladakh terrane is beyond the scope of the project. However, in order to characterize the boundary between the NPHM and the Ladakh arc terrane, the general lithology and chemistry of the western Ladakh rocks near NPHM must be characterized. To this end, reconnaissance mapping and sampling of the major lithologic units was completed.

The two primary objectives of this part of the study are 1) to verify that the terrane east of the fault zone is truly a remnant section of an oceanic island arc and 2) to determine whether and how lithologies and metamorphic grade of the arc terrane change as the boundary with the NPHM is approached. Blocks of various lithologies are found within the boundary zone and knowledge of the Ladakh terrane rocks will help to unravel the geometry, and ultimately the geologic history, of the fault zone. Two other objectives of a more regional tectonic nature are to compare the lithologies of the western Ladakh arc and the eastern Kohistan arc and to see if there is any evidence for continental crust underlying the Ladakh terrane. By comparing the lithologies adjacent to the massif, I hoped to understand better whether the massif separates two related terranes or whether the Ladakh and Kohistan terranes are different.

The work was conducted along the Skardu road from Talu near NPHM eastward to Dasu, a village at the mouth of the Tormik River (Plate

A2). Because the Indus Valley is much broader east of the massif, reconnaissance mapping is difficult, but the maps amd lithologic descriptions of Zanettin (1964) proved to be accurate and useful. The eastern boundary of the study area is the mouth of the Tormik River. This limit was selected to avoid suspected structural complexities north of the Tormik, where Zanettin (1964) mapped a major change in lithology from amphibolite to limestone. Parallel to this lithologic change additional evidence for this structural complexity includes serpentinite and talc actinolite schist near the town of Dasu.

Major units were sampled for geochemical and petrographic analysis. Wherever possible, the contact relationships were evaluated, but many contacts are covered at lower elevations by surficial deposits.

This section of the paper will consist of a detailed description of the lithologic and chemical character of the major units, a comparison with units adjacent to the west side of the massif, and a conclusion.

Lithology Section

The western part of the Ladakh arc consists dominantly of intermediate plutons, which have been metamorphosed to varying degrees. The plutons intrude well-foliated, plagioclase-rich amphibolite intercalated with subordinate schists and marble. No volcanic rocks were observed; this is consistent with the work of Zanettin (1964).

The units will be discussed in the same order in the lithology section and in the chemistry section. The order is based on the chemistry, the most primitive unit to the most evolved. The chemical

evolution is likely to reflect the geochronologic variation. The discussion starts with the amphibolitic country rock, the Talu amphibolite, followed by the Twar tonalite, Shuat diorite, Dasu tonalite porphyry, and finally the felsic dikes (Plate A2). Table 3.1 is a tabulation of the mineralogy of the western Ladakh samples.

Talu Amphibolite

The oldest exposed rock in the western Ladakh terrane is a fine- to medium-grained amphibolite, referred to as the Talu amphibolite. The mineralogy and chemistry are variable. Two samples were studied in detail. Both samples have a well developed foliation defined by euhedral hornblende crystals. Near Dasu, alternating plagioclase- and hornblende-rich layers give the rock a distinctive color banding. Under the microscope the hornblende appears to be in equilibrium, and the albite twins in the plagioclase are poorly developed. Subordinant sphene, scapolite, and epidote are present. The foliation is oriented north/south and dips 45° to the south.

Adjacent to the Stak fault zone another sample of the Talu amphibolite (4126) was collected. Fine- to medium-grained hornblende defines the foliation which trends N70E 70N. Hornblende makes up 80% of the unit with 13% labradorite and the remaining minerals being quartz, epidote, and pyroxene. The labradorite composition of the plagioclase was derived from poorly defined albite twins. The hornblende is euhedral, appearing to be in equilibrium. The biotites are subparallel to the foliation, thus a late stage mineral. Numerous aplitic and calcareous veinlets are concordant to the foliation. The aplites

Table 3.1

Modal Mineralogy of Ladakh Samples.

	Talu Amphibolite		Shuat Gabbro			Twar Tonalite	Dasu Porphyry	Felsic Dike
Mineral	5018B	4126	5007A	5008	4125	5018A	5017	5007B
Plagioclase	43	15	75	50	60	65	65	30
K Feldspar						5		25
Quartz		t	2		5	10	7	35
Clinopyroxene			10		t		t	
Orthopyroxene		1						
Hornblende	50	80	5	35	20	3	5	
Epidote	4	1	3	3	3	5	2	
Biotite		3	5	12	12	12	14	3
Muscovite							5	2
Almandine								
Scapolite	1							
Calcite						t	t	
Sphene	2	t				t	t	
Zircon								
Apatite								
Opaques			t		t			
Allanite							t	

consist of quartz, potassium feldspar, and plagioclase +- biotite and muscovite. The carbonates consist of calcite.

The Talu amphibolite is similar to the hornblende gneiss described by Zanettin (1964). In his description, he stresses the schistose nature of the gneiss. He also notes the occurrence of calcareous rocks: marbles, calciphyres, and calc hornfels, "interbedded with the amphibole epidote gneiss". Although the western part of Ladakh is dominated by intrusive rocks, it is likely that the amphibolite was a major lithology of the preintrusive metamorphic terrane.

Twar Tonalite

Near the village of Twar, an equigranular tonalite, informally called the Twar Tonalite, crosscuts the foliation of Talu amphibolite. Inclusions of amphibolite are present in the tonalite and have various orientations. The fabric of the tonalite is poorly developed and defined by hornblende and biotite.

Under the microscope, the tonalite consists of oligoclase and subequal amounts of quartz, potassium feldspar, hornblende, biotite, and epidote. Interlocking grains of hornblende, biotite, and epidote define a weak fabric. Sphene and calcite are present as trace phases. Igneous textures, such as well defined grain boundaries between quartz, potassium feldspar, and plagioclase, are easily recognized. The oligoclase exhibits well developed albite twins, some of which are kinked.

Shuat Diorite Complex

An intrusive complex comprised of diorite and gabbro lies to the west of the Twar tonalite. These rocks, informally called the Shuat Complex, are in unknown contact relationship with the Twar tonalite.

Just to the west of the Shuat bridge, sample 5007A was collected. The gabbro has been intruded by felsic dikes (5007B). The dominant mineral of 5007A, roughly 40%, is labradorite (An_{50}-An_{55}) with well developed albite twins. The mafic minerals: hornblende, clinopyroxene, and biotite, make up 50% of the rock. The remaining 5% is primarily quartz with some pyrite.

A slight fabric can be recognized in both the field and in thin section. This fabric is less pronounced than that in the tonalite. Igneous textures are readily apparent. An example is the overgrowth of hornblende on the clinopyroxene.

A diorite, 4125 and 5008, crops out along the Indus River at Talu. A fabric is developed, with the foliation oriented N70E 70N. Interlocking grains of biotite and hornblende define the foliation. Although the plagioclase, An_{45}-An_{50} has been altered, albite twins are still apparent.

Dasu Tonalite Porphyry

A porphyritic pluton is exposed to the west of the mouth of the Tormik River near the village of Dasu. The unit can be traced westward along the Indus for approximately 3 km. The most striking feature of the porphyry is large, zoned, unoriented, euhedral

plagioclase crystals up to 2 cm long. Plagioclase accounts for fifty percent of the rock with subordinate quartz and potassium feldspar. In thin section, alteration of plagioclase to epidote and muscovite is evident. The quartz occurs as well defined grains and as small aggregates. Primary magmatic biotite, hornblende, clinopyroxene, sphene, and epidote are present in varying quantities. The epidote is euhedral and in places has recognizable allanite cores. The rock is slightly altered with secondary epidote, muscovite, and calcite.

Zanettin (1964) mapped this unit as plagioclase gneiss, because he believed the plagioclase phenocrysts to be augen. Based on petrographic analysis, the plagioclase is zoned and undeformed, quite dissimilar to the augen within the massif. This rock is massive, not foliated. In his field descriptions, Zanettin recognized porphyritic plagioclase dikes intruded into the surrounding amphibolite and the presence of amphibolitic inclusions in the porphyry. He also noted the existence of a fabric in the more mafic sections of the porphyry near the contacts. The outline of the porphyry on his geologic map gives the appearance of an intrusion into the amphibolite/hornblende schist. Although the contact between the porphyry and the amphibolite was not examined in this study, no evidence for metamorphism or deformation was observed in thin section or at the outcrop and it is likely that the marginal foliation formed during emplacement from flow of the magma. It is doubtful that the porphyry was emplaced prior to deformation of the amphibolite.

Felsic Dikes

Adjacent to the fault zone are three sets of felsic dikes. Near Talu the dikes account for about 15% of the exposed rock. This continues eastward for approximately 3 km. The dikes occur from the level of the river, 2000 m, to the tops of the ridges, 4000 m. The dikes are generally 1-2 m wide but are up to 20 m wide. The oldest set of muscovite-, biotite-bearing, medium-grained dikes is folded along with the Talu amphibolite. Two younger sets of dikes, a set of hornblende-bearing pegmatites and a set of biotite, muscovite aplites, crosscut the fabric of the country rock. The extent of intrusion of dikes progressively decreases eastward from the fault zone.

Geochemistry

A suite of seven samples from the Ladakh arc terrane were collected for chemical analysis. The suite was collected along the Indus gorge from Talu to Dasu. The data (Table 3.2) are compared with data of other workers in Kashmir and Ladakh and with that from arc related lithologies within the fault zone. The data show a complex history ranging from primitive mantle derived material to evolved continental material.

Sample no.	5007A	5007B	5008	5017	5018B	4125	4126	Percent Uncertainity
SiO2 %	51.6	73.1	56.0	65.7	50.1	57.9	54.2	1-3
TiO2	0.87	0.18	0.62	0.40	0.83	0.77	0.57	1-3
Al2O3	18.4	13.3	16.5	15.3	15.2	16.8	15.7	1-3
Fe2O3	3.42	1.02	2.64	1.57	3.05	2.14	2.58	1-3
FeO	6.02	0.94	5.52	2.39	6.80	4.71	5.64	1-3
MnO	0.18	0.02	0.16	0.07	0.19	0.13	0.15	1-3
MgO	4.85	0.42	5.31	3.03	8.82	4.23	6.93	1-3
CaO	9.27	1.01	7.21	5.06	10.40	7.18	9.00	1-3
Na2O	3.46	2.50	3.26	3.77	3.52	3.39	3.19	1-3
K2O	1.22	6.38	1.87	1.59	0.33	1.55	1.05	1-3
P2O5	0.31	0.07	0.19	0.15	0.07	0.25	0.14	1-3
H2O-	0.01	0.03	0.04	0.02	0.02	0.04	0.03	1-3
H2O+	0.93	0.43	1.16	0.86	1.46	0.96	1.57	1-3
Sc PPM	20	1.2	33	11.9	17	69	35	1-2
Cr	30	1.0	-	-	-	90	240	2-4
Co	30	2.2	25	14	44	32	40	2-3
Ni	40	10	-	-	100	40	-	10-20
Rb	27	140	42	12	8.0	51	20	10-30
Sr	840	420	300	580	290			10-30
Cs	0.86	0.74	1	1.2	0.2	1.6		10-30
Ba	530	980	240	230		240	130	5-10
La	16.0	180	7.7	8.4	2.4	14.3	6.3	1-3
Ce	29	280	15	18	6.3	31	14	5
Nd	15	66	-	-	-	18	6.5	10-30
Sm	3.44	7.59	3.09	1.71	2.34	3.47	2.35	1
Eu	1.30	1.36	0.94	0.62	0.66	1.00	0.79	1-3
Tb	0.53	0.40	0.48	0.21	0.47	0.55	0.60	5-10
Yb	1.3	0.84	2.1	0.68	2.1	2.1	1.8	5-10
Lu	0.20	0.10	0.18	0.07	0.33	0.32	0.33	5-10
Zr	60	200	50	60	80	-	-	30
Hf	0.9	4.6	1.9	0.1	1.2	2.3	1.3	5-10
Ta	0.20	0.68	0.07	0.21	0.19	1.4	0.7	5-15
Th	1.8	32	1.1	3.1	0.1	3.7	0.98	5-15

Table 3.2. Chemistry of Ladakh Samples.
Note: Percent uncertainty derived from statistical error and reproducibility of data.

Major Element Data

Talu Amphibolite

Two samples of the Talu amphibolite, 5018B and 4126 were analyzed. Sample 5018B has lower SiO_2 and FeO* concentrations. Chemically, the amphibolite is similar to low potassium basalt (Gill, 1981). Plotted on FeO*/MgO vs. SiO_2 and FeO*/MgO vs. FeO* diagrams, the sample lies within the tholeiitic field (Fig. 3.1). Tholeiitic basalts can be formed at mid-ocean ridges (MORB) and at oceanic islands (OIT) or continental volcanic arcs. Green (1980) uses TiO_2 content greater than 1.2% as an indicator of MORB. Sample 5018B contains 0.83% TiO_2 thus fits in an oceanic island arc setting.

In contrast to 5018B, 4126 is a calc-alkaline, basaltic andesite. When plotted on FeO*/MgO vs. SiO_2 and FeO*/MgO vs FeO* diagrams (Fig. 3.1), the sample lies well within the calc-alkaline field. TiO_2 and MgO are lower, while K_2O is higher than in 5018B.

Shuat Diorite Complex

Three samples of Shuat complex, 5007A, 5008, and 4125, were collected. Sample 5007A plots within the tholeiitic field on both FeO*/MgO vs. SiO_2 and FeO*/MgO vs.FeO* diagrams; 5008 and 4125 plot within the calc-alkaline field (Fig. 3.1). All three samples cluster together on the ACF diagram (Fig. 3.2). Overall, the chemistry of calc-alkaline suites of volcanic and plutonic rocks from oceanic island arcs and continental margin arcs is similar. Small consistent

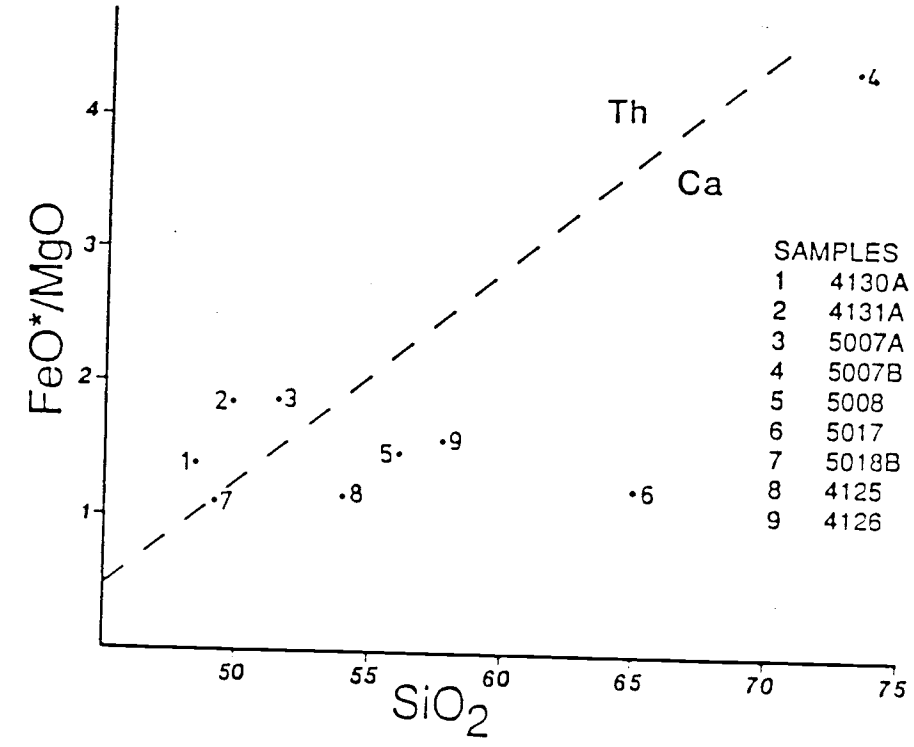

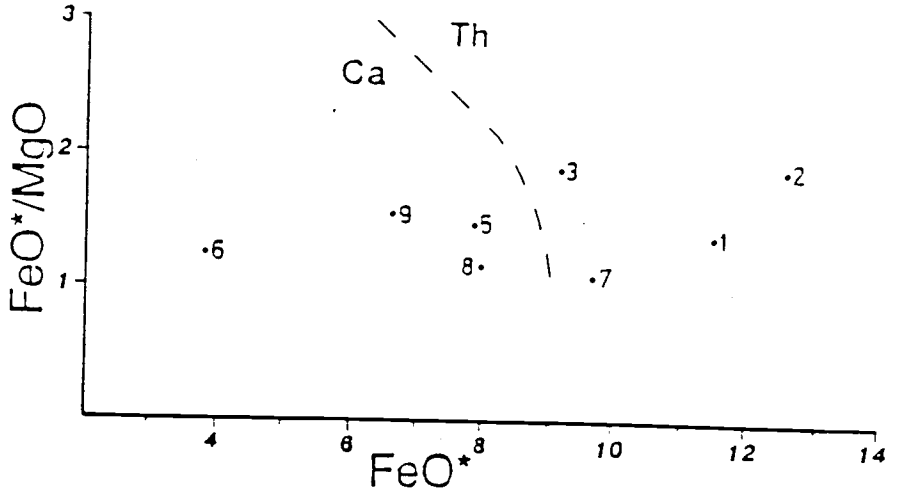

Figure 3.1. Feo* vs. SiO_2 and FeO*/MgO vs. FeO* for the Basaltic Dikes and Ladakh Lithologies. Tholeiitic and calc-alkaline discrimination line from Miyashiro (1974).

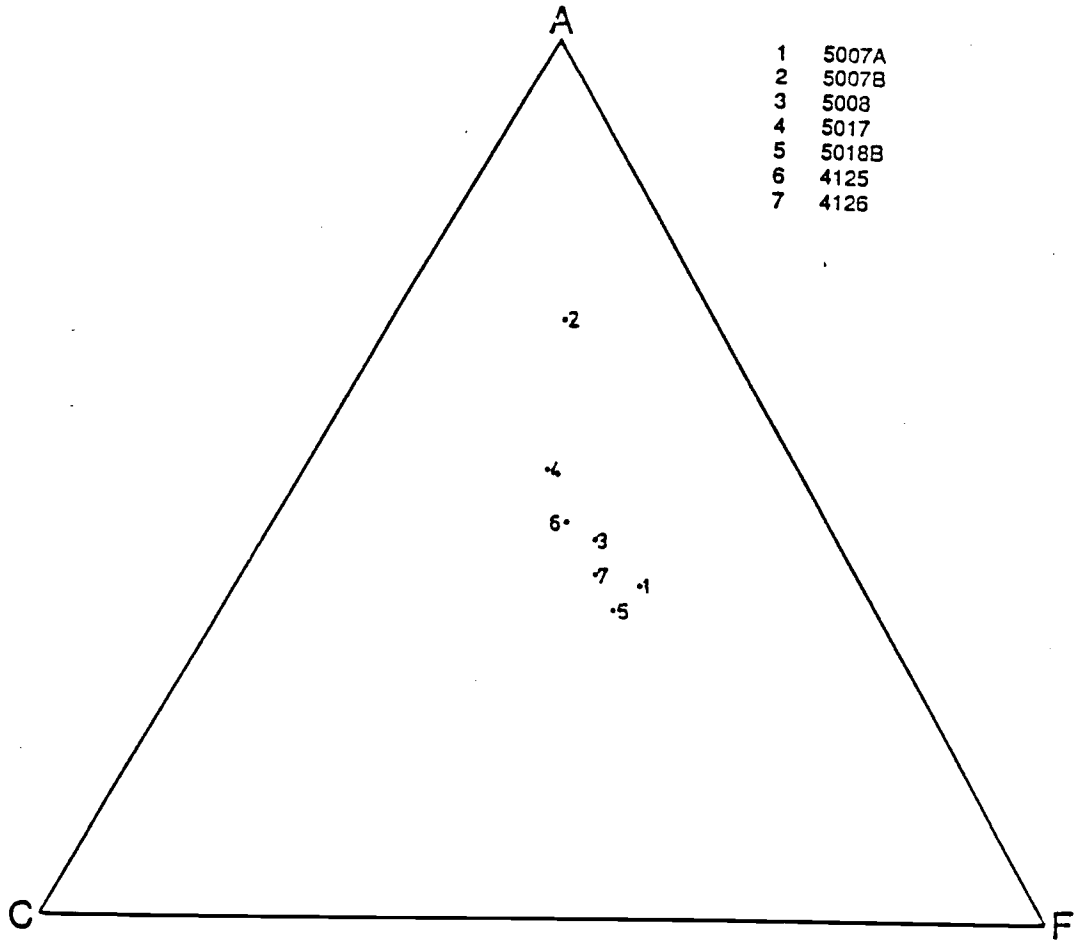

Figure 3.2. ACF Diagram of Ladakh Units.

differences are apparent, for example K_2O, TiO_2, and P_2O_5 (Ewart, 1976). These oxides tend to have lower concentrations in oceanic island arc basalts and basaltic andesites compared to continental margin ones. The total iron as FeO to MgO ratio is generally greater than two in continental margin calc-alkaline suites and less than two in oceanic island arc suites (Jakes and White, 1972). These generalities are useful for large suites of rocks and can be misleading when comparing a few samples.

The TiO_2 and K_2O concentrations in all three samples is within the range of oceanic arcs, while the P_2O_5 concentration lies within both ranges. The $FeO+Fe_2O_3/MgO$ is near or below two.

Dasu Tonalite Porphyry

The Dasu tonalite porphyry, 5017, is texturally, mineralogically, and chemically distinct. The silica value of the plagioclase-rich tonalite is the highest of the suite, except for the late stage dike. The sample plots well within the calc-alkaline field. The tonalite is depleted in FeO, MgO, and MnO relative to the rest of the suite.

Felsic Dikes

Sample number 5007B is a granitic dike that cuts the fabric of the Shuat complex. The sample is located 8 km east of the Stak fault zone. Chemically, the sample is unlike arc granites. Instead, the chemistry is similar to that of S-type granite (Chappel and White,

1974). In particular the ratio of the molecular portion of Al_2O_3/Na_2O+K_2O+CaO is 1.1, which is at the transition of the 1.1 lower limit of S-type granites. The low Na_2O concentration is also like that of an S-type granite with this K_2O value.

Trace Element Data

Trace element data on the same suite of rocks were obtained by INAA. The concentrations of the trace elements reflect the nature of the source region of the arc lithologies.

Talu Amphibolite

Although the two samples of the Talu amphibolite (5018B and 4126) have similar trace element concentrations, some distinctions are apparent. Sample 5018B is a tholeiitic basalt with an approximately flat REE pattern at 10X (Fig. 3.3). This pattern is consistent with a MORB or OIT.

Other sets of trace elements have been used to differentiate between these two enviroments. Large, low valence cations (e.g Cs, Rb, K, Ba, Pb, Sr); intermediate, high valence cations (e.g. Th, U, Zr, Hf); and ferromagnesium (e.g. Sc, Cr, Co, Ni) trace elements are the sets generally employed. The data on the large, high valence cations and the ferromagnesium trace elements are not conclusive, for the data overlap both environments. Large, low valence cations are generally less depleted in OIT relative to MORB (Basaltic Volcanism Study Project (BVSP), 1981). The K_2O, Rb, Sr, and Cs concentrations in 5018B are all

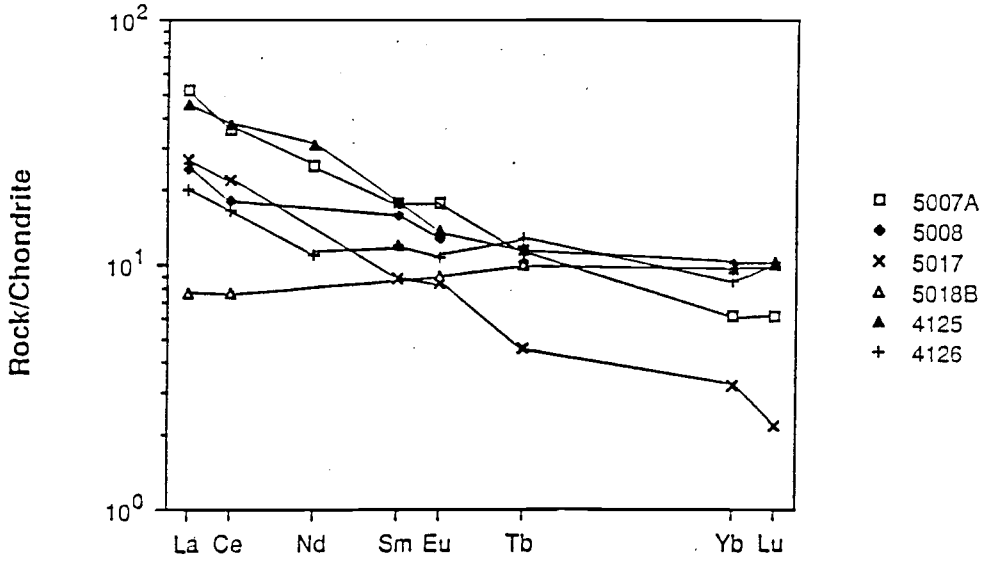

Figure 3.3. REE Diagram of Ladakh Units. Samples normalized to C1 chondrites.

in the range of OIT (Fig. 3.4).

The REE pattern of 4126 shows LREE enrichment relative to a flat HREE. The LREE enrichment, 20X, is consistent with an oceanic island arc enviroment (Ewart, 1976). The other trace elements are within the range of data for basaltic andesite from an oceanic arc.

Shuat Dorite

The three REE patterns of the Shuat complex (5007A, 5008, and 4125) exhibit LREE enrichment (25X-50X) and a relatively flat to slightly fractionated HREE pattern. These patterns are consistent with both oceanic arc and continental margin mafic complexes.

Other trace elements (Rb, Sr, Cs, and Ba) can be useful to help distinguish between oceanic and continental arc settings (Jakes and White, 1972). Continental crust is enriched in these elements, and if the magma interacts with continental crust, these elements would likely be enriched. Not all magmas in continental margins are contaminated with continental crust, the southern Andes is an example.

The two calc-alkaline samples (5008 and 4125) and the one tholeiitic sample (5007A) have K_2O, Rb, Cs, Ba, and Th values in the range of oceanic arc suites or continental margin suites that do not show continental crustal contamination (Deruelle, 1982, Frey et al, 1984, Dostal et al, 1977). The Sr concentration and HREE fractionation of sample 5007A is more consistent with a continental margin basaltic-andesite, than an oceanic arc one.

	Type I basalts	Ocean-Island tholeiites
K	1064 ppm	1600 — 8300 ppm
Rb	1.0 ppm	5 — 12 ppm
Ba	12.2 ppm	70 — 200 ppm
Sr	127 ppm	150 — 400 ppm
Cs	13 ppb	—
K/Rb	1046	≈ 400
K/Ba	109	25 — 40
Sr/Rb	127	20 — 70
$^{87}Sr/^{86}Sr$	0.7024 — 0.7030	0.7030 — 0.7050

Figure 3.4. Range of Trace Elements in MORB and OIT. Normal mid-ocean ridge basalts (Type 1) vs. oceanic island arc tholeiites (BVSP, 1981).

Dasu Tonalite Porphyry

The REE plot is distinctive and shows LREE enrichment as well as HREE depletion. A steep, fairly consistent, negative slope extends from Th to Sc. A slightly positive Eu anomaly may break this slope, but the resolution of the data is not great enough to tell if the anomaly is truly present. The (La/Lu)cn is 20. This pattern is different from those of the previously described samples.

Felsic Dikes

The REE pattern (Fig. 3.5) of 5007B shows extreme LREE enrichment and HREE depletion. The (La/Lu)cn is 161, and no Eu anomaly is present. This pattern is not consistent with that of a granite derived from fractional crystallization. All the incompatible elements measured (Rb, Sr, Ba, LREE, Zr, Hf, Ta, and Th) are highly enriched.

Geochemical Synopsis

The geochemistry of a suite of seven samples from the western edge of Ladakh has been evaluated. The chemical data interpreted within the framework of the field relationships and petrography show a complex geologic history. These data combined with other geologic data from Ladakh proper (Honnegar et al, 1982 and Srimal, 1986) and Kohistan (Peterson and Windley, 1985), reveal distinct chemical and metamorphic variations with time.

In this study the chemically most primitive rock sampled is 5018B,

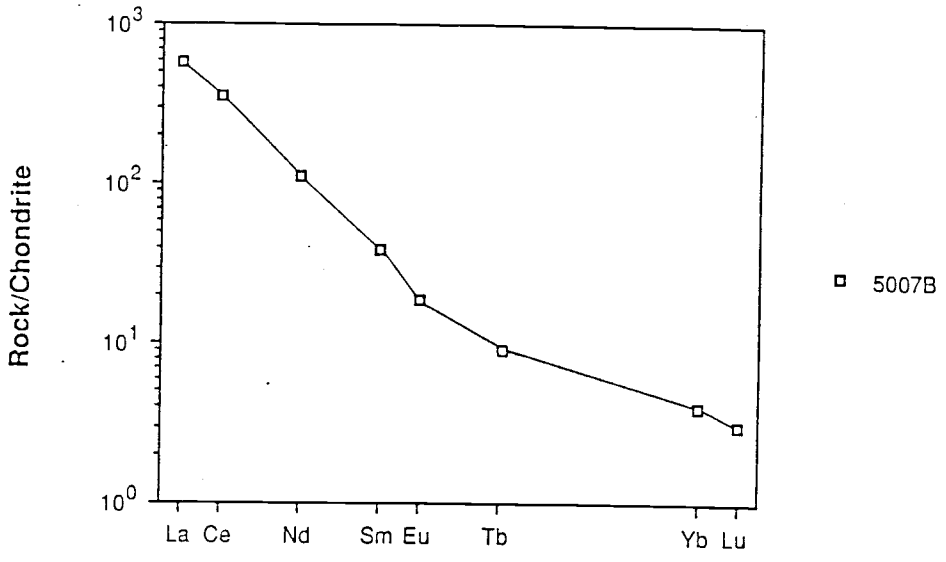

Figure 3.5. REE Diagram of Late Stage Granitic Dikes. Samples normalized to C1 chondrites.

an epidote, plagioclase amphibolite. Because it occurs as inclusions in the tonalite and is the host rock for the tonalite and Dasu porphyry, it is older than these units. Chemically, this sample is identical to low potassium ocean island tholeiite. Sample 4126 is also relatively primitive but is calc-alkaline. Overall, this unit is chemically correlative to the Dras volcanics of Ladakh and the Kamila amphibolite of Kohistan.

The Talu amphibolite likely represents the early stages of arc formation. Primitive tholeiitic basalts are formed in present day immature oceanic arcs (Miyashiro, 1974). Examples of these arcs are the Tonga-Kermadecs arcs, the New Britain arc, and the South Sandwich arc (Gill, 1981). The average chemical concentrations of the Kermadecs tholeiitic series are almost identical to those of sample 5018B.

The Shuat complex contains both tholeiitic and calc-alkaline bodies. The range in major and trace element data is consistent with an oceanic or continental setting. Isotopic analyses need to be employed to try to constrain the nature of the arc.

Unlike the mafic samples, the chemistry of the Dasu porphyry is not consistent with a simple crystal fractionation model of a calc-alkaline or tholeiitic magma. Multiple fractionation or fractionation with garnet in the source is needed to create such a REE pattern. To have garnet in the source the crustal thickness would be thicker than that measured at most island arcs. The porphyry has magmatic epidote which suggests that it initially crystallized at a moderate depth (Zen, 1984).

Late stage felsic dikes crosscut the foliation of the amphibolite, and metadiorite. A granitic dike sample that crosscuts the fabric of

the Shuat gabbro about 8 km east of the NPHM yields a REE pattern different from that of a granite end product of fractional crystallization in an island arc setting. Instead, it is more likely that the magma formed by partial melting of evolved continental material. Thus the source of the dikes is likely partially melted continental material, sediments or basement rocks, which according to most tectonic reconstructions (Reynolds et al, 1983; Klootwijk, 1985; and Madin, 1986) lies below the Ladakh arc.

Ladakh-Kohistan Comparison

Another objective of this study was to compare the lithologies on the east and west side of the massif. Wadia (1933) was the first to notice the similarities during his work along the Astor River. More recently, some geologists have concluded that Kohistan represents the older more mafic component, while Ladakh is the more siliceous section (Andrews-Speed and Brookfield, 1982).

The western part of the Ladakh terrane near the boundary with NPHM consists of metadorite as well as older amphibolite. The region has been intruded by numerous felsic dikes. As described earlier, at least three sets of dikes are present. Madin (1986) in a cooperative study has described the lithologies adjacent to the west side of the massif in the Kohistan region. He defined the Kohistan group as consisting of the Hanuchal amphibolite that has been intruded by the Shuta gabbro. The Hanuchal amphibolite is mineralogically and geochronologically contemporaneous to the amphibolitic host rock of western Ladakh. The Shuta gabbro is a series of slightly foliated gabbros, norites, and

diorites that are analogous to the Shuat series of western Ladakh. Finally, both units have been extensively intruded by at least two sets of felsic dikes.

Approaching the Raikot fault from the west, the most striking feature of the dark 3000 m high ridge is the felsic dike swarm. Forty kilometers to the east passing from the Stak fault zone into the Ladakh terrane, the same striking feature is present. Although the dikes were emplaced after the island arc rocks were juxtaposed against the continental rocks of the NPHM, the similarities between the arc rocks from opposite sides of the massif are striking. It would be unreasonable to hypothesize that the same structural and lithologic level of two chemically identical island arcs were juxtaposed against the NPHM at about the same time. Instead, it is more likely that the once continuous island arc which extended from Kohistan to Ladakh was severed by rocks of the NPHM by some structural mechanism similar to that discussed in later sections of this report.

Conclusions and Implications

Although this part of the project was done in reconnaissance fashion, some conclusions can be drawn by integrating the field, petrographic, and chemical data in light of previous studies. The field and petrographic data document three stages of magmatic development of the Ladakh terrane; an early stage of tholeiitic to calc-alkaline basaltic magmatism with subsequent regional metamorphism to epidote amphibolite facies, a middle stage of dominantly calc-alkaline magmatism and subsequent slight deformation without metamorphism, and

a post-deformational stage represented by felsic dikes. The chemical data document a progressive evolutionary sequence of arc development as well; early primitive tholeiitic series, intermediate calc-alkaline series, and a final stage of highly evolved dikes.

The transition from a tholeiitic to a calc-alkaline series has been observed in many arcs, mostly in oceanic island arcs but also in some continental arcs. Tholeiitic magmas are generated early in arc genesis, while calc-alkaline magmas mark the more mature stage. The tholeiitic and calc-alkaline series are believed to form by fractional crystallization of a primary basaltic magma derived by partial melting of mantle peridotite that has been fluxed by a component released from the underlying subducted oceanic slab (e.g., Grove and Kinzler, 1986). Fractional crystallization of tholeiitic magmas occurs at low pressures, while fractional crystallization of calc-alkaline magmas occurs at moderate pressures and higher water contents (Grove and Kinzler, 1986).

This transition is associated with the thickening of arc crust and a greater subduction angle. A slower rate of subduction and subduction of older oceanic crust have been correlated to an increase in calc-alkaline relative to tholeiitic volcanism (Miyashiro, 1974; Verplanck, 1985). The systematics involved with the change in magmatism is poorly understood. The transition is not instantaneous but is gradational and can last for millions of years.

In this study the transition from tholeiitic to calc-alkaline magmatism appears to roughly coincide with amphibolite facies metamorphism. The most likely event associated with the amphibolite facies metamorphism is the accretion/obduction of the arc onto a continental

mass. The thickening of the arc's crust may not be from the maturing of an island arc, but may be from the accretion or obduction onto a continental block.

At least two stages of magmatism are documented in Kohistan and in Kashmir. Peterson and Windley (1985) document two stages of growth of the Kohistan group near Gilgit. The first stage has experienced a regional metamorphic event and the second stage intrudes the metamorphosed arc sequence. Finally, a set of late stage aplitic and pegmatitic dikes intrude both stages. Their data show that the early stage of magmatism is in an oceanic island arc environment and the second stage represents Andean-type continental margin setting. The age of deformation is pre 75 My, and the extent of deformation increases northward, thus they believe that the island arc collided with the Asian plate around 75-80 My. This is consistent with Klootwijk et al's (1985) paleomagnetic evidence showing that the Ladakh group did not collide with Indian plate till 55 My.

The studies in the Ladakh region of Kashmir document the transition from tholeiitic to calc-alkaline magmatism, but curiously, no major metamorphic event has been reported until now. Honneggar et al (1982) show that the magmatic transition occurs within the Dras volcanics. Rai and Pande (1982) describe the same compositional transition in the Kargil intrusives.

Finally, the third stage, intrusion of felsic dikes, is spatially associated with the Stak fault zone, for the abundance of dikes decreases away from the zone. The dikes appear to be partial melts of an evolved material. The most likely candidate is the water-rich, continental sediments that were sandwiched between the obducted arc and

the underlying continental mass. An anomalously high geotherm would be created by the obduction of the arc and could cause the partial melting of the water-rich sediments at relatively shallow depths, 10-12 km. The fault zone would provide a channel for the ascent of the melts.

THE STAK FAULT ZONE

The transition zone between Ladakh and Nanga Parbat has been thought to be the northern continuation of the Main Mantle thrust (Tahirkheli, 1979). Tectonic maps of northern Pakistan show a variety of orientations and locations of the transition zone (Desio, 1964; Tahirkheli, 1979; and Andrews-Speed and Brookfield, 1982). In reality a careful study of the exact location and nature of the boundary had not been completed until this study. The previous confusion exists because of the nature of the boundary and the lithologies on either side of it and because the area has been inaccessible until recently.

The Nanga Parbat massif and the Ladakh arc terrane are separated by a 3-5 km wide fault zone, the Stak fault zone. Two photograghs (Fig. 4.1) show the Indus river exposing a cross section of the fault zone. The fault zone intersects the Indus gorge at the mouth of Stak valley (Fig. 4.3). Within this zone are four major faults and numerous minor faults, which have been mapped along the Indus River. The major faults separate large elongate blocks of varying lithologies.

The rocks of the easternmost section of the massif are not typical Nanga Parbat gneiss as described above; instead they are high grade continental, micaceous gneiss that have been extensively hydrothermally altered and have been intruded by large mafic and felsic dikes. This is best exhibited to the east of Chutran (Plate A2) where the augen-rich, finely laminated, biotite gneiss of the massif grades to a more schistose gneiss. Mafic and felsic dikes have intruded the gneiss. Approaching the fault zone, the schistose gneiss becomes highly fragmented due to brittle deformation and extensive hydrothermal

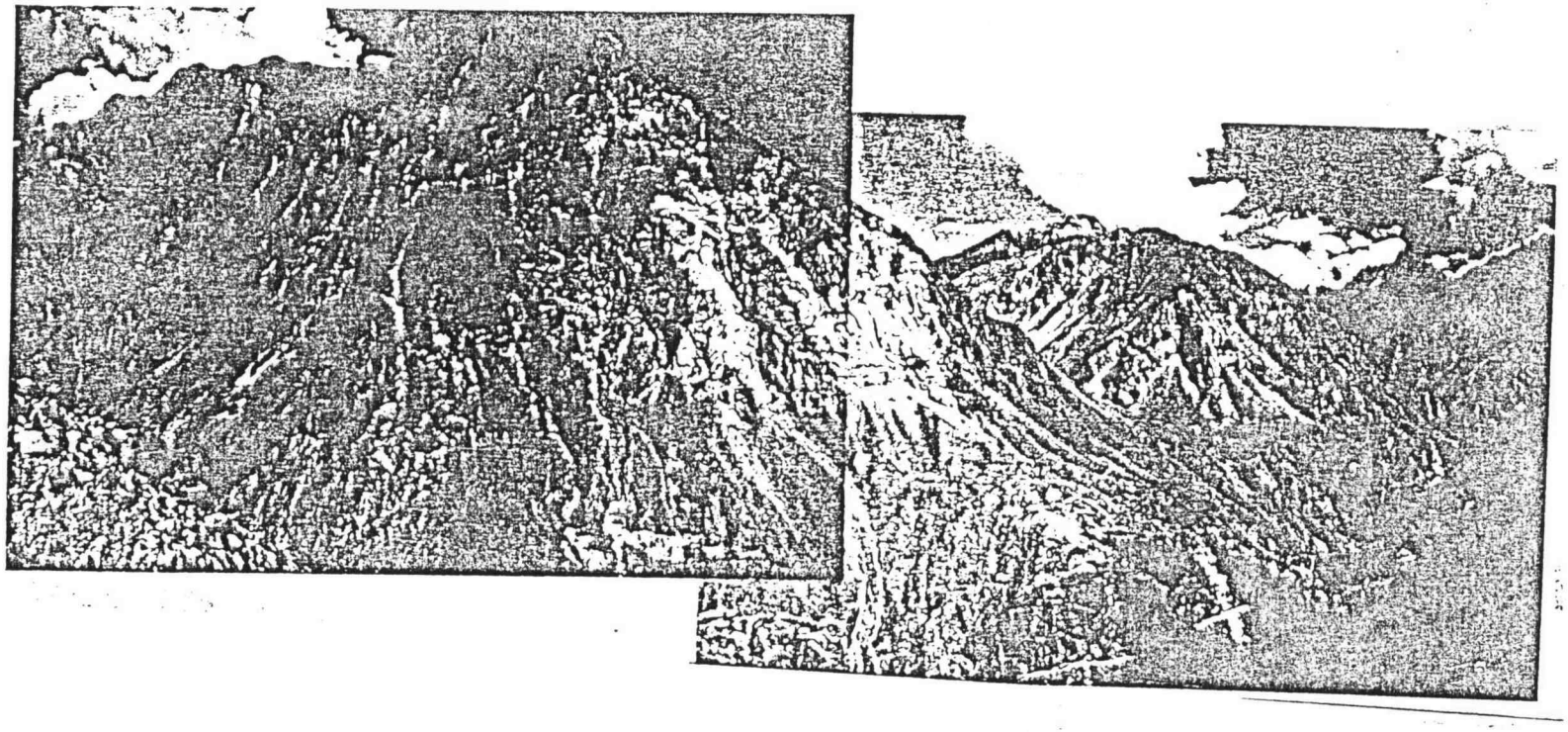

Figure 4.1. Photograph of Stak Fault Zone. View looking east-northeast across Stak fault zone. Relief exposed on ridge on the left side is approximately 2500 m.

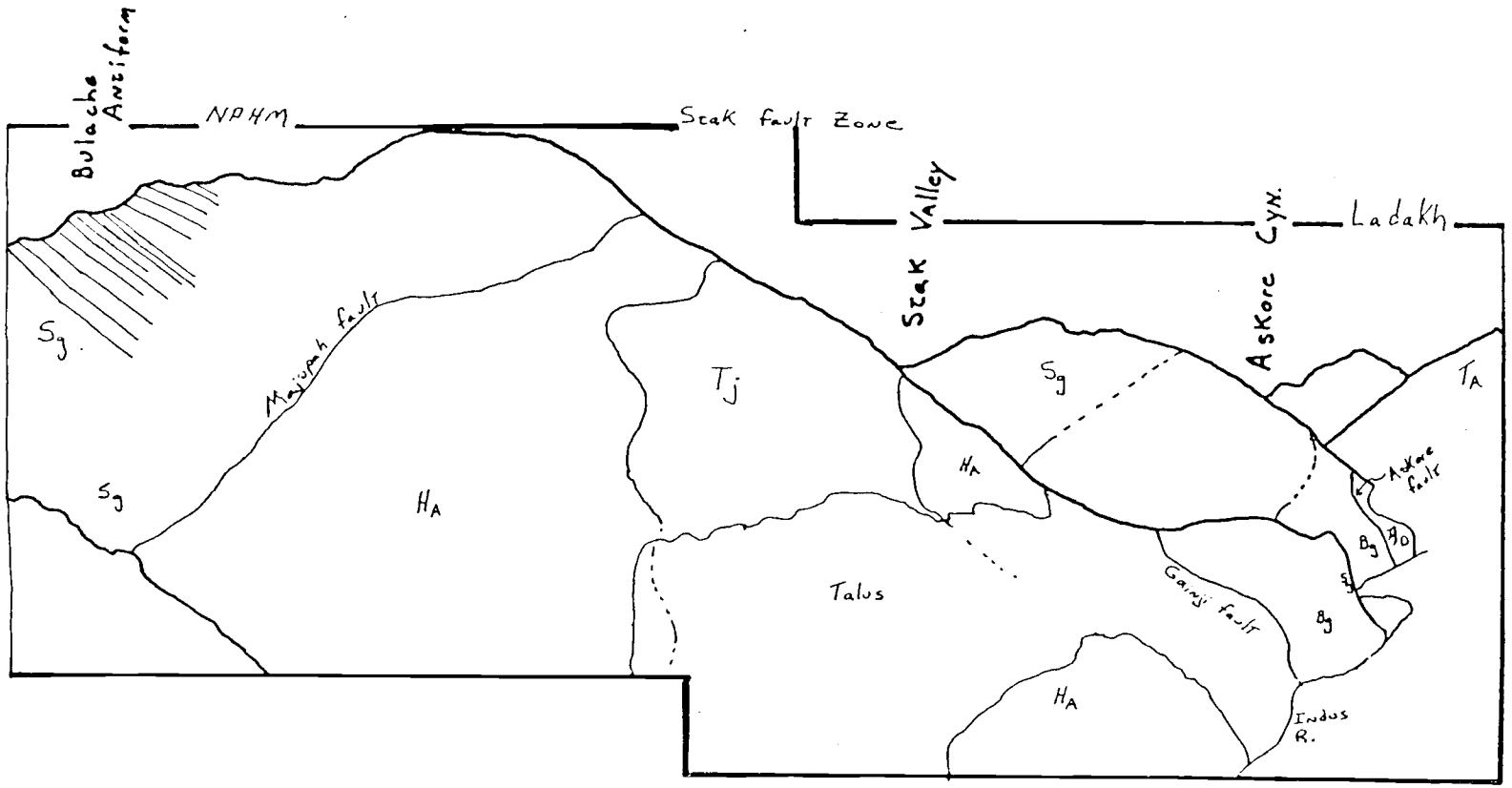

Figure 4.2 Sketch of Units within Figure 4.2.

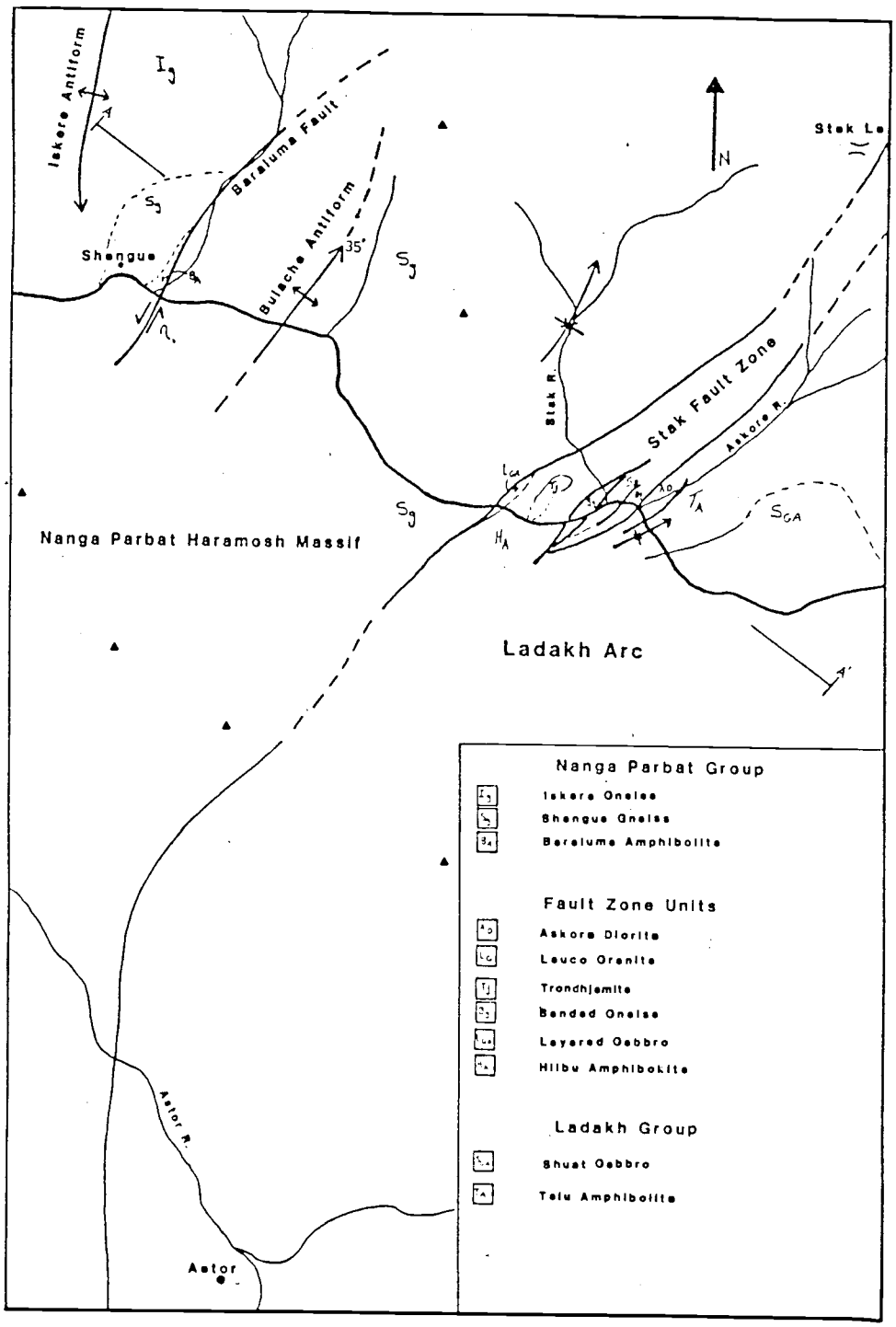

Figure 4.3. Generalized Geologic Map.

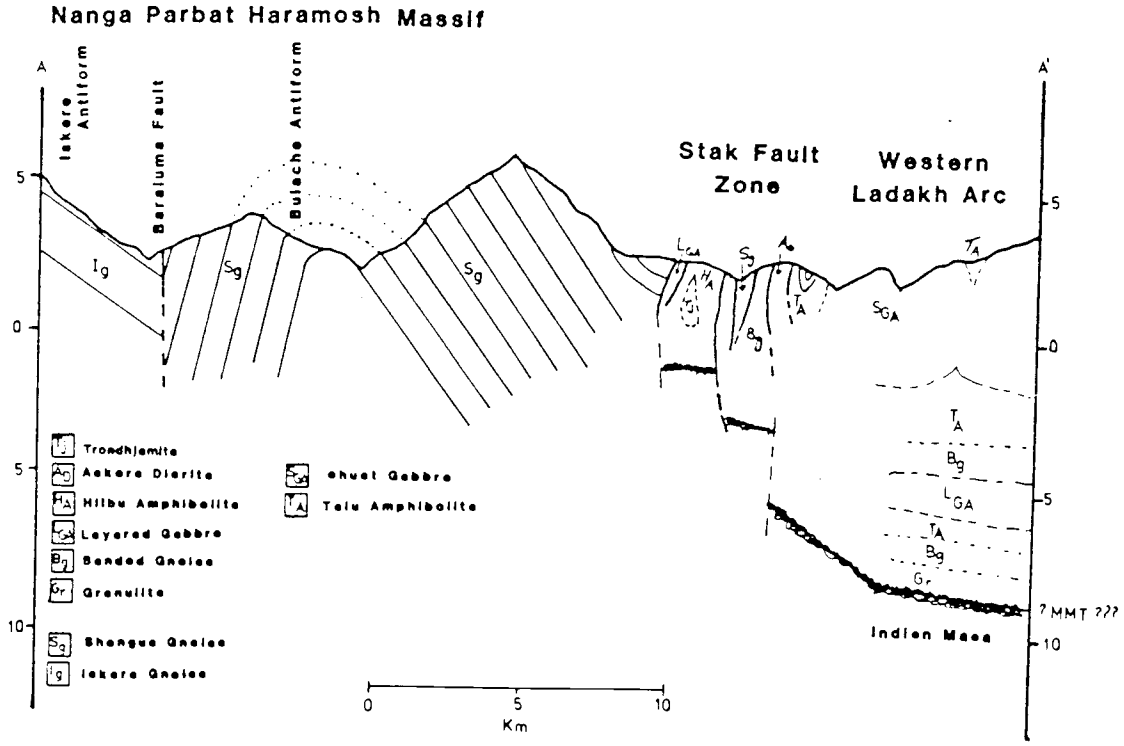

Figure 4.4 Generalized Cross Section.

activity.

The nature of the fault zone adds to the difficulty in delineating a boundary between the massif and the arc, for no one fault can mark the transition from continental to arc material. Along strike, the zone varies in width and lithology. Within the fault zone is a mixture of blocks of Nanga Parbat gneiss and schist, foliated units from deep within the arc, and nonmetamorphosed arc lithologies. The zone is dominated by arc related lithologies. Boundaries between strikingly different lithologies are not in all cases easily recognized because the foliation of the blocks is parallel to the strike of the faults. The fault zone has a complex deformational history; single outcrops within the zone may exhibit both mylonitization and brecciation.

Finally, the deformational history and lithology of the western edge of the Ladakh terrane are complex. The arc has undergone at least one and possibly more deformational and metamorphic events. The lithologies range from amphibolite to plagioclase tonalite porphyry. One does not pass out of the fault zone into a plutonic complex but instead into a series of amphibolites and metadiorites. The metamorphism has masked many of the once obvious igneous textures. Small shear zones also disrupt the edge of the arc.

The objectives of this part of the study are th following.

1) Locate the boundary between the massif and the arc.
2) Map and sample the zone in detail along the Indus gorge.
3) Extend the structures along strike by reconnaissance mapping and compilation of previous work.
4) Petrographically characterize the major lithologies in an attempt to unravel the metamorphic and deformational history.

5) Chemically characterize the major lithologies in an attempt to identify their source region.
6) Compare the eastern and western boundaries of the massif.
7) Attempt to interpret the nature of the fault zone in a regional tectonic framework.

The discussion of the Stak fault zone is organized into four parts. First, the major faults of the zone that intersect the Indus gorge are described. Second, lithologies of the blocks within the zone are described. Third, the geochemistry of the blocks within the zone is described. And fourth, variation of the fault zone along strike is described in light of previous studies.

Discussion of the Major Faults

Four major faults were identified during field work in the falls of 1984 and 1985. The faults will be described from west to east and are informally named the Majupah fault, the Gainji fault, the Stak Chi fault, and the Askore fault (Plate A2).

Majupah Fault

The westernmost major fault, the Majupah fault, separates hydrothermally altered schistose Shengus gneiss from layered gabbro, ultramafic pods, and amphibolite of island arc affinity. The fault intersects the Skardu road 4.5 km east of Chutran. Landslide debris covers much of the roadcut and part of the road, and the debris chokes

the river creating an impressive set of rapids, including a 15 m drop.

To the north the fault trends N60E with a vertical dip. In the fault zone fine-grained, schistose, garnet-biotite gneiss is oriented N85W 52N. For 500 m to the west the gneiss is extensively altered and fractured, making lithologic identification difficult. To the east of the fault a small section of layered gabbro is exposed. The layered gabbro contains highly contorted pods of ultramafic material, talc schist, peridotite, and hornblendite (Fig. 4.5). The pods are small, up to 3 m long and 0.5 m wide but most are 20-40 cm long and 5-10 cm wide. Some are isoclinally folded. Due to the highly deformed nature of the ultramafics, the most probable origin is by tectonic emplacement, but the ultramafic rocks could have originally formed in a layered complex.

The best exposure of the fault is 800 m above the road and 500 m east of the village of Majupah. A 40 m wide mylonitic zone cuts the Nanga Parbat gneiss. To the west, the foliation of the Shengus gneiss has a similar orientation to the other attitudes on the east limb of the Bulache antiform. To the east, scattered blocks of Shengus gneiss occur with an array of orientations. Immediately to the east, the dominant lithologies are layered gabbro and associated amphibolites.

Approaching the fault zone, the Shengus gneiss contains progressively more mylonitic lenses. A 20-30 m wide mylonite/ultramylonite marks the fault. Fractured lenses of quartz and potassium feldspar are recognizable. The mylonite is truncated by a 5-8 m wide siliceous breccia. To the east of the breccia, a fine-grained intermediate rock with hornblende augen and mylonitic lenses is present. Scree and landslide debris dominate the adjoining terrain.

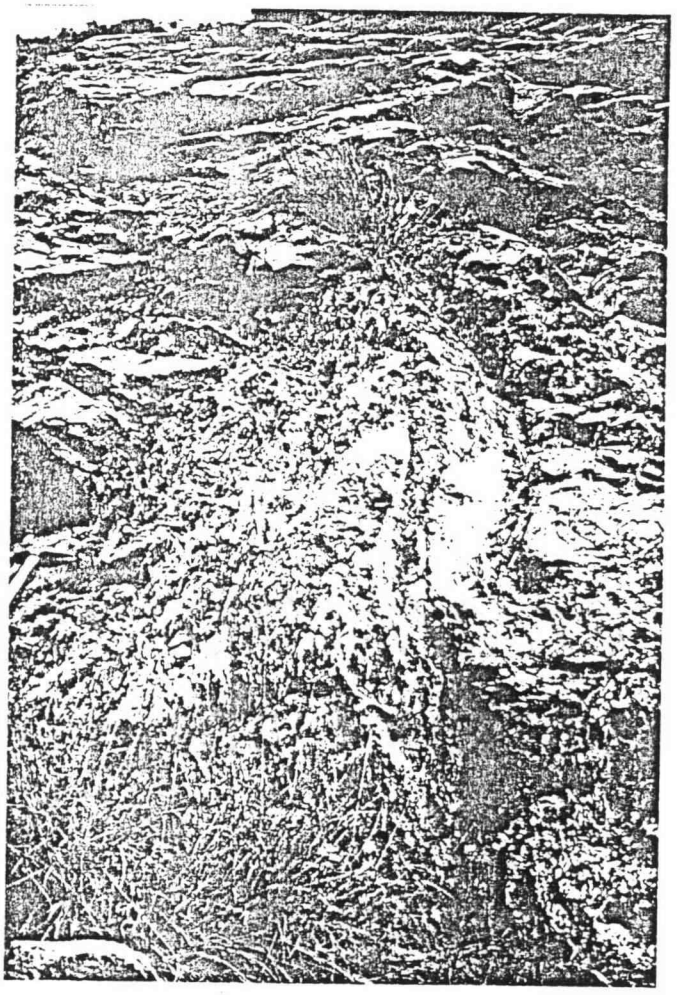

Figure 4.5. Photograph of Folded Ultramafic Pod. From near Majupah.

In thin section the mylonite consists of a crushed matrix of quartz, plagioclase, muscovite, chlorite, calcite, and biotite fragments with porphyroblasts of quartz, plagioclase, and potassium feldspar. The porphyroblasts are rounded, rotated, and fractured with undulose extinction. The albite twins in the plagioclase are kinked. Elongated epidote crystals are parallel to the fabric. Some are cracked. Garnets too are fractured.

This section of the fault shows a complex history, for both mylonitization and brecciation occurred. The mylonite formed during earlier, deeper activity on the fault and after significant unroofing, fault movement caused brecciation along the same zone. The breccias have provided fluid pathways for extensive hydrothermal alteration.

The fault can be traced to the northeast over the ridge and into the Stak Valley, trending N60E. The fault can also be traced southwestward. Three obvious fault traces can be observed on the ridge on the south side of the Indus Gorge. The traces are marked by alteration, gouge zones, and notches in the ridgeline. The westernmost trace is the most prominent and is oriented S70W from the mylonite zone east of Majupah. Past the ridge, the fault swings southward, for the next ridge to the south is dominated by the impressive dipslopes of the Shengus gneiss.

Gainji Fault

The next major fault of the Stak fault zone crosses the Skardu road 2.5 km to the east (Plate A2). The fault is marked by a 150 m of iron-stained, garnet-muscovite schist. The garnet porphyroblasts are

0.5-1 cm in diameter. Much of the schist is friable with some gneissic layers. The schist separates a banded gneiss to the west and a coarse-grained amphibolite with some banded gneiss to the east. Elongated pods, 5-8 m long, of ultramafic material occur within the highly deformed schist. The pods consist of pyroxenite, talc and actinolite schist, and biotite schist. These pods must have been tectonically emplaced.

The fault can be traced for a few hundred meters to the northeast, on a bearing of N40E with a vertical dip. To the south across the Indus, the fault is well exposed. An irrigation channel runs along the east side of Gainji Canyon exposing a cross section of the fault. A 100 m wide shear zone, oriented N35E, controls the course of the canyon. It is not clear which units the fault separates, for alluvium covers the adjacent terrain.

Approaching the fault zone, the banded gneiss becomes contorted and progressively more fractured and fragmented. The lithologies within the fault zone are chlorite-biotite schist, garnet schist, banded gneiss, and small ultramafic inclusions. The lithologies of the inclusions are similar to those along the Skardu road.

The canyon follows the trace of the fault for about one kilometer. Fault splays cross out of the drainage and can be mapped along the ridge to the west. The foliation of the iron-stained, garnet, muscovite schist at the southernmost exposure is oriented N65E 83S. The schist separates the banded gneiss to the northwest from a garnet amphibolite and diorite to the southeast.

Stak Chi Fault

Continuing eastward along the Skardu Road, the third major fault from the west side of the Stak fault zone is difficult to observe, for it strikes parallel to the foliation. The fault runs along the bend in the Skardu road and Indus River approaching Stak Chi. The fault is along a section of Shengus gneiss. Elongated pods of ultramafic material occur along the transition but are dominantly within the base of the gneiss/schist. The best exposure of the fault is below the road along the base of the walls of the Indus gorge. Ultramafic pods are elongated in a N40E direction and appear to plunge 45° to the northeast. The pods consist of talc schist, hornblendite, and dunite. The size of the pods ranges from a few centimeters to 20 meters in length. The fault can not be traced along strike, for the Indus cuts both directions. To the north side at the base of the Stak Valley, landslide and glacial debris mask the bedrock. To the south across the river, glacial and alluvial material mask the bedrock.

Askore Fault

The fourth and easternmost fault studied intersects the road 2 km east of the confluence of Stak Nala and Indus River near the Askore drainage. The fault is marked by a narrow, washed out tributary. The Askore fault separates banded gneiss and amphibolite to the west and epidote hornblende diorite to the east. The foliation in the banded gneiss adjacent to the fault is N50E 83W, and the foliation in the diorite is N42E 78E. At the fault these units appear quite similar. The

fault is marked by a 50 m wide zone of chlorite-biotite schist with small, fist-sized inclusions of ultramafic material. The attitude of the fault is approximately N40E 90°.

Because of the similar lithologies and their orientations adjacent to the fault, it is difficult to trace the fault across the river. When the river level is low exposing the bedrock in the channel, the fault can be seen. Above this level, the exposure is obscured by alluvium and scree.

To the north the fault can be traced. The gouge zone is readily apparent for a distance of 1.5 km. to the northeast. The fault cuts a young, simple pegmatite. The pegmatite crosscuts the foliation in the amphibolite (Fig. 4.6). Although the fault splays, the orientation remains northeast along the northwest wall of the Askore canyon. Along the canyon wall the fault appears to cut glacial till, creating a large scarp. This was observed through binoculars, for the access was too difficult.

Other Faults

To the east of Askore Canyon, lithologic and structural inconsistencies suggest the presence of a fifth fault. The fault trace is not exposed along the base of the Indus gorge. A transition from epidote hornblende diorite to Talu amphibolite is covered by scree. The foliation in the diorite is N55E 75E in contrast to the foliation, N70E 70N, in the amphibolite. The transition is rather sudden. On the southwest wall of the Indus, a narrow gully mirrors the transition. The lithologic transition follows along a scree filled drainage to the

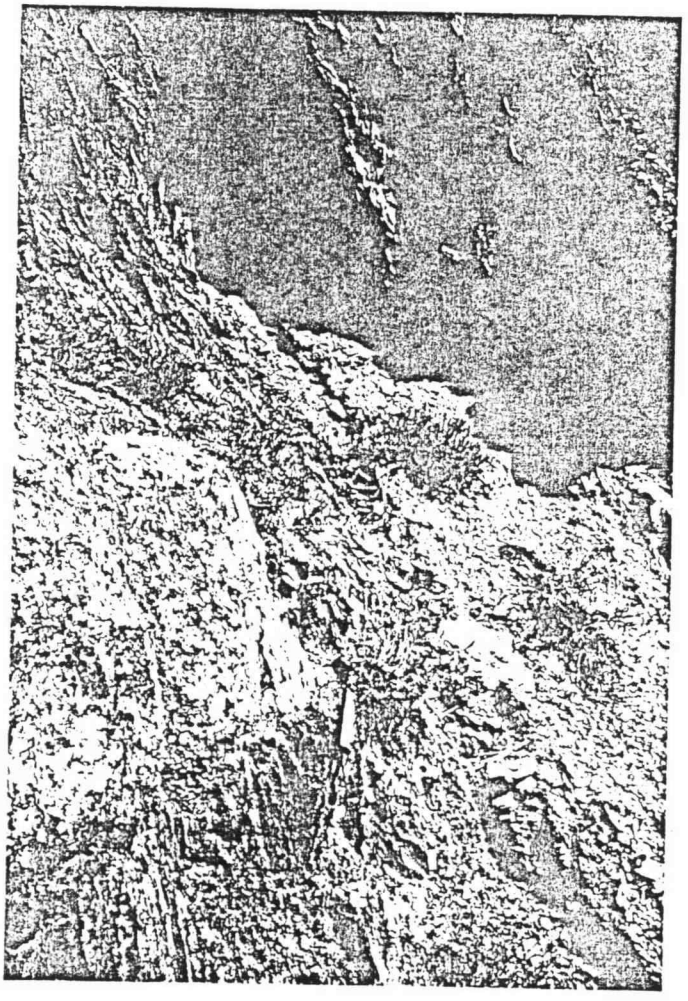

Figure 4.6. Photograph of Faulted Pegmatite. Along Askore Fault displaced late stage pegmatitic dike. Pegmatite is approximately 1 m thick.

northeast. Much of the scree is biotite schist and pyroxenite. The top of the wall is marked by a distinct V.

Another likely fault contact is along the western boundary of the highly contorted augen gneiss/biotite schist and the eastern boundary of the banded gneiss is likely a fault (between the Stak River and the Askore fault). Subsequent deformation has masked the contact, but the lithologies are from contrasting terranes.

Structural Synopsis

The northeast trending Stak fault zone is 3 to 6 km wide and contains blocks of various lithologies separated by major faults. The Indus River cuts across the strike of the structure exposing a cross section that wonderfully displays the overall character of the zone. The lithologies are dominantly of the same chemical, mineralogical, and metamorphic character as those found within the Ladakh-Kohistan arc and the massif.

The faults separating these blocks are dominantly of a nature intermediate between brittle and ductile. The westernmost fault contains a true mylonite zone that has been cut by a younger brittle fault. The eastern most fault shows evidence for recent activity. The four major faults trend from N70E to N40E and generally have a steep dip. Minor amounts of small ultramafic pods are smeared out along the faults. The lithologies are talc, chlorite, and actinolite schists, peridotites, dunites, pyroxenites, and hornblendite. These pods are usually a few cm across but can be up to 5 m across. The elongation of the pods is parallel to the strike of the fault, plunging about 45N.

Little structural data were taken in this study. The foliation of the lithologies of the blocks is generally parallel to the strike of the fault zone with steep dips. The blocks are also elongated parallel to the fault zone. Slickensides were measured along the Askore fault. They were on a plane N42E 78E and plunged 30N. Tight isoclinal folds in the gneiss are oriented N18E 66E and plunge 44N. The sense of motion associated with this structure would be west side up and right lateral.

Variation of fault zone along strike

Reconnaissance mapping along with evaluation of previous work has been done to extend the structure to the north and south. The units seen within the zone along the Indus pinch out along strike thus direct correlation could not be done. To the south, the westernmost fault changes trend from N70E to about N40E at the village of Hilbu. The boundary between the Shengus gneiss and the amphibolites can be traced with binoculars along the ridge that separates the Indus Gorge from the Astor River. Reconnaissance work in the Astor Valley showed the strike of the fault boundary between the gneiss and amphibolite changes to north/south with a vertical dip. The road passes through the contact approximately 3 km past the village of Harchu. Wadia(1933) mapped the transition along the Dichil Canyon. He also mapped the boundary southward as a N/S contact between gneiss and epidiorites and basic intrusions.

To the north of the Indus River the transition between the Shengus gneiss and the amphibolites can be traced with binoculars along the NW side of the Askore canyon. Access along this part of

the canyon is nearly impossible. Zanettin (1964) mapped the contact along the canyon wall and then near Stak La, the glaciated pass between the Stak and Tormik river valleys.

The eastern boundary of the fault is not as easy to map in reconnaissance fashion, for the lithologies of the eastern part of the fault zone and the western part of Ladakh are too similar. The most striking feature of the westernmost section of Ladakh is the felsic dike swarm.

Reconnaissance work to the south along Gainji Canyon was done in an attempt to map the change in lithologies along the strike of the fault zone and to map the eastern boundary. A few kilometers south of Gainji, the eastern ridge becomes dominated by felsic dikes. Ultramafic rocks, dunite dominantly, can be found as float coming down narrow canyons near this transition.

Lithology Section

Introduction

The lithologies of the assorted blocks within the fault zone are described in this section. They are presented in occurrence from west to east across the fault zone, except that the continental gneiss will be discussed last. The order is fragmented layered complex, amphibolite, banded gneiss, diorite, felsic units, and finally continental blocks. The mineralogy is presented in Table 4.1.

Fragmented Layered Mafic Complex

On the east side of the Majupah fault is a well exposed section of a layered gabbro. The unit is exposed in drainages that cut through the landslide debris. Primary igneous structures are present including size- and mineral-grading, crossbedding, and rhythmic layering. The mafic layers consist of hornblende and pyroxene and the felsic layers are plagioclase and quartz.

The section cropping out near Majupah exhibits the most variety of lithologies and structures. Mineral grading is evident. Ultramafic xenoliths have been incorporated into the layering. One pod of peridotite has been cut by hornblendite dikes, but the surrounding complex has not. Another peridotite breccia has been cut by chloritized dikes. Lower in the section talc schist and pyroxenite lenses along with the host rock have been tightly isoclinally folded.

Many of the lithologies described above have been observed in

Table 4.1

Characteristic Mineralogy of Stak Fault Zone Units

X = major component, x = minor component, t = trace component.

Mineral	Hilbu Amphibolite	Banded Gneiss M	Banded Gneiss F	Askore Diorite	Trond-hjemite	Continental Gneiss
Plagioclase	X	X	X	X	X	X
K Feldspar					t	X
Quartz	t	t	x	x	X	X
Biotite	x	x	x	x	x	x
Muscovite					x	x
Almandine	x	x	x		t	x
Sillimanite						t
Kyanite						X
Hornblende	X	X	x	X		
Epidote	x	x	x	x	x	
Orthopyroxene	t					
Epidote	x			x	x	
Calcite	t					
Sphene				t		t
Zircon	t	t	x	x		t
Apatite	t					t
Opaques	t	t			t	

the Chilas Layered Complex of Kohistan. The easternmost exposure of the Chilas Layered Complex is reportedly 35 km to the west of the Stak fault zone (Jan et al., 1984). Chilas proper, 60 km to the west, has been studied in great detail, for the exposures are good and easily accessible. Jan et al. (1984) describe a similar layered section with ultramafics, hornblende dikes, and peridotite breccias.

Current workers believe the Chilas Complex, the world's largest layered mafic complex (Jan et al., 1984), has a two stage emplacement history, one during the initial stages of the Kohistan island arc formation and a second post metamorphic magmatic phase. The exposures within the fault zone are limited, but the lithologies are analogous to those of the Chilas Complex.

To the southeast of the fault zone, in Kashmir, another cumulate section is exposed. The sections of the Kargil complex are postulated to represent the cumulate material associated with the Dras volcanics (Honeggar, 1983). Detailed field descriptions are not available to compare to the lithologies observed in the layered complex exposed in the fault zone.

Amphibolites

Much of the Stak fault zone is dominated by mafic units ranging from amphibolite to diorite. Intimately associated with the layered complex are medium- to coarse-grained, extensively recrystallized amphibolite and hornblende gniess. Metadiorite is also present but has not experienced the same amount of recrystallization. The lithologic, metamorphic and chemical variations of this mafic suite are somewhat

consistent across the fault zone.

South of the Indus, above the village of Hilbu, is the westernmost occurrence of amphibolite (5016). The foliation of garnet-epidote amphibolite is defined by the orientation of hornblende, epidote and flattened quartz and feldspar. The foliation trends N50E, parallel to the strike of the fault zone, and the dip is dominantly vertical but varies from 34°SE to 68°NW.

The mineralogy consists of hornblende (50-65%), plagioclase (20-35%), epidote (5%), quartz (5-10%), garnet (2-4%) and opaques (1-2%), along with trace amounts of zircon, sphene and chlorite. Calcite stringers cut parallel to the foliation. The quartz and plagioclase occur in ribbons. The quartz has undulose extinction, and the twins in the plagioclase are deformational. The garnets are prograde, for the crystal boundaries are well developed and inclusions of hornblende, plagioclase and opaques are present.

Along the Majupah fault the amphibolite (4084) is associated with the layered gabbro. The mineralogy is quite complex. The amphibolite contains pods of ultramafic material, talc and altered peridotite, as well as calcsilicates, calcium garnet and diopside. The package has been hydrothermally altered, masking the original mineralogy. The general orientation of the foliation strikes N70E with a vertical dip. Numerous fractures occur oblique to the foliation. Again, the texture and mineralogy of the original rock has been obliterated by an extensive epidote amphibolite facies metamorphic overprinting.

Sample 5038 is an epidote garnet amphibolite adjacent to the layered gabbro. The metamorphic grade of this amphibolite is lower than the amphibolite to the west. Minerals consists of plagioclase (40-50%),

hornblende (30-40%), quartz (5%), epidote (5%), garnet (5%), biotite (3-4%), with trace amounts of zircon, sphene, opaques and chlorite. Two generations of hornblende are present: a coarser one and a finer more euhedral one. Both are aligned with the foliation. The foliation is defined by the flattened mafic minerals. The quartz and plagioclase lamellae have undulose extinction. Few of the remnant zoned plagioclase are recognizable. The nature of the garnet is similar to that of the amphibolite at Hilbu, which has well defined grain boundaries and inclusions of various matrix minerals. These three amphibolites have been mapped as one unit, the Hilbu amphibolite.

Banded Gneiss

The banded gneiss is a distinctive lithology which occurs throughout much of the central portion of the fault zone. The unit, consisting of alternating mafic and felsic bands, is well exposed at the base of Gainji Canyon and along the Skardu road west of the Askore fault. The lithology can be confused with the rhythmically layered section of the layered gabbro. The mafic bands consist of coarse-grained hornblende, epidote, and subordinant plagioclase +-garnet and biotite, and the felsic bands consist of coarse-grained plagioclase and quartz +-garnet, muscovite, and biotite. The ratio of mafic to felsic bands ranges from 50/50 to 90/10. The mafic portions of the banded gneiss are indistinguishable from amphibolite.

At the base of Gainji canyon the banded gneiss is bounded on the west by the Gainji fault. The bands strike parallel to the fault, N40E, and the dip is vertical. Approaching the fault, the fabric

becomes highly contorted. The edge of the fault contains sheared off blocks of the banded gneiss.

Diorite

Continuing eastward across the fault, another mafic unit, a diorite with a slight fabric (4116), is exposed along the east side of Gainji Canyon. The diorite is along the east side of the fault. The mineralogy consists of plagioclase (35%), hornblende (35%), quartz (10%), biotite (10%), epidote (6%) along with zircon. The hornblende, biotite, and epidote are coarse-grained and are vaguely aligned, forming a slight fabric. The epidote contains inclusions of coarse biotite. The plagioclase has cross hatched, wedge-shaped twins and tends to have undulose extinction.

On the eastern edge of the fault zone is another mafic unit, a hornblende gneiss/metadiorite. The mineralogy consists of plagioclase (andesine/labradorite), hornblende, epidote and biotite of varying amounts. Two generations of hornblende are present, a coarse set and a finer idioblastic set. Some of the plagioclases contains well preserved albite twins, while others have wedge-shaped twins with undulose extinction.

Felsic Units

In addition to the mafic units, a set of felsic units are present. The nature of these felsic units is not well defined, for the contact relationships are not well exposed and the mineralogical and chemical

data are not definitive.

The best exposed unit is a trondhjemite that intrudes the amphibolite between the Majupah and Gainji faults. Along the Skardu road the trondhjemite occurs approximately 2 km east of the Majupah fault. No preferred mineral orientation is recognizable in the field, but this could be due to the lack of mafic minerals to exhibit the fabric. The pluton appears to be elongated parallel to the strike of the fault zone. Dikes of similar composition extend into the amphibolite and a block of banded gneiss is included in the trondhjemite (Fig. 4.7). The block is somewhat assimilated, particularly the felsic portions.

The thin section (5039) is dominated by plagioclase (65%) crystals, some are zoned and most exhibit poor albite twins. Quartz with undulose extinction makes up the bulk of the rest of the sample. The minor phases are biotite, muscovite, garnet and epidote. These four phases appear to be primary, for they are coarse and do not have a preferred orientation. The epidote is crudely zoned with allanite cores.

The trondhjemite definitely intrudes the banded gneiss and associated amphibolite and has not experienced the amphibolite facies metamorphic event. It is not clear whether the pluton intruded the banded gneiss and amphibolite after they were emplaced in the fault zone or before. It has experienced some brittle deformation, for a mortar texture is developed around some of the larger grains.

One kilometer east of the confluence of the Stak River another felsic unit, a biotite muscovite gneiss, is highly contorted and associated with a schistose unit. Because of the numerous folds in the schist and gneiss, the contact relations are masked. The gneiss

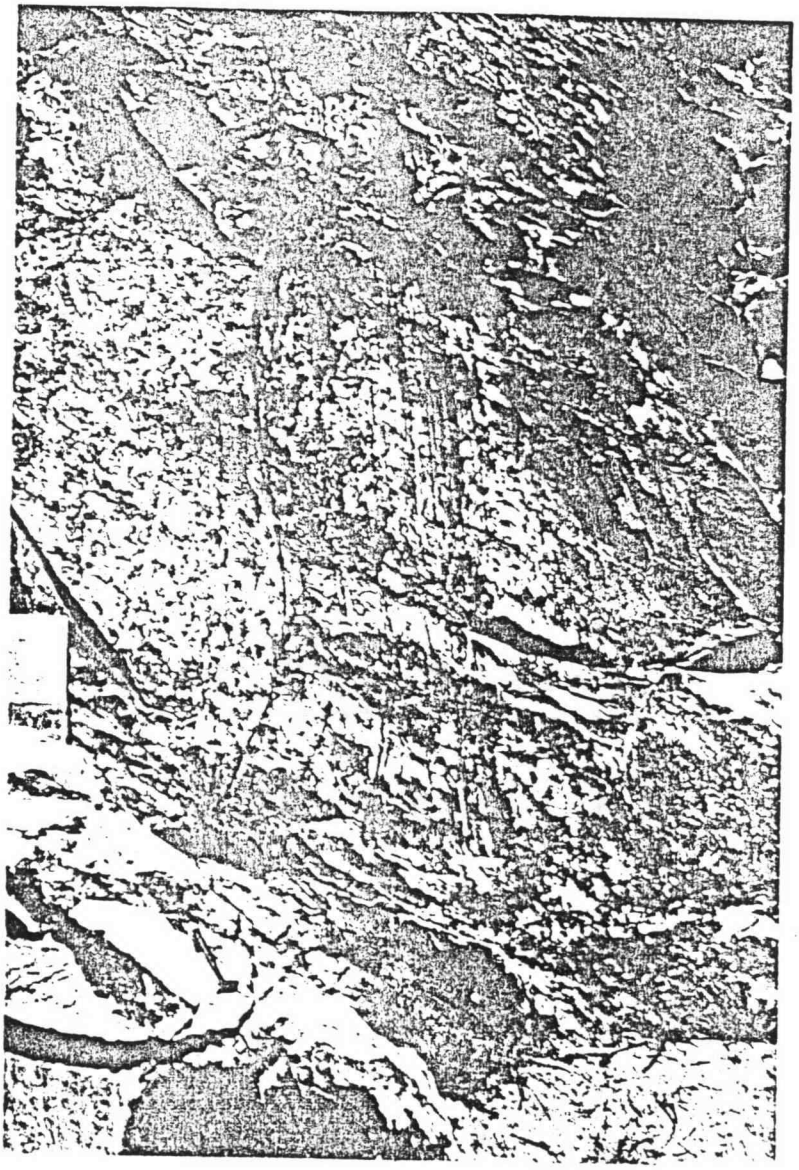

Figure 4.7. Photograph of Trondhjemite. Note banded gneiss inclusion in trondhjemitic pluton.

consists of subequal amounts of plagioclase, quartz, and potassium feldspar with muscovite, biotite and garnets. The potassium feldspar occurs predominantly as ribbons parallel to the foliation. The foliation is also defined by the alignment of muscovite and biotite. The quartz has undulose extinction. Most of the grains exhibit flattening and grain size reduction.

On the north side of the Indus, across from the village of Hilbu, a medium-grained muscovite-biotite gneiss occurs as a metamorphosed dike within the foliation of the schistose section of the Shengus gneiss. The mineralogy consists of plagioclase, quartz, potassium feldspar, biotite, muscovite, epidote and garnet with accessory pyrite and chlorite.

This gneiss has experienced a major metamorphic event and hydrothermal alteration. The plagioclase has kinked albite twins, sutured grain boundaries, and altered cores. The quartz displays undulose extinction. The muscovite and biotite are aligned with the foliation and some have been kinked. The epidote is zoned and formed parallel to the foliation.

Continental Blocks

Along with the units associated with the Ladakh arc complex, slices of gneiss and schist that are texturally, mineralogically, and chemically similar to the Shengus gneiss occur within the fault zone. The most prominent slice is just west of the confluence of the Stak River. The finely laminated, fine-grained augen gneiss is bounded by large faults. Within this slice the lithology is quite variable.

Sections consisting of garnet, muscovite, kyanite gneiss are identical to the kyanite gneisses of the upper Stak Valley. The felsic bands consist of quartz ribbons and plagioclase and the dark bands consist of biotite, muscovite, and kyanite. Porphyroblasts of potassium feldspar and garnets interrupt the banding.

Approaching the fault boundaries the gneiss exhibits greater deformation. The quartz is mashed with undulose extinction. The micas are bent and kinked. The garnets are broken and elongated.

Another deformed schistose gneiss similar to the Shengus gneiss occurs along the Gainji fault. The distinguishing features of the schist are the large garnet porphyroblasts, up to 1 cm in diameter, and the extensive iron staining. Fluids must have passed through the fault zone oxidizing the iron. Actinolite schist, peridotite, and biotite schist occur as pods included in the schist. The schist has a complex metamorphic history. Clues to the nature of the metamorphic events are preserved in the mineralogy. Two phases of muscovite development are seen, an earlier blocky muscovite and a later finer muscovite associated with the breakdown of kyanite. The kyanite is retrograding to muscovite. Staurolite is also preserved from an earlier event.

East of the Stak River confluence, a biotite, muscovite schist is interfolded with a felsic orthogneiss. The schist grades to fine-grained biotite, muscovite, gneiss. The fabric is strong, including deformed biotite, plagioclase, and quartz.

Geochemistry Section

To gain insight into the source region of the major blocks within the fault zone, major and trace element geochemical data were determined on twenty-five samples. The results are used to define the nature of the lithologies within the fault zone and to reconstruct the geometry of the fault zone. First, the units of arc affinities will be discussed and then the gneisses and schists of continental affinities. All results are tabulated in Table 4.2.

Major Element Geochemistry

Layered Gabbro

No geochemical samples of the layered gabbro were analyzed. A bulk composition could not be determined, for no chilled border rocks were located. Reconstruction of the layered complex was not possible, thus the location of the slices within the parent complex is unknown.

Mafic Units

The mafic units, amphibolites and metadiorites, within the fault zone show a general trend of tholeiitic composition on the west side to calc-alkaline on the east side. Four amphibolites (5016, 5038, 5040A, and 5040BM) and the banded gneiss (4132 and 5033M), are tholeiitic, and two units, the epidote-hornblende metadiorite (5032) and a diorite (4116) are calc-alkaline.

Sample no.	5016	5032	5033M	5038	5040A	5040BM	5053	4066	4112	4116	Percent Uncertainity
SiO2 %	48.1	55.2	48.3	50.9	52.9	52.5	51.6	58.2	43.9	55.9	1-3
TiO2	1.08	0.79	1.44	0.95	0.75	0.68	0.90	0.82	1.39	0.89	1-3
Al2O3	17.9	17.8	18.5	17.6	19.8	20.0	19.6	17.5	18.4	17.5	1-3
Fe2O3	3.38	2.91	4.24	3.57	2.88	2.89	2.46	2.48	4.97	2.64	1-3
FeO	7.68	4.86	7.53	6.24	5.21	6.11	7.15	4.44	9.76	5.30	1-3
MnO	0.18	0.15	0.21	0.15	0.12	0.25	0.17	0.12	0.44	0.15	1-3
MgO	6.49	4.27	4.99	5.81	4.02	4.34	4.61	7.41	6.14	3.95	1-3
CaO	10.30	7.97	9.43	9.67	9.61	8.32	9.54	3.30	12.20	7.79	1-3
Na2O	2.65	3.53	3.57	3.06	3.44	3.83	2.91	3.72	1.01	3.34	1-3
K2O	0.32	1.32	0.69	0.50	0.30	0.22	0.59	1.54	0.45	1.47	1-3
P2O5	0.10	0.31	0.29	0.15	0.08	0.13	0.07	0.27	0.35	0.27	1-3
H2O-	0.03	0.00	0.01	0.00	0.00	0.02	0.04	0.00	0.00	0.04	1-3
H2O+	1.80	1.15	1.47	1.54	1.07	1.05	0.81	1.04	1.80	0.99	1-3
Sc PPM	36	19	30	33	26	21	28	17	44	21	1-2
Cr	100	50	-	70	-	5	-	-	30	30	2-4
Co	40	22	32	37	23	26	-	34	42	31	2-3
Ni	50	30	-	10	-	10	-	-	-	-	10-20
Rb	7.0	38	17	12	13	1.3	10	47	4.5	48	10-30
Sr	350	540	420	280	510	500	590	-	-	-	10-30
Cs	1.8	1.0	1.5	0.15	0.17	0.27	0.9	1.2	-	1.4	10-30
Ba	50	260	-	100	260	90	100	410	-	200	5-10
La	2.9	18.7	12.6	6.0	3.1	3.3	4.2	22.8	33.1	17.1	1-3
Ce	7.6	37	27	15	6.0	7.9	8.1	46	86	36	5
Nd	5.9	12	-	10	-	5.2		20	35	24	10-30
Sm	2.00	4.30	4.58	2.60	1.29	1.35	1.62	4.11	7.05	4.09	1
Eu	0.84	1.17	1.58	0.95	0.71	0.76	0.76	1.16	3.71	1.25	1-3
Tb	0.48	0.61	0.75	0.52	0.27	0.24	0.33	0.59	1.7	0.59	5-10
Yb	1.7	2.1	2.6	1.6	0.84	1.1	1.1	2.4	4.6	2.3	5-10
Lu	0.28	0.29	-	0.23	-	0.15	-	0.39	0.80	0.39	5-10
Zr	40	-	70	40	-	-	60	90	600	200	30
Hf	1.6	2.2	3.1	1.7	0.74	0.45	1.4	-	1.2	4.1	5-10
Ta	0.03	0.33	0.21	0.13	0.06	0.09	0.06	1.6	0.85	1.1	5-15
Th	0.21	4.3	0.9	0.15	-	0.11	0.71	6.0	8.0	1.5	5-15
U	0.1	-	-	0.4	-	0.2	-	-	-	-	5-10

Table 4.2. Chemistry of Stak Fault Zone Samples.
Note: Percent uncertainty derived from statistical error and reproducibility of data.

			Gneisses					Felsic Units		Jijal Gran.	Ultra Malics			Trondhjemite		Percent
Sample no.	5012B	5036R	5041	5055	4092	4097	5027	4064B	4132	5057	5012A	5012C	5035	5039	5040BF	Uncertainity
SiO2 %	68.8	67.8	59.6	65.0	72.8	71.7	64.3	68.3	70.6	50.9	47.6	40.4	74.2	76.9	72.9	1-3
TiO2	0.66	0.68	1.29	0.62	0.11	0.28	0.38	0.25	0.19	0.67	2.41	0.02	0.07	0.08	0.10	1-3
Al2O3	15.7	16.3	14.3	16.2	15.6	14.9	19.7	17.2	16.5	18.5	14.6	1.0	14.5	13.4	15.6	1-3
Fe2O3	1.21	1.19	1.43	0.79	0.55	0.49	1.38	1.25	0.72	4.28	1.21	1.48	0.33	0.53	0.68	1-3
FeO	3.46	3.00	6.81	2.84	0.63	1.75	1.35	1.24	1.01	5.78	3.46	7.01	0.64	0.63	1.36	1-3
MnO	0.14	0.14	0.13	0.07	0.05	0.04	0.04	0.04	0.03	0.18	0.22	0.11	0.02	0.05	0.16	1-3
MgO	1.25	1.20	3.80	1.49	0.37	0.91	0.77	0.60	0.54	5.73	7.31	44.80	0.19	0.33	0.53	1-3
CaO	1.32	1.61	5.23	2.37	3.53	2.74	6.34	5.66	4.07	10.70	11.80	0.16	0.74	3.21	4.46	1-3
Na2O	2.03	2.53	1.74	3.95	4.77	3.90	5.28	4.66	5.31	2.43	1.45	0.15	3.54	4.01	4.10	1-3
K2O	3.56	4.26	2.63	5.17	0.97	2.82	0.18	0.09	0.37	0.28	0.58	0.02	4.44	0.54	0.04	1-3
P2O5	0.09	0.11	0.21	0.27	0.05	0.09	0.14	0.07	0.06	0.05	0.24	0.05	0.23	0.05	0.07	1-3
H2O-	0.08	0.00	0.06	0.03	0.02	0.04	0.00	0.03	0.07	0.00	0.08	0.00	0.04	0.00	0.00	1-3
H2O+	0.93	0.97	1.56	0.85	0.36	0.33	0.35	0.37	0.34	0.74	0.93	0.96	0.63	0.28	0.12	1-3
Sc PPM	12	11	22	6.6	2.3	5.3	4.6	3.0	3.0	38	42	5.1	3.0	2.3	3.1	1-2
Cr	-	30	-	-	1	20	2	2	2	50	-	3000	5	1	-	2-4
Co	10	9	27	7.2	31	24	4.6	32	2.3	36	48	110	1	1.2	2.3	2-3
Ni	-	-	60	40	-	20	10	30	-	20	80	2400	-	-	-	10-20
Rb	150	180	97	210	28	120	8.0	2.0	15	7.0	4.1	-	250	20	-	10-30
Sr	220	300	2200	480	-	-	600	-	540	200	160	390	70	400	-	10-30
Cs	8.5	6.8	5.5	8.5	1.9	5.6	0.34	0.05	0.89	-	0.15	-	9.4	1.1	0.08	10-30
Ba	950	930	470	1230	410	790	70	50	150	120	40	-	290	210	-	5-10
La	38.1	40.2	40.9	120	3.7	30.4	2.0	1.7	1.6	2.6	20.6	-	7.9	6.5	10.7	1-3
Ce	88	91	84	238	7.2	53	4.1	3.0	3.3	6.6	43	11	17	13	22	5
Nd	-	-	-	58	3.2	21	4.4	2.4	2.4	4.3	-	-	-	6.4	-	10-30
Sm	-	8.35	-	13.8	0.83	4.23	1.23	7.23	0.65	1.30	4.93	-	2.18	1.27	1.58	1
Eu	1.51	1.89	1.90	3.01	0.34	0.81	0.67	0.51	0.40	0.70	1.45	0.01	0.46	0.43	0.65	1-3
Tb	1.1	1.0	1.2	1.3	0.28	0.53	0.25	0.12	0.13	0.50	0.74	-	0.57	0.18	0.29	5-10
Yb	3.7	4.5	4.0	2.9	0.84	2.1	0.60	0.58	0.66	1.4	3.1	-	1.1	0.9	1.5	5-10
Lu	0.45	0.56	0.45	0.29	0.14	0.31	0.08	0.13	0.10	0.20	0.41	0.01	0.15	0.13	0.21	5-10
Zr	150	300	190	350	70	150	150	100	80	70	70	-	-	70	-	30
Hf	8	-	7	14	1.9	3.4	2.7	2.8	2.1	0.6	3.9	-	1.6	1.9	2.4	5-10
Ta	0.81	0.90	1.1	4.1	2.4	1.9	0.05	2.2	0.06	0.02	1.0	-	1.6	0.1	-	5-15
Th	15	14	14	39	1	14	0.03	0.06	0.06	0.03	6	0.15	3.7	1.5	0.73	5-15
U	-	-	-	-	-	-	-	-	0.1	-	-	-	-	0.5	-	5-10

Table 4.2. Continued

Western Mafic Units

Amphibolites

The Hilbu amphibolite (5016) has the lowest SiO_2 value of any mafic block within the fault zone. FeO*, MgO, Al_2O_3, P_2O_5 and CaO are enriched relative to the rest of the suite while Na_2O and TiO_2 are not. The sample plots well within the tholeiitic field on the FeO*/MgO vs. SiO_2 and FeO*/MgO vs. FeO* (Fig. 4.8). The K_2O content is low, 0.32%, but it is comparable to that of Gill's low potassium basalts. The TiO_2 concentration (1.08%) is consistent with Green's (1980) ocean island or continental arc tholeiitite, not a mid-ocean ridge basalt. Overall the major element data are correlative with the Talu amphibolite of the western Ladakh terrane.

Two other samples of amphibolite, 5040A and 5040B, were collected just east of the Majupah fault. Chemically, the amphibolite is classified as a basaltic-andesite of the tholeiitic series (Fig. 4.8). Compared to 5016 and 5038, the Al_2O_3 is high, 20%, but the sample has correspondingly low values of Na_2O and K_2O and thus plots within the tholeiitic field, not the high alumina basalt field. The high Al_2O_3 content is reflected on the ACF diagram, for the samples plot above the rest of the samples (Fig. 4.9).

Another amphibolite (5038) has major element concentrations which are almost identical to those of 5016, but it is slightly more felsic. It too is an island arc tholeiitite. The total mafic elements, FeO*+MnO+MgO, equals 16.5% versus 18.6% for the Hilbu sample (5016). Potassium is slightly greater as well.

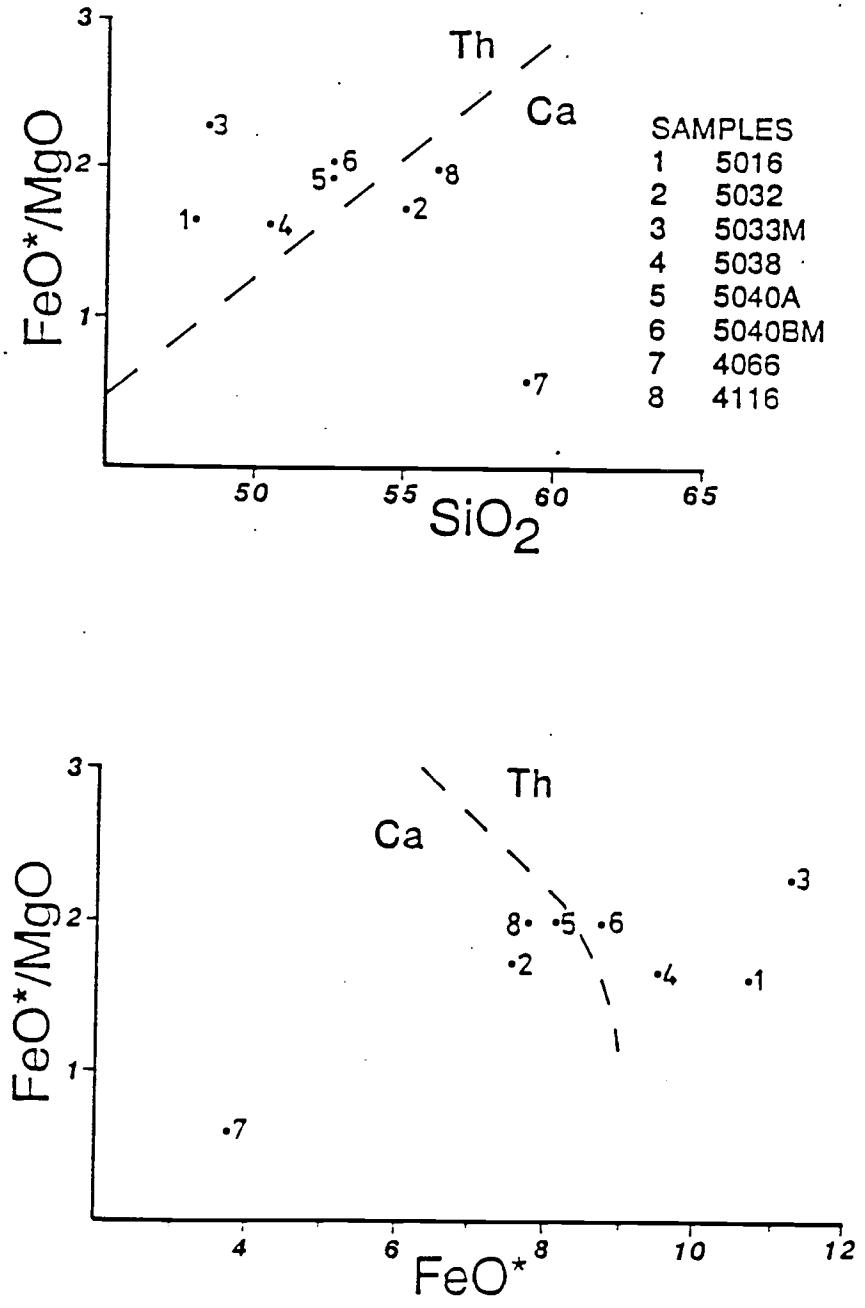

Figure 4.8. Feo* vs. SiO_2 and FeO*/MgO vs. FeO* for Fault Zone Mafic Samples. Tholeiitic and calc-alkaline discrimination line from Miyashiro (1974).

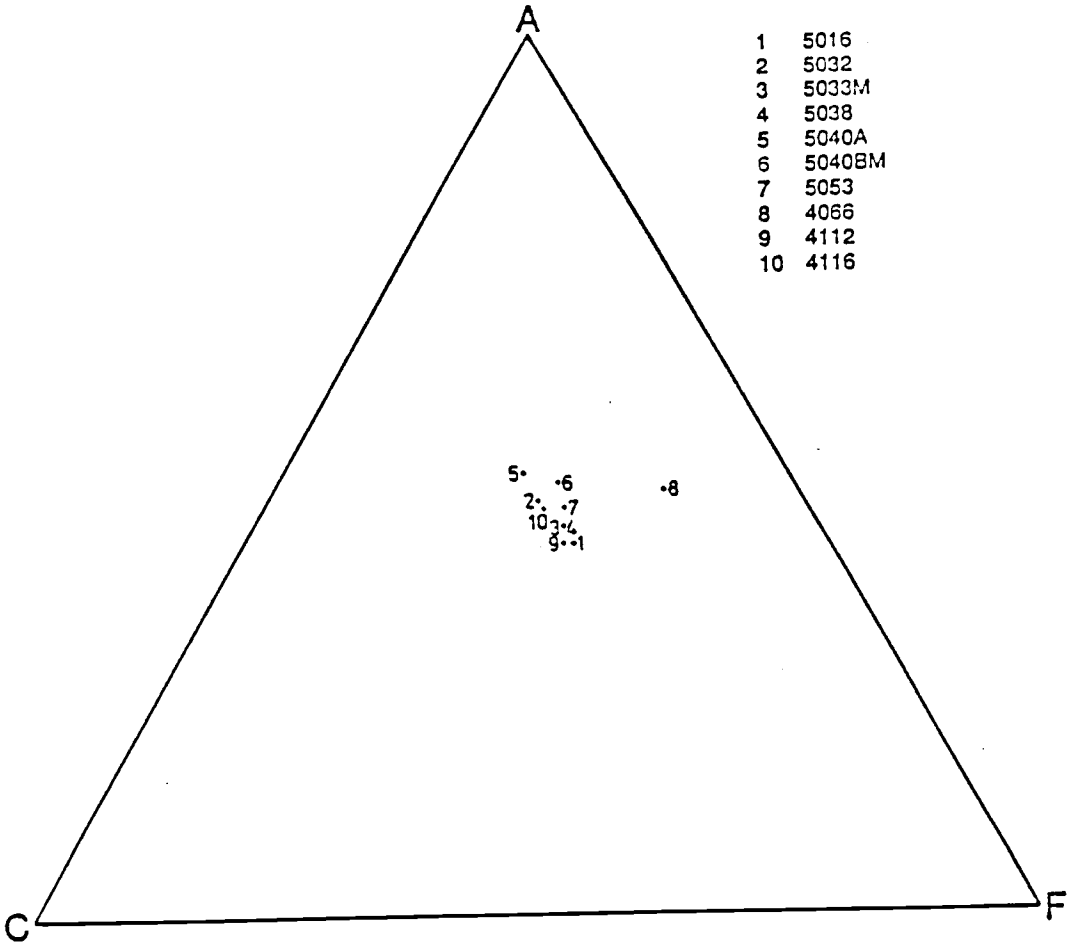

Figure 4.9. ACF Diagram of SFZ Mafic Units.

Banded Gneiss

The mafic and felsic bands of the banded gneiss were individually analyzed. Sample 5033M is a mafic band from the banded gneiss east of the mouth of the Stak River. It has the chemical composition comparable to Jakes and Gill's island arc tholeiitic basalt. Although the SiO_2 content is similar to 5016 and 5018B, the other major elements differ; TiO_2, Al_2O_3, Fe_2O_3, Na_2O, and K_2O are greater and MgO and CaO are lower.

The chemistry of felsic bands (5027, 4132, and 4064B) are analogous to a trondhjemite, for the SiO_2 is high (70.60%) and the K_2O is low (0.37%). Average granite has 71.30% SiO_2 and 4.07% K_2O. Compared to average granite the Al_2O_3, CaO, and Na_2O are enriched. The mineralogy is reflective of the chemistry, for the samples contain plagioclase and quartz with no potassium feldspar.

Eastern Mafic Units

In contrast to the above units, samples 5032 and 4116 (epidote hornblende metadiorites) are calc-alkaline and occur on the eastern side of the fault zone. Both lie within the calc-alkaline field on the FeO*/MgO vs. SiO_2 and FeO*/MgO vs. FeO* diagrams (Fig 4.8). The major and trace element chemistry of these two units is almost identical. On the ACF diagram they plot on the same spot (Fig. 4.9). The chemical data are correlative with that of the younger mafic units of the western Ladakh terrane.

Felsic Units

Three felsic units within the fault zone were sampled. The felsic pluton (5039) that intrudes the tholeiitic amphibolites is a trondhjemite. The silica value is high 73-77% while the K_2O is very low, less than 0.5%. The mineralogy is dominated by plagioclase and quartz. On the plot of K_2O vs. SiO_2 and on the normative fieldspar triangular diagram the samples plot on the transition from continental to oceanic trondhjemite delineated by Coleman and Peterson (1975) (Fig. 4.10).

Equigranular gneiss which is in intrusive contact with the Shengus gneiss just east of the Majupah fault is also a trondhjemite. The K2O is slightly greater than the previously described unit. The other major elements are quite comparable.

The equigranular gneiss (5035), that crops out east of Stak and is folded with a schist, is of granitic composition. The K_2O is 4.5% which is similar to the average granitic composition. The major element data are dissimilar to the trondhjemites, on the ACF diagram (Fig. 4.9) the point is indistinguishable from the felsic layers of the banded gneiss.

Continental Blocks

Within the fault zone are schist and gneiss that are mineralogically and chemically identical to those of the massif. The lithologies were described in the previous section. The gneiss (5036, 5012B, and 4097) that occurs just west of the mouth of Stak River is rich in SiO_2 (68-69%), Al_2O_3 (16%) but low in CaO and Na_2O. The samples plot within the group of NP material on the ACF (Fig. 4.11).

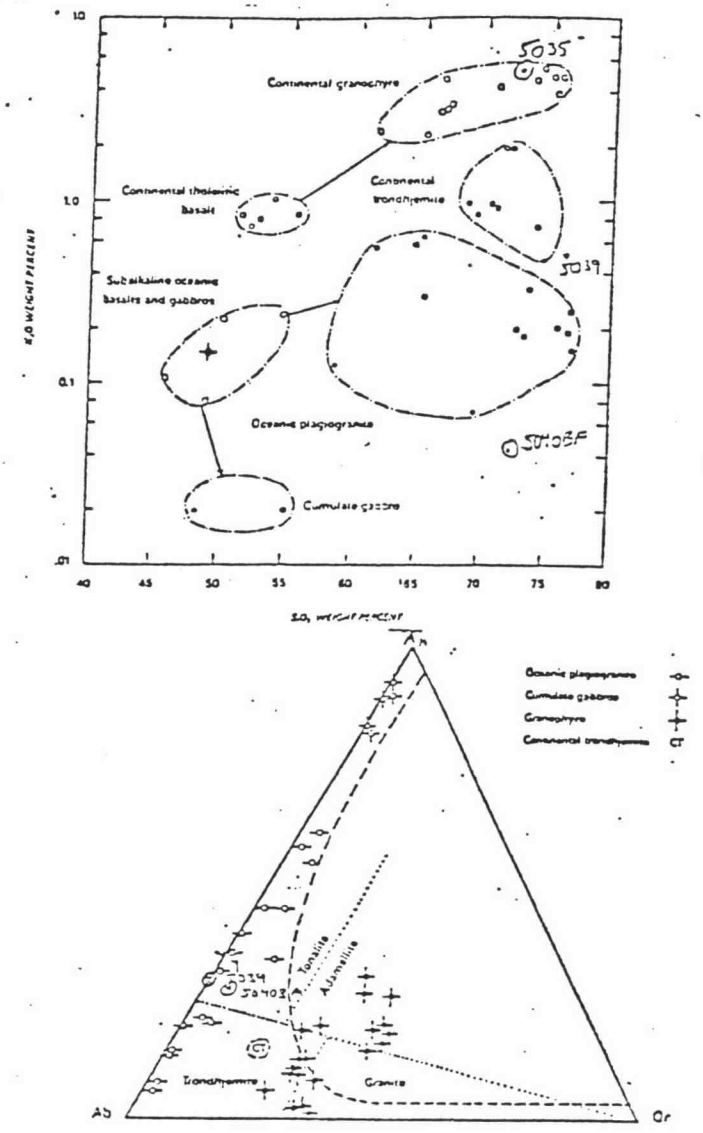

Figure 4.10. Classification of Trondhjemites (from Coleman and Peterman, 1975). A: Triangular diagram of normative Ab, An, and Or content. B: Semilog plot of SiO2 vs. K2O (From Coleman and Peterman, 1975).

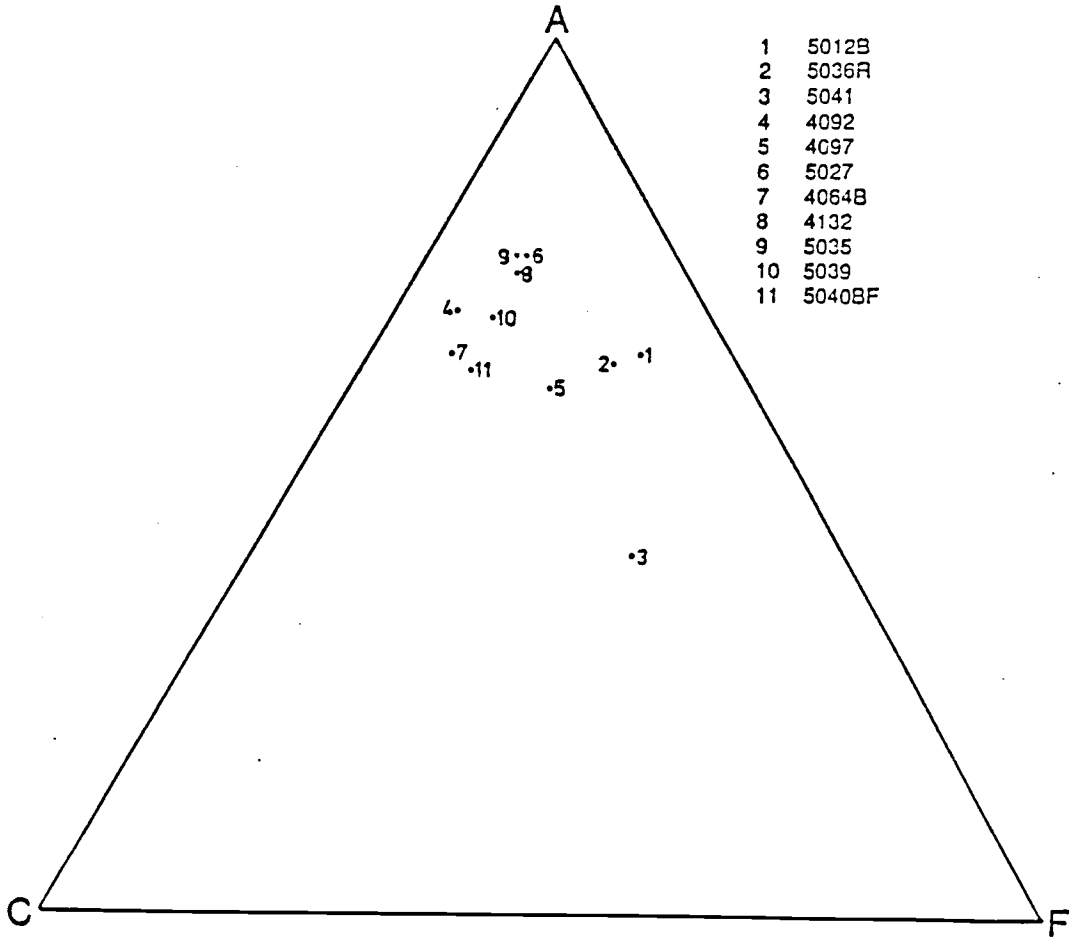

Figure 4.11. ACF Diagram SFZ Gneisses.

The chemistry of the iron stained, garnet schistose gneiss from Gainji Canyon (4112) is somewhat anomalous. The SiO_2 is low while the Al_2O_3, FeO*, MgO and CaO are extremely high. On the ACF plot the high CaO shifts the point to the center of the diagram. The hydrothermal fluids passing along the fault zone could have affected the major element chemistry.

Trace Element Geochemistry

The trace element data have been utilized to further categorize the suite of samples from within the fault zone. Using the data from the arc and the massif, one can try to correlate the similar lithologies and speculate on the origin of the others.

Amphibolites

The REE plot (Fig. 4.12) of the Hilbu amphibolite, 5016, is generally flat at approximately 10 times chondrite (10X). This composition is comparable to the amphibolitic country rock of the Ladakh terrane. A tholeiitic basalt with a flat pattern of 10X could be from a MORB or an OIT. The arguments from the major element data suggest an arc setting. Other trace elements are needed to determine which is the most likely source.

Studies comparing trace element concentrations in MORBs and OIT have shown that OIT are less depleted in large, low valence cations, Cs, Rb, K, Ba, and Sr (BVSP,1981). The K, Rb, and Sr are well within the range of OIT. Large and intermediate high valence cations,

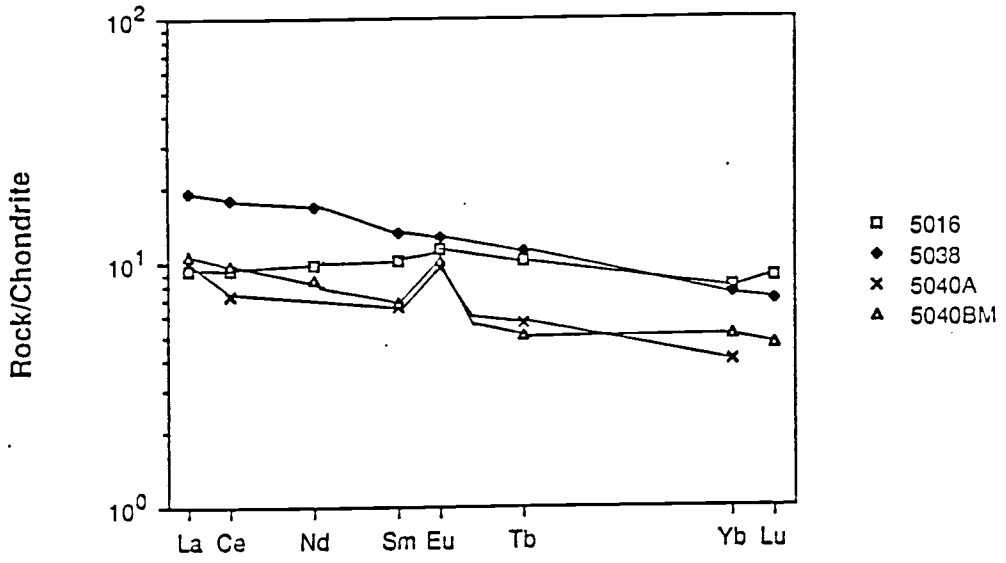

Figure 4.12. REE Diagram of SFZ Amphibolites. Samples normalized to C1 Chondrite.

Th, U, Zr, and Hf, are also in the range of OIT.

The REE plots of two other amphibolites 5040A and 5040BM are parallel, but 5040BM is slightly higher except for Eu. The REE plot has a negative slope with (La/Yb)cn ratio of 2.4. Europium is enriched by 1.4 relative to Sm. The samples contains much plagioclase, which appears to dominate the REE pattern. The relatively high Sr concentration is consistent with plagioclase domination. Thorium is depleted relative to La, and Hf is slightly enriched relative to Sc and Ta in both samples.

The REE plot of 5038 is within the range of OIT. The pattern has slight LREE enrichment and a flat HREE pattern at about 10X. The pattern is comparable to the Talu amphibolite. The large low and high valence cation concentrations are consistent with an oceanic arc environment.

Banded gneiss

The REE plot (Fig. 4.13) of the mafic band, sample 5033M, is slightly LREE enriched, approximately two times the HREE. No Eu anomaly occurs and the HREE are relatively flat. The total REEs are slightly greater than those of the other amphibolites. Thorium is not enriched compared to La, while Hf is enriched relative to Sc and Ta.

Trace element data for the felsic bands (4132 and 5027) are interesting, for Rb and Ba are low for a rock this rich in SiO_2 while Co and Ni are somewhat enriched. The REE plot (Fig. 4.14) is controlled by plagioclase. The total amount of REE is low. The LREE are slightly enriched, and HREE are flat at about 3.5X. Europium is enriched to 7X,

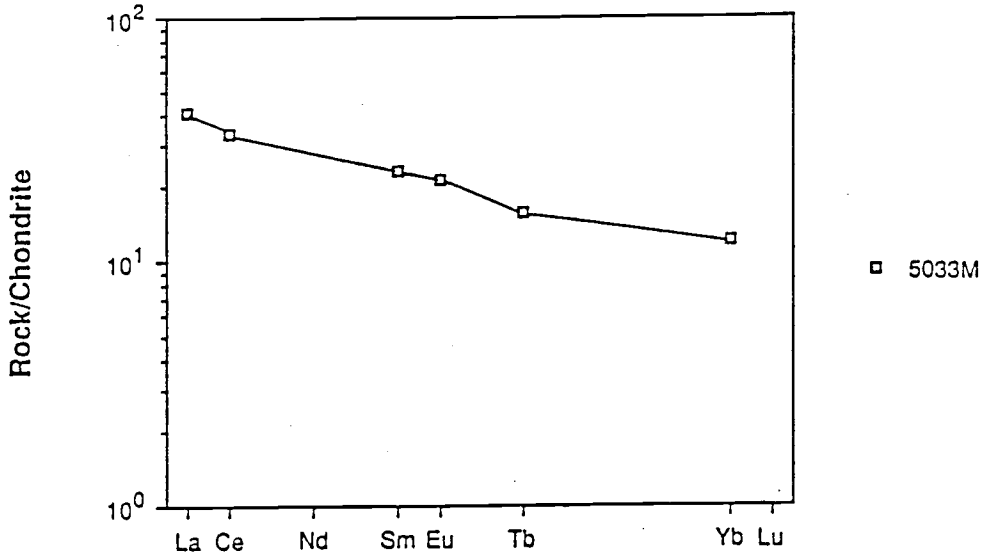

Figure 4.13. REE Diagram of Mafic Band of Banded Gneiss. Samples normalized to C1 Chondrite.

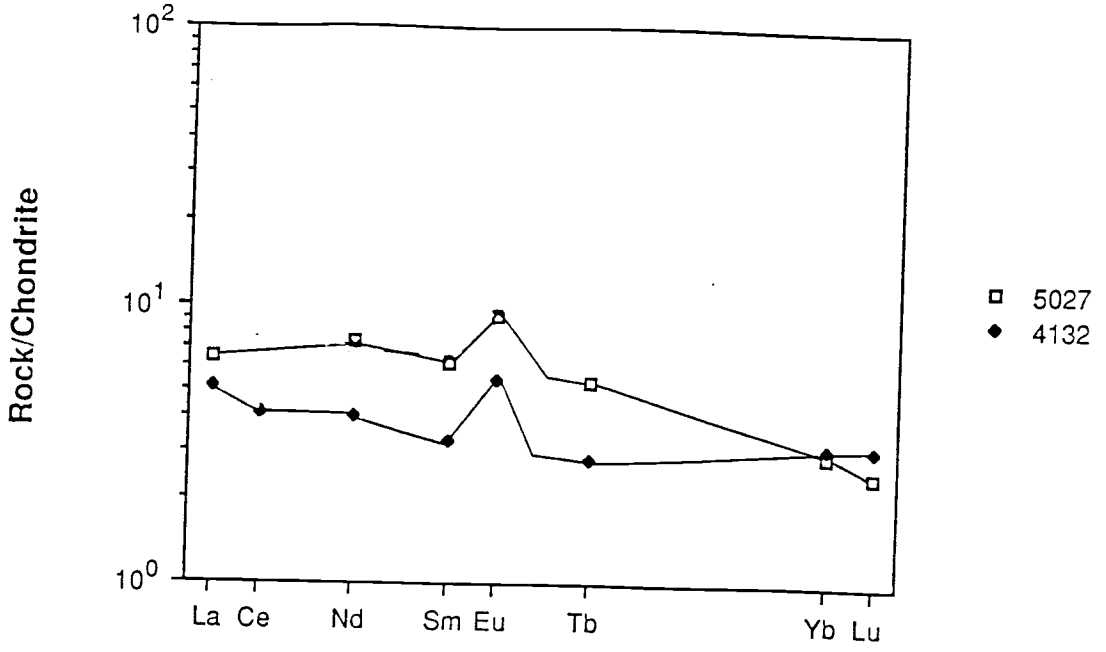

Figure 4.14. REE Diagram of Felsic Band of Banded Gneiss. Samples normalized to Cl Chondrite.

about two times higher than the other REE. Comparing this pattern to plagioclase separates from mafic rocks, one sees quite a similarity, although the total REE are lower in abundance. The Eu anomaly in the plagioclase separates is about three times enriched compared to the rest of the REEs. La is slightly enriched as well as Lu. Although plagioclase dominates the felsic layers, the presence of other constituents would raise the concentration of the REE and change the pattern.

Diorites

The REE patterns of 5032, 4066, and 4116 (Fig. 4.15) are identical and are similar to those of the slightly deformed gabbros and diorites of the western Ladakh terrane. The plots show a LREE enrichment (40X-60X) and relatively flat HREE (10X-15X). The patterns are within the range of oceanic or continental arc basaltic andesites. The high Rb, Sr, Ba, and Th could reflect a continental influence.

Felsic Units

The REE plots (Fig. 4.16) of the trondhjemitic intrusive (5039 and 5040A) are distinctive. The LREE are strongly enriched and the HREE are flat. Europium is slightly enriched, due to the plagioclase. Although the low concentration of REE is consistent with an oceanic island arc setting, this pattern is not consistent with either the continental or oceanic trondhjemite REE pattern described by Coleman and Peterson (1975). Rubidium and Sr are low for a rock of this high SiO2 but are

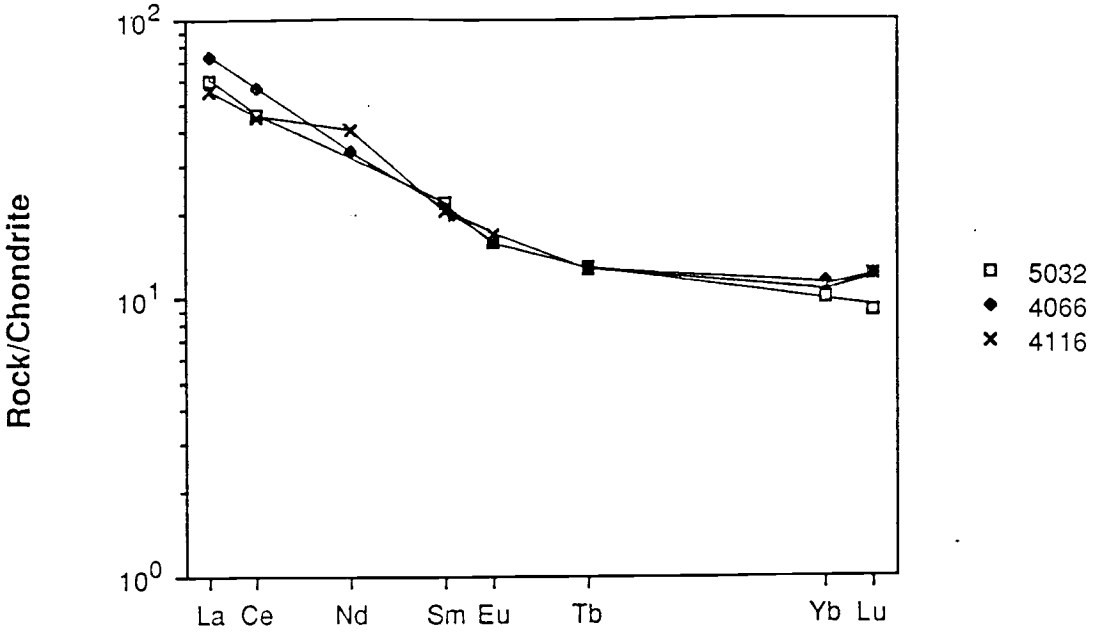

Figure 4.15. REE Diagram of SFZ Metadiorites. Samples normalized to C1 Chondrite.

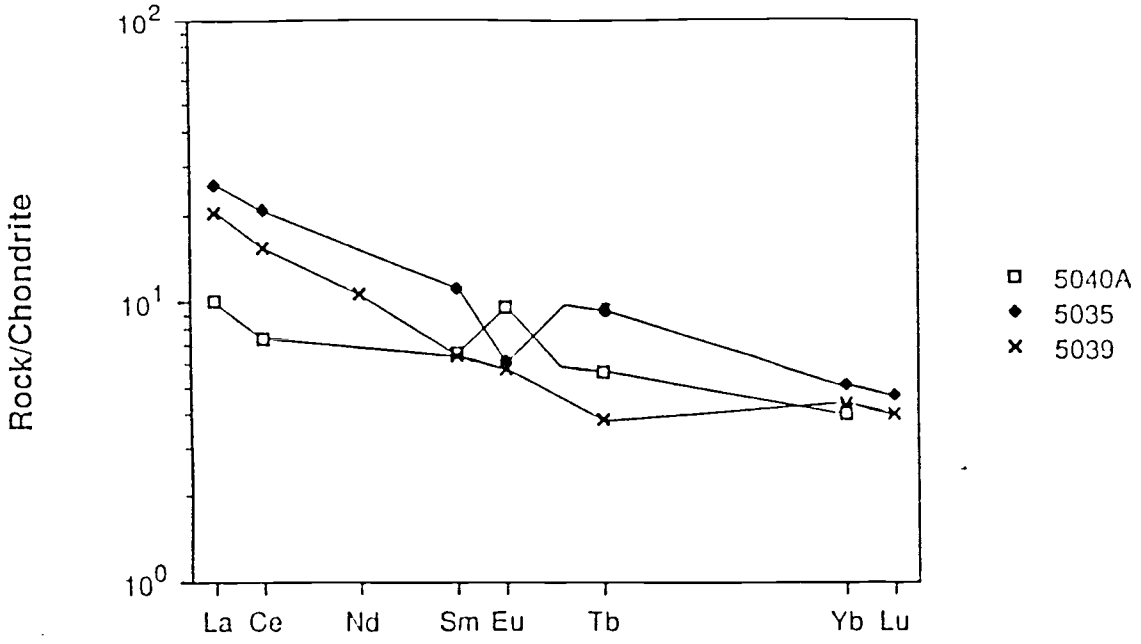

Figure 4.16. REE Diagram of SFZ Felsic Units. Samples normalized to C1 Chondrite.

consistent with the low K_2O concentration. Scandium, Co, Cr, and Ni are barely detectable.

The REE concentrations (Fig. 4.17) of the equigranular gneiss (4092) that intrudes the Shengus gneiss are extremely low. The LREE are slightly enriched while the HREE are flat. This dike is definitely of arc parentage.

The trace element data for the gneiss that crops out just east of the Stak Valley, 5035, are enriched in Rb, Sr, Ba, Cs, and Th, while Sc, Co, and Cr are depleted. The REE pattern has a negative slope, for the LREE are enriched and the HREE are depleted. A large negative Eu anomaly breaks the slope. The overall concentrations are low, La=35X and Lu=4X. The gneiss is intimately associated with a continental schist (4097). The trace elements could have been remobilized if a fluid phase was present, which would explain the anomalous concentrations.

Continental Blocks

The incompatible elements (REEs, Rb, Sr, Cs, Ba, Zr, Hf, and Th) are greatly enriched in the samples of the gneisses lithologically similar to the Shengus gneiss. The total REEs are less than those of the gneiss of NPHM, but quite similar to the more schistose units and the equigranular gneiss. The LREE are enriched while the HREE are slightly depleted (Fig. 4.18). A small, negative Eu anomaly is present. When the pattern is compared to 5041, the NPHM schist just east of the fault zone, no distinction can be made.

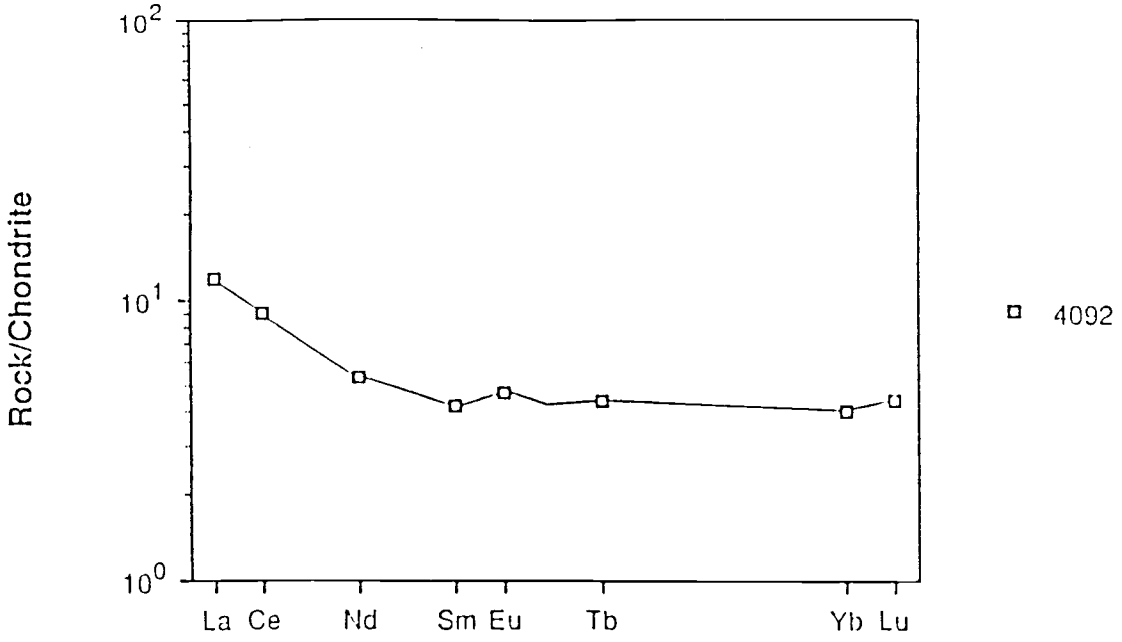

Figure 4.17. REE Diagram of a Gneiss. Sample normalized to C1 Chondrite.

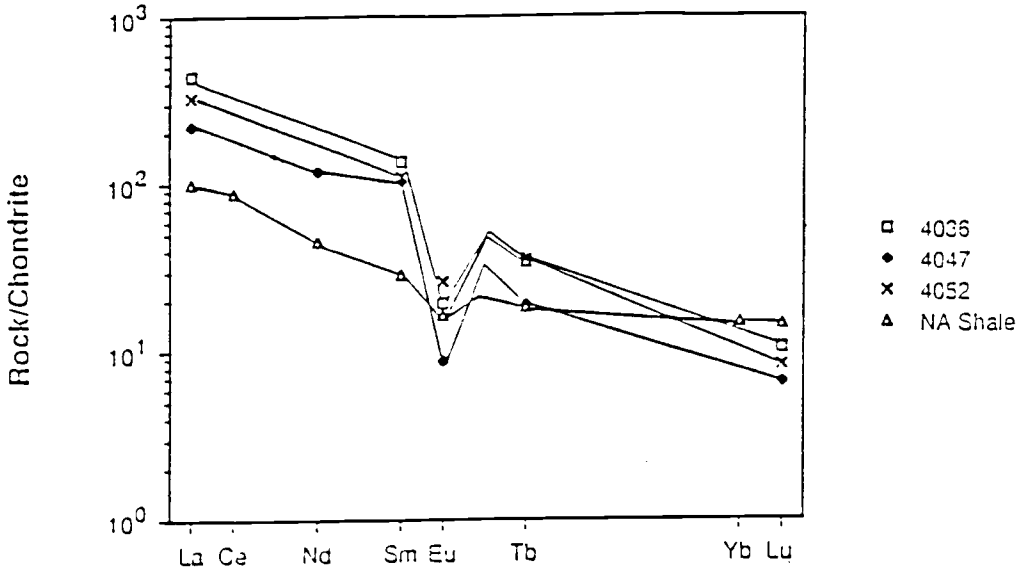

Figure 4.18. REE Diagram of SFZ Continental Gneisses. Samples normalized to Cl Chondrite.

Lithologic and Chemical Synopsis

The major and trace element data can be utilized to constrain the likely source region of the assorted blocks within the fault zone. By comparing these data with data from the adjacent terrains, conclusions can be drawn concerning the nature of the fault zone.

The amphibolites on the west side of the fault zone are island arc tholeiites. The metamorphic grade is epidote amphibolite and the extent of recrystallization ranges from wholly to partially recrystallized. This unit is chemically and mineralogically similar to the amphibolitic host rock of the western Ladakh terrane.

Associated with the amphibolites is a section of layered gabbro. Although this unit was not studied in detail in the field, graded bedding, rhythmic layering, and crossbedding were observed. The unit is likely correlative to the Chilas layered complex, a large mafic complex exposed in the Kohistan terrane.

The trace element chemistry of the banded gneiss is consistent with an arc parent. The mafic bands are mineralogically and chemically similar to the amphibolites. The protolith was likely a basaltic sequence that was intruded by a series of trondhjemitic dikes, for the package is dominated by the mafic layers.

The eastern mafic units are calc-alkaline diorites. The diorites have a fabric, but are not totally recrystallized. Igneous textures are recognizable. The trace element chemistry is consistent with an oceanic or continental volcanic arc source. The diorites are texturally and chemically correlative with the younger mafic units of the western Ladakh arc.

A large felsic pluton occurs within the middle of the fault zone. The pluton likely intruded into the fault zone, for dikes of the same composition intrude the surrounding rock. Amphibolite and blocks of the banded gneiss are included in the pluton. Chemically, this pluton plots between oceanic and continental trondhjemites.

A large block of kyanite gneiss with schistose interbeds crops out in the middle of the fault zone. The block is mineralogically and chemically analogous to the upper section of the finely laminated Shengus gneiss.

Conclusions

The Stak fault zone consists of four major faults that separate assorted blocks derived from the adjacent terranes. The faults are high-angle and trend N70E to N40E. The westernmost fault is marked by a 40 m wide mylonite zone along with minor brecciation. The other three faults consist of 50-150 m wide shear zones containing garnet, mica schist with inclusions of ultramafic pods. The only evidence of recent activity is along the easternmost fault, the Askore fault, where a late stage pegmatitic dike has been faulted and where remains of fault scarps are preserved in the glacial till along the west wall of the Askore canyon.

A structural analysis was beyond the scope of this study, but a few observations were made. The trend of the fault zone is approximately N45E. The fault zone was traced from Stak La southward to the north side of the Astor River for a total distance of 50 km. At the Astor River the fault zone changes strike from N45E to roughly north/south but the dip remains nearly vertical. The sense of motion inferred from tight folds in the units adjacent to the Askore fault is right lateral and west side up.

The faults separate blocks derived from the adjacent terranes, except for the trondhjemitic intrusive. Within the arc derived lithologies in the fault zone, a general trend is from deeper derived lithologies on the west to upper arc lithologies. The units on the western side consist of a section of a layered complex, amphibolite, and banded gneiss. The amphibolite and banded gneiss are chemically analogous to tholeiites from an immature oceanic island arc. The

units on the east side of the fault zone are slightly deformed gabbros and diorites, which are mineralogically and chemically correlative to the mafic plutons exposed in the adjacent western Ladakh terrane.

Interrupting this trend is a slice of kyanite gneiss and banded gneiss exposed in the middle of the fault zone. This package is a crude repetition of the units on the west side of the fault zone and could have been emplaced by thrusting/strike slip motion or a combination of the two mechanisms.

Previously, the eastern and western boundaries of the NPHM were mapped as a continuation of the MMT/Indus Tsangpo suture zone. This conclusion was based on the belief that a parallel belt of granulite and amphibolite wrapped around the west, north and east sides of the massif. Lawrence and Ghauri (1983) and Madin (1986) have documented that the western boundary of the massif is an active fault. Their detailed mapping shows that no belts of granulite and amphibolite are exposed along the boundary. Similarly, this study does not document the presence of parallel belts of granulite and amphibolite along the eastern boundary of the massif.

The Main Mantle thrust is believed to be a western continuation of the Indus Tsangpo suture zone (Lawrence et al, 1983) because similar lithologies are present along both sutures. The lithologies along the east-west trending suture zones are large ultramafic blocks, sections of ophiolite complexes, and blueschist assemblages. These exotic blocks are derived from the oceanic crust and sedimentary cover that once separated the Indian mass and the Kohistan-Ladakh island arc. In contrast, the lithologies within the Stak fault zone have been derived from the adjacent terranes, except for the possibly trondhjemitic

intrusive. The recent mapping and geochemical data from this study prove the necessity for a re-evaluation of the tectonic history of this section of northern Pakistan.

CONCLUSIONS AND IMPLICATIONS

To conclude this study a brief summary of the first three chapters will be reviewed to build a foundation for a tectonic reconstruction of northern Pakistan. The tectonic reconstruction is developed by incorporating the data from this study with a suite of data from other recent studies and models.

The chemical, mineralogical, and structural data from this study show that the northeast section of the NPHM is dominated by the Shengus gneiss, a multiply deformed paragneiss with continental affinities. Madin (1986) described evidence for three deformational events. The earliest event was the folding of the original (?) layering creating tight, isoclinal, intrafolial folds in the gneiss. Madin speculates that this structure was formed during a pre-Himalayan event, possibly Proterozoic or early Paleozoic. The second deformational event was responsible for the set of folds with east/west oriented fold axis. This deformational event is likely related to the obduction of the Kohistan-Ladakh arc onto the northern margin of the Indian plate. The third and most recent event was the formation of the upright, assymetric antiforms, the Bulache and Iskere antiforms. The Cenozoic uplift was likely responsible for these structures (Madin, 1986).

The data from the western Ladakh terrane document three magmatic phases; an immature oceanic island arc plutonic phase, a mature oceanic island or continental margin arc plutonic phase, and an intrusive phase of chemically evolved, continental, felsic dikes. The three phases are exposed along the Indus River east of the Stak fault zone as well as west of the Raikot fault in eastern Kohistan. The Kohistan and Ladakh

terranes are correlative, as first proposed by Wadia (1933), and represent the same structural level of the once continuous arc. The present day exposed structural level is the upper part of the Kohistan-Ladakh arc, where the volcanic and sedimentary cover has been removed by erosion.

The Stak fault zone marks the boundary between Precambrian gneiss and Cretaceous arc lithologies. Evidence from geologic mapping, petrography, and geochemistry shows that the Stak fault zone does not represent the early Cenozoic suturing event which created the Main Mantle thrust/Indus-Tsangpo Suture Zone. The lithologies within the fault zone are derived from the adjacent terranes, in contrast to the assortment of exotic blocks that are exposed along the east-west trending MMT/Indus Tsangpo Suture Zone. The lithologies of the blocks within the Stak fault zone represent a trend, from east to west of the exposure of progressively deeper arc lithologies. This trend culminates at the Majupah fault, which contains the only mylonite exposed in the study area. The easternmost fault, the Askore fault, exhibits the most recent activity, for a late stage felsic dike is faulted and glacial till contains features that are likely fault scarps.

Data from this study can be evaluated in light of other recent studies to try to unravel the tectonic history of northern Pakistan. A six stage tectonic model, from the initiation of the Kohistan-Ladakh arc to the present, has been created (Fig. 5.1).

The model starts with the mid-Cretaceous development of the Kohistan-Ladakh arc. Chemically primitive, deformed, and metamorphosed mafic units are the relics of this stage. The arc is believed to have been separated from the southern margin of Asia (or a microcontinent

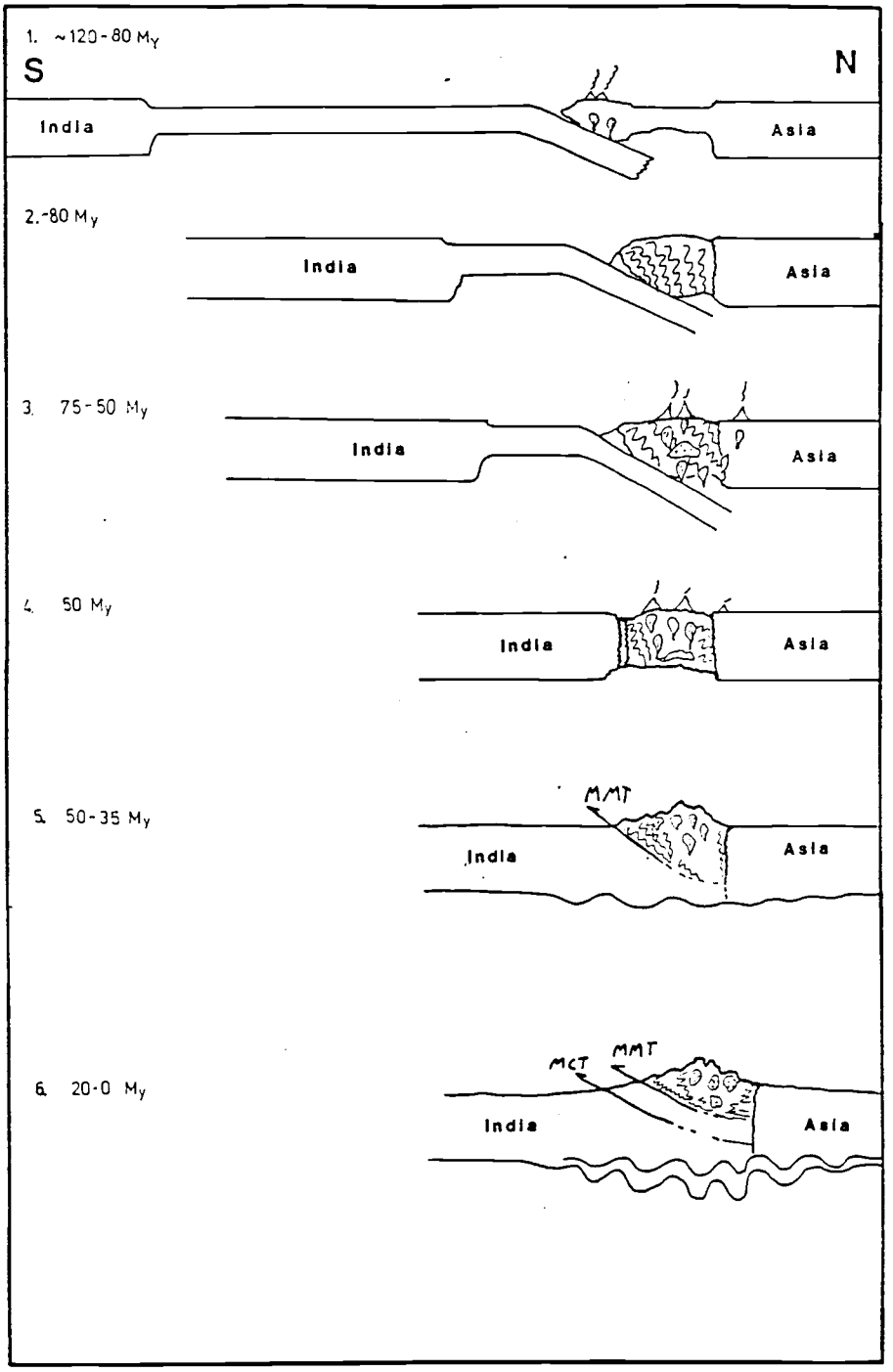

Figure 5.1. Tectonic Reconstruction. Crosssection oriented north/south.

attached to the southern Asian margin) by a back-arc basin (Peterson and Windley, 1985; Pudsey, 1986; and Hanson, pers. comm., 1986).

The second stage is closure of the back-arc basin and collision of the Kohistan-Ladakh arc with the Asian margin. A 75 Ma $^{40}Ar/^{39}Ar$ age determination of a hornblende from a mafic dike that crosscuts deformed and metamorphosed stage one units constrains the timing of the collision (Peterson and Windley, 1985). The event is likely responsible for the metamorphism of the Talu amphibolite.

The third stage of the model is marked by the second phase of magmatism in the Kohistan-Ladakh arc. The mafic to intermediate, calc-alkaline plutons are chemically more evolved than the phase one units. The trace element data are consistent with a mature oceanic island arc or a continental margin arc.

The fourth phase is the collision of the Indian continent with the southern margin of the Kohistan-Ladakh arc. Klootwijk et al. (1985) suggest that the initial collision occurred between 55 and 50 My. This is based on the abrupt decrease in the India-Asia relative movement at approximately 50 My. It is doubtful that magmatism ended at this point (Zhou, 1985).

The fifth phase is what Klootwijk et al. (1985) refer to as the indentation of Greater India. The continued indentation lasted from 50 My to approximately the early Miocene and ended with the onset of the major intracontinental underthrusting (Klootwijk et al., 1985).

The sixth phase is marked by the rotational underthrusting of the Indian continental mass beneath the Tethyan Himalaya. Klootwijk et al., (1985) document 45° of counterclockwise rotation of the underthrusted Indian mass. The pivot point is near the southern part of the NPHM.

The rotational underthrusting during the past 20 My is likely the driving force of the recent uplift of the massif (Madin, 1986). Zeitler (1985) calculates 8 +- 3 km of uplift during the past 7 My with 5.2 +- 0.7 km of the uplift during the past 2 m.y. Zeitler's uplift profile from Gilgit to Skardu shows that the uplift across the massif is relatively uniform (Fig. 5.2). Gradients across the western and eastern boundaries of the massif are different; this suggests a fundamental difference between the Raikot fault and the Stak fault zone. The gradient across the western boundary is steep, 10 km wide, and is gradual (60 km wide) across the eastern boundary.

The Raikot fault is a major tear, possibly the western terminous of the Main Central thrust (Yeats and Lawrence, 1983). The Stak fault zone is also formed in response to the recent uplift, but it does not represent the major tear (Fig. 5.3). Instead, the fault zone is created from bending of the Indian plate between the uplifted massif and the underthrusted section of the Indian plate below the Ladakh terrane.

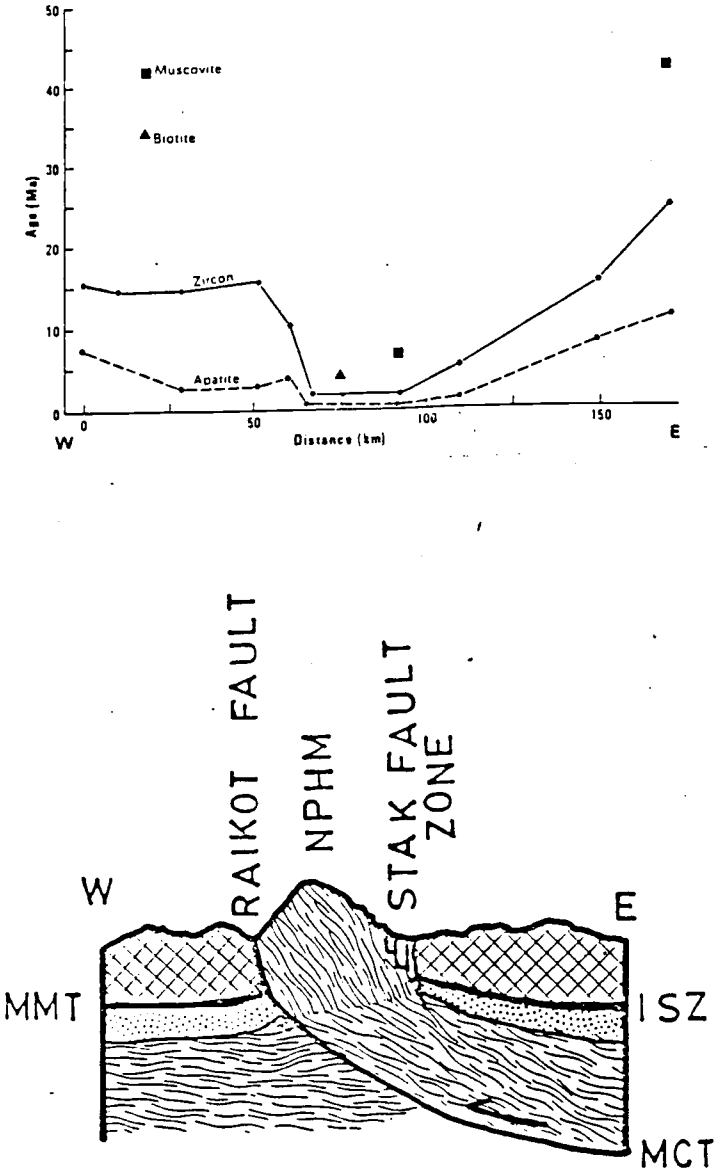

Figure 5.2. Uplift Profile. East/West oriented profile across the massif and adjoining terranes (from Zeitler, 1985) with corresponding cross section.

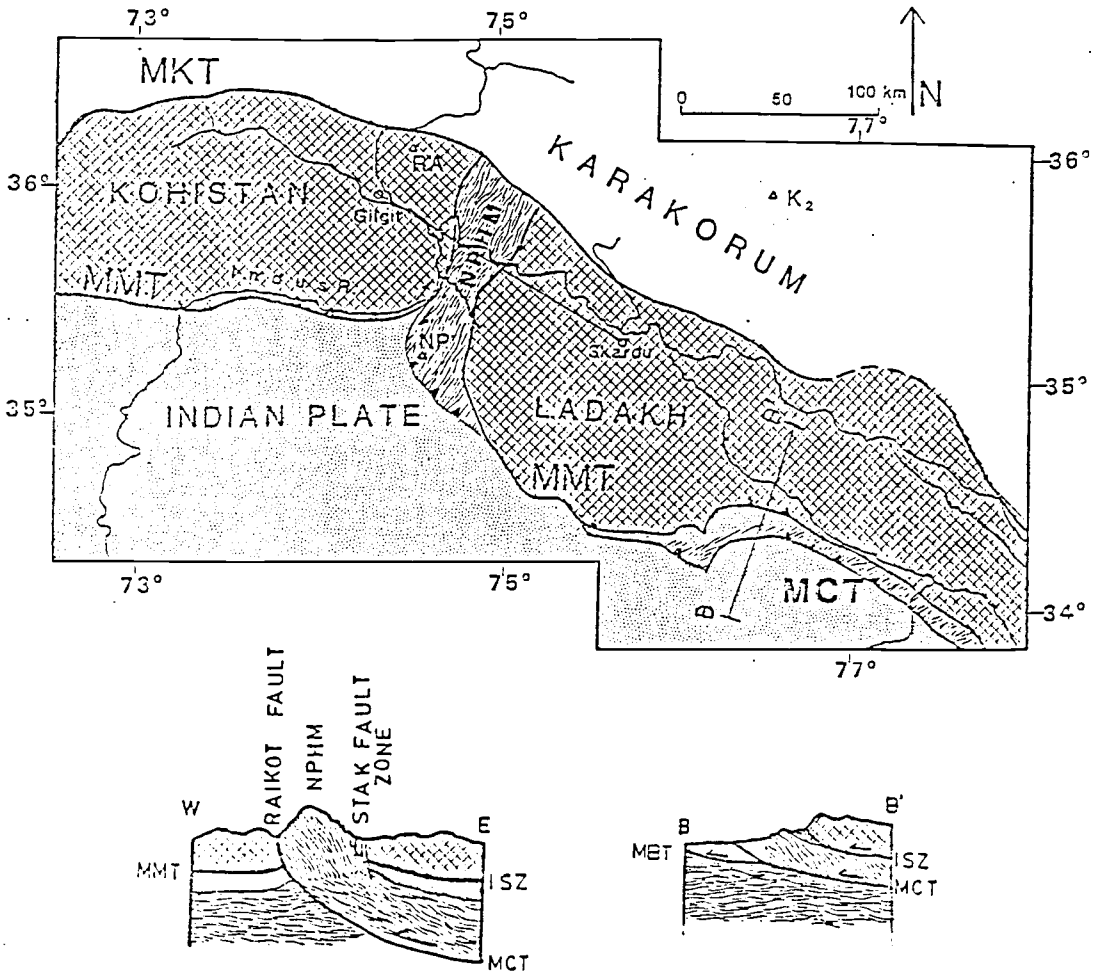

Figure 5.3. Redrawn Regional Map and Cross Sections (adapted from Madin, 1986).

Dot pattern = Indian sedimentary sequence. Wavey pattern = Indian basement. Grid pattern = Kohistan-Ladakh arc. MBT = Main boundary thrust. MCT = Main central thrust. MMT = Main Mantle thrust. ISZ = Indus Suture Zone. MKT Main Karakorum thrust.

REFERENCES

Anders, E., and Ebihara, M., 1982, Solar-system abundances of the elements: Geochem. Cosmochem. Acta, 46:2363-2380.

Andrews-Speed, C.P. and Brookfield, M.E., 1982, Middle Palaezoic and Cenozoic geology and tectonic evolution of the northwestern Himalaya: Tectonophysics, 82:253-275.

Basaltic Volcanism Study Project, 1981, Basaltic Volcanism of the Terrestrial Planets: Pergamon Press, New York, 1286 p.

Champnes, P.E. and Lorimer, G.W., 1976, Exsolution in Silicates: in Electron Microscopy: In Mineralogy. Wenk, H.R. ed. Springer, New York. pp. 228-234.

Chappell, B.W. and White, A.J.R., 1974, Two contrasting granite types: Pacific Geol., 8:173-174.

Coleman, R.G. and Peterman, Z.E., 1975, Oceanic plagiogranites: Jour. Geophy. Res., 80:1099-1108.

Coward, M.P., Jan, M.Q., Rex, D., Tarney, J., Thirlwall, M., and Windley, B.F., 1982, Geo-tectonic framework of the Himalaya of N. Pakistan: J. Geol. Soc. London, 139:299-308.

Coward, M.P., Windley, B.F., Broughton, R., Luff, I.W., Petterson, M.G., Pudsey, C., Rex, D., and Kahn, M.A., 1986, Collisional tectonics in the northwest Himalaya: In Collision Tectonics. Coward M.P. and Reis, A.C. eds., Geol. Soc. London., pp. 203-219.

Debon, F., LeFort, P., Dautel, D., Sonet, J., and Zimmerman, J.L., Plutonism in western Karakorum and northern Kohistan (Pakistan): a composite Mid-Cretaceous to Upper Cenozoic magmatism: in press.

Deruelle, B., 1982, Petrology of the plio-quaternary volcanism of the south-central and meridional Andes: J. Volc. Geoth. Res., 14: 77-124.

Desio, A., 1964, Geological tentative map of the western Karakorum: Instituto di Geologia, Milan.

Dostal, J., Zentilli, M, Caelles, J.C., and Clark, A.H., 1977, Geochemistry and origin of volcanic rocks of the Andes (26°-28° S.): Contrib. Mineral. Petrol., 63:113-128.

Dusel-Bacon, C. and Aleinikoff, J.N., 1985, Petrology and tectonic significance of augen gneiss from a belt of Mississippian granitoids in the Yukon-Tanana terrane, east-central Alaska: Geol. Soc. Am., 96:411-425.

Eskola, P. 1939, Die metamorphen gesteine: In Barth,T.F.W., Correns, C.W., and Eskola,P., Die entstehung der gesteine, ein lehubuch der petrogenese: Springer, Berlin, 422p.

Ewart, A., Bryan, W.B., and Gill, J.B., 1973, Mineralogy and Geochemistry of the younger volcanic islands of Tonga, S. W. Pacific: J. Petrol., 14:429-465.

Ewart, A., 1976, Mineralogy and geochemistry of modern orogenic lavas-some statistics and implications: Earth Plan. Sci. Lett., 31: 417-432.

Frey, F.A., Haskin, M.A., Poetz, J.A., and Haskin, L.A., 1968, Rare earth abundances in some basic rocks: Jour. Geophy. Res., 73:6085-6098.

Frey, A.F., Gerlach, D.C., Hickey, R.L., Lopez-Escobar, L., and Munizaga-Villavicenceio, F., 1984, Petrogenesis of the Laguna del Maule volcanic complex, Chile (36° S.): Contrib. Mineral. Petrol., 88:133-149.

Gansser, A., 1964, Geology of the Himalayas: Interscience, London, 289 p.

Gill, J., 1981, Orogenic andesites and plate tectonics: Springer, New York, 390 pp.

Green, T.H., 1980, Island arc and continental building magmatis a review based on experimental petrology and geochemistry: Tectonophysics, 63:367-385.

Grove, T.L. and Kinzler, R.J., 1986, Petrogenesis of andesites: Ann. Rev. Earth Planet. Sci., 14:417-454.

Haskin, L.A., Haskin, M.A., Frey, F.A., and Wildeman, T.R., 1968, Relative and absolute terrestrial abundances of the rare elements: In Origin and Distribution of elements, Ahrens L.H. ed., Pergamon, Oxford, pp. 889-912.

Haskin, L.A., 1984, Petrogenetic modelling-use of rare earth elements: in Rare earth element geochemistry, Henderson, P. ed., New York, Elsevier, 510 p.

Honeggar, K., Deitrich, V., Frank, W., Gansser, A., Thoni, M., and Trommsdorf, V., 1982, Magmatism and metamorphism in the Ladakh Himalaya: Earth Planet. Sci. Lett., 60:253-292.

Jakes, P. and Gill, J., 1970, Rare earth elements and the island arc tholeiitic series: Earth Planet. Sci. Lett., 9:17-28.

Jakes, P. and White, A.J.R., 1972, Major and trace element abundances in volcanic rocks of orogenic areas: Geol. Soc. Am. Bull., 83:29-40.

Jan, M.Q., 1979, Petrgraphy of the amphibolites of Swat and Kohistan: Geol. Bull. Univ. Peshaware, 2:65-88.

Jan, M.Q., Khattak, M.U.K., Parvez, M.K., and Windley, B.F., 1984, The Chilas Stratiform Complex: field and mineralogical aspects: Geol. Bull. Univ. Peshawar, 17:153-169.

Kazmi. A.H. and Rana,R.A., 1982. Tectonic map of Pakistan: Geol. Surv. Pakistan, Quetta, Pakistan.

Kazmi, A.H., Lawrence, R.D., Dawood, H, Snee, L.W., and Hussain, S.S., 1984. Geology of the Indus suture zone in Mingora-Shangla area of Swat, N. Pakistan: Geol. Bull. Univ. Peshawar, 17:127-144.

Klootwijk, C.T., Conaghan, P.J., and Powell, C.McA., 1985, The Himalayan arc: large-scale continental subduction, oroclinal bending, and back-arc spreading: Earth Planet. Sci. Let., 75:167-183.

Kureshy, K.U. and Elahi, M.K., 1975, Geographic map of Pakistan: Geol Surv. Pakistan, Quetta, Pakistan.

LaFort, P., 1975, Himalayas: the collided range: present knowledge of a continental arc: Am. Jour. Sci., 275A:1-44.

Laul, J.C., 1979, Neutron activation analysis of geological materials: At. Energy Rev., 17:603-695.

Lawrence, R.W. and Ghauri, A.A.K., 1983, Evidence for active faulting in the Chilas district, northern Pakistan: Geol Bull. Univ. Peshawar, 16:185-186.

Lawrence, R.D., Kazmer, C., and Tahirkheli, R.A.K., 1983. The main mantle thrust: a complex zone: Geol. Soc. Amer. Abst. with Programs, 15:624.

Madin, I.P., 1986, Structure and neotectonics of the northwestern Nanga Parbat-Haramosh massif: Oregon State University, Ms thesis, 160 p.

Misch, P., 1935, Geologische rundschau, 26:157-158.

Misch, P., 1949, Metasomatic granitization of batholithic dimensions: Am. Jour. Sci., 247: 209-245.

Miyashiro, A., 1974, Volcanic rock series in island arcs and active continental margins: An. Jour. Sci., 274:321-355.

Miyashiro, A., 1978, Metemorphism and metamorphic belts: Wiley, New York, 492 p.

Mueke, G.K., Pride, C., and Sarkar, P., 1977, Rare-earth element geochemistry of regional metamorphic rocks: In Origin and distribution of elements; Proceedings of the second symposium. Ahrens, L.H. ed., Pergamon Press, New York, p. 449-464.

Nockolds, S.R., 1954, Average chemical composition of some igneous rocks: Bull. Geol. Am., 66:1007-1032.

Page, B.G.N., Bennett, J.D., Cameron, N.R., Bridge, D.McC., Jeffrery, D.H., Keats, W., and Thiab, J., 1979, A review of the main structural and magmatic features of northern Sumatra: Jour. Geol. Soc. London, 136:569-574.

Peterson, M.G. and Windley. B.F., 1985, Rb-Sr dating of the Kohistan arc-batholith in the Trans-Himalaya of N. Pakistan, and tectonic implications: Earth Planet. Sci. Lett., 74:45-57.

Pudsey, C.J., 1986, The northern suture, Pakistan: margin of a Cretaceous island arc: Geol. Mag., 123:405-423.

Rai, H. and Pande, I.C., 1982, Study of the norite from the Kargil igneous Complex, Indus Suture Zone, Ladakh, India: in Cont. Geos. Res. in Hamalaya, Sinha, A.K. ed., 2:41-47.

Reynolds, P.H., Brookfield, M.E., and McNutt, R.H., 1983, The age and nature of Mesozoic-Tertiary magmatism across the Indus suture zone in Kashmir and Ladakh (N.W. India and Pakistan): Geol. Rundschau., 3:981-1004.

Ronov, A.B. and Khlebnikova, Z.V., 1957, Geochemistry, 6:527-552.

Srimal, N., 1986, A tectonic, geochemical, and isotopic study of the Ladakh arc, N. India: University of Rochester. PhD dissertation, 400 p.

Tahirkheli, R.A.K., 1979, Geology of Kohistan and adjoining Eurasian and Indo-Pakistan continents: Pakistan. Geol. Bull. Univ. Peshaware, 2:1-30.

Verplanck, E.P., 1985, Temoral variations in volume and geochemistry of volcanism in the western Cascades, Oregon: Oregon State University, M.S.thesis. 115 p.

Wadia, D.N., 1933, A note on the geology of Nanga Parbat (Mt. Diamir) and adjoining portions of Chilas, Gilgit District, Kashmir: Records Geol. Sur. India, 66:212-234.

Wadia, D.N., 1937, The Cretaceous volcanic series of Astor-Deosia, Kashmir, and its intrusions: Records Geol. Sur. India, 72:151-161.

Winkler, H.G.F., 1979, Petrogenesis of metamorphic rocks (fifth edition): Springer, New York, 348 p.

Yeats, R.S. and Lawrence, R.D., 1983, Tectonics of the Himalayan thrust belt in northern Pakistan: in Marine geology and oceanography of the Arabian sea and coastal Pakistan, Haq, B.U. and Milliman, J.D. eds., Reinhold, p. 177-198.

Zanettin, B., 1964, Geology and petrology of the Haramosh-Mango Gusor area. Italian Expeditions to the Karakorum and Hindu Kush: Brill, Leiden, 304 p.

Zeitler, P.K., 1985, Cooling history of the NW Himalaya, Pakistan: Tectonics, 4:127-151.

Zen, E. and Hammarstrom, J., 1984, Magmatic epidote and its petrologic significance: Geology, 12:515-518.

Zhou, J., 1985, The timing of calc-alkaline magmatism in parts of the Alpine-Himalayan collision zone and its relevance to the Caledonian magmatism: Jour. Geol., 16:305-317.